Monitoring chemically-induced myelin damages in the central nervous system via surface-recorded cerebellar auditory evoked potentials and radioimmunoassay of myelin basic protein in the cerebrospinal fluid

Xuguang Liu, B.M., M.Med.,

This thesis is submitted for the degree of

Doctor of Philosophy

Gough-Cooper Department of Neurological Surgery, Institute of

Neurology, Queen Square, London.

December, 1996

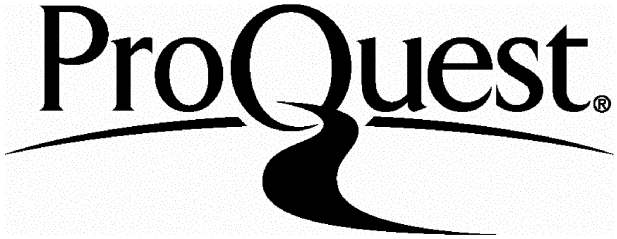

ABSTRACT

This study aimed to evaluate two novel *in vivo* approaches to quantifying chemically-induced myelin damage in rats which might be useful for clinical monitoring of demyelination in humans. These were surface recording of the cerebellar auditory evoked potential (AEP), and radioimmunoassay of myelin basic protein (MBP) in the cerebrospinal fluid (CSF).

The cerebellar AEP was characterized using a range of experimental manipulations, repeated CSF sampling techniques developed, and a radioimmunoassay shown to be practicable for detection of MBP in rat CSF. Two toxic models were established: lysolecithin (LPC) induced focal demyelination and triethyltin (TET) induced myelin oedema. The cerebellar AEP was recorded chronically via pre-implanted skull electrodes, and MBP concentration in the CSF was assayed in both models over the period of intoxication. Lesions were also characterized morphologically.

Destruction of myelin by LPC produced a significant but transient decrease in AEP amplitude and rapid appearance of MBP in the CSF peaking at 24 hours. Myelin disruption without demyelination by TET intoxication produced a significant decrease in AEP amplitude at 24 hours, significant delay in latency, prolongation in conduction time and increase in the temperature dependence of conduction velocity at 72 hours, but no MBP was detected in the CSF.

The surface-recorded cerebellar AEP was an effective indicator for monitoring progression of dysfunction associated with both LPC and TET induced lesions, although interpretation is complicated by interference from non-cerebellar components of the response. MBP was a sensitive and selective indicator which further distinguished myelin destruction from reversible myelin disruption. Both methods could therefore usefully be extended to clinical applications.

PREFACE

After six years of training in Neurosurgery at Beijing Neurosurgical Institute, the busiest neurosurgical centre in China, and after two years of experimental research on electrophysiological monitoring of acute cerebral ischaemia in the Department of Neurological Surgery, Institute of Neurology, London, I determined to start a systematic PhD training in neuroscience, having a preference of experimental neurophysiology, with loads of good wishes and also family responsibilities.

The surface-recorded cerebellar AEP and radioimmunoassay of MBP in the CSF was evaluated for *in vivo* monitoring chemically-induced myelinopathy, which forms a part of collaborative investigations among five European nations on developing effective indices for *in vivo* monitoring toxicity (Manzo, *et al.*, 1996). The study covered by this thesis commenced at the beginning of 1992, at the MRC Toxicology Unit, Carshalton, and it was then continued after the Unit was relocated in Leicester.

This thesis was actually completed during my time working as a Research Scientist at the University Laboratory of Physiology, Oxford, after I had left the MRC Toxicology Unit in February, 1995.

Xuguang Liu, B.M., M.Med.

Oxford, December, 1996

ACKNOWLEDGEMENTS

I would like, first of all, to express my deep appreciation to Dr Neil M. Branston, Department of Neurological Surgery, Institute of Neurology, London, and Dr David E. Ray, Neurotoxicology Section, MRC Toxicology Unit, Leicester, for both their supervision of the project and their encouragement to me to carry out the study, and more importantly, their great efforts to teach me 'thinking in a scientist's way'.

I am also indebted to Dr Paul Glynn, MRC Toxicology Unit, for his supervisory and detailed instructions on Immunochemistry and constructive criticisms of the relevant chapters in this thesis. I would like to thank Dr Nigel Groome, Brookes University, for his kindness in providing essential agents of the immunoassay employed in my study. Many thanks to Professor Lindsay Symon, Institute of Neurology, for allowing me to register myself through his department, and to Professor John B. Cavanagh, Institute of Psychiatry, for his expert input to the design of the toxicological experiments. I am extremely grateful to the colleagues at the Neurotoxicology Section: Mr Christopher Nolan and Mrs Jean Edwards for their excellent technical support in obtaining pathological sections and photographs; Mr Tim Lister for his skilful support of setting up and maintaining the electronic apparatus; Drs Martin Johnson, Philip Forshaw, Mike Mulheran, Richard Verschoyle, Janice Holton for their valuable discussions about this study. Thanks to Drs John Stein and R Christopher Miall, my superiors in the University Laboratory of Physiology, Oxford, for their unforgettable support to me to complete my thesis.

Thanks to Dr Anling Rao, my dear wife, for her understanding and supporting in both academic and domestic terms over this period of years.

I was kindly supported by a EC grant (EC BIOMED grant, STEP EV5V-CT91-0005) for a period of three years from February, 1992 to February, 1995.

CONTENTS

	page
ABSTRACT	2
PREFACE	3
ACKNOWLEDGEMENTS	4
TABLE OF CONTENTS	5
LIST OF TABLES	10
LIST OF FIGURES	11
GLOSSARY OF ABBREVIATIONS	14
CHAPTER 1. RESEARCH BACKGROUND	17
1.1. The question	18
1.2. Myelin and myelinated nerve fibres	19
1.2.1. Ultrastructure of myelin and myelinated fibres	20
1.2.2. Molecular constituents of myelin	21
1.2.3. Physiological properties of myelin and myelinated fibres	24
1.3. Demyelination	25
1.3.1. Physiological impairment	26
1.3.2. Components of myelin breakdown products	30
1.3.3. Pathological features	31
1.3.4. A common mechanism in demyelination?	34
1.4. Animal models of chemically-induced myelinopathy	35
1.4.1. Classification of demyelinating chemicals	39

1.4.2. Myelinopathies induced by TET 39

1.4.3. Acute focal demyelination induced by LPC 48

1.4.4. Chronic demyelination induced by cuprizone 51

1.4.5. Focal myelinopathy induced by oral intoxication of diphenamid 56

1.5. Monitoring central demyelination *in vivo* 57

1.5.1. Recording evoked potentials 58

1.5.2. Detecting myelin breakdown products in body fluids 61

1.5.3. Computerized imaging systems 65

1.6. The surface cerebellar AEP: An index of cerebellar conduction? 66

1.7. Hypotheses and protocols of the present investigation 67

CHAPTER 2. EXPERIMENTAL METHODS 70

2.1. Animals 71

2.2. Toxic chemicals 72

2.3. Experimental anaesthesia in rats 72

2.4. Surgical implantation of cannulae for repeated CSF sampling 75

2.5. Estimation of clearance rate of MBP from CSF circulation 78

2.6. Radioimmunoassay for detecting MBP in the CSF 79

2.6.1. Preparation of rat MBP 80

2.6.2. Preparation of CSF samples 81

2.6.3. Protocol of labelling the peptides 34T for RIA 81

2.6.4. RIA procedures 82

2.6.5. Standard curves of rat MBP and parallelism test of rat CSF samples 85

2.7. Recording AEP 85

2.7.1. Surface-recording of AEP 86

2.7.2. Depth-recording of AEP 87

2.7.3. Calibration and application of sound stimulus 87

2.7.4. Recording parameters 88

2.7.5. Analyses of AEP 88

2.8. SEP recording 93

2.9. Histopathological methods 94

2.10. Statistical analysis of data 97

CHAPTER 3. AUDITORY AFFERENTS TO THE CEREBELLUM: THE SURFACE-RECORDED CEREBELLAR AEP IN ANAESTHETIZED RATS 98

3.1. Summary 99

3.2. Introduction 99

3.3. Materials and methods 101

3.4. Results 103

3.4.1. Spatial distribution of the surface-recorded cerebellar AEP 103

3.4.2. Effects of stimulating and recording parameters on the cerebellar AEP 105

3.4.3. Binaural interaction of the cerebellar and neocortical AEPs 109

3.4.4. Monopolar depth recordings of AEP at different levels of the auditory pathway 114

3.4.5. Effects of intracerebellar injection of procaine on the cerebellar AEP 120

3.5. Discussion 120

CHAPTER 4. MONITORING THE LYSOLECITHIN-INDUCED FOCAL DEMYELINATION IN THE CEREBELLAR WHITE MATTER USING THE SURFACE-RECORDED CEREBELLAR AEP AND DETECTION OF MBP IN THE CSF 129

4.1. Summary 130

4.2. Introduction 131

4.3. Materials and methods 132

4.4. Results 135

4.4.1. The clearance rate of MBP from the CSF 135

4.4.2. Changes in the cerebellar and neocortical AEPs 136

4.4.3. Appearance of MBP in the CSF 137

4.4.4. Histopathological findings 137

4.5. Discussion 137

CHAPTER 5. TRIETHYLTIN-INDUCED ACUTE OTOTOXICITY AND MYELINOPATHY IN RATS: MONITORED BY SURFACE-RECORDED AEP, SEP AND RADIOIMMUNOASSAY OF MBP IN THE CSF 152

5.1. Summary 153

5.2. Introduction 153

5.3. Materials and methods 155

5.4. Results 158

5.4.1. Clinical assessments of acute systemic toxicity in rats 158

5.4.2. Interaction of TET with anaesthetics 158

5.4.3. Monitoring TET toxicity with cerebellar AEP and cortical SEP 159

5.4.4. No MBP detectable in the CSF 160

5.4.5.Histopathological findings 160

5.5. Discussion 160

CHAPTER 6. CONCLUSIONS 175

6.1. Conclusions from the present investigation 176

6.2. Pointers for further investigations 180

REFERENCES 182

APPENDICES 198

1. Preliminary results of cuprizone intoxication in rats 198

2. Preliminary results of diphenamid intoxication in rats 207

3. Publications related to this study 210

LIST OF TABLES

		page
Table 1-1.	Classification of different toxins inducing primary or secondary demyelination	37
Table 1-2.	Classification of different chemicals with effects on the central, peripheral or both nervous systems	38
Table 2-1.	Stereotaxic positions of various brain structures	91
Table 3-1.	Alteration of the surface-recorded cerebellar AEP following intracerebellar injection of procaine	122
Table 4-1.	Measurements of latencies, amplitudes of the cerebellar AEP and CCT before and after focal LPC injection	138
Table 4-2.	Measurements of MBP in the CSF over the period of LPC intoxication	139
Table 5-1.	Measurements of latencies, amplitudes of the cerebellar AEP and CCT before and after acute TET intoxication	161

LIST OF FIGURES

		page
Figure 2-1.	Cannula implantation into the cisterna magna for repeated CSF sampling in rats	77
Figure 2-2.	Standard curve of radioimmunoassay for detection of rat MBP	83
Figure 2-3.	Parallelism tests for CSF samples from four rats using logit-log plot.	84
Figure 2-4.	Arrangement of implanted surface electrodes for chronic AEP recordings	89
Figure 2-5.	The spatial distribution of the surface-recorded AEP under monaural stimulation	90
Figure 2-6.	Calibration of sound intensity and apparatus set up for monaural and binaural stimuli	92
Figure 2-7.	Analyses of AEP	95
Figure 2-8.	Analyses of SEP	96
Figure 3-1.	The spatial distribution of the surface-recorded AEP under binaural stimulation	104
Figure 3-2.	Positive linear correlation between stimulus intensity and potential amplitudes	106
Figure 3-3.	Effect of stimulus frequency on the evoked potential	107
Figure 3-4.	Effect of band-width setting on potential recordings	108
Figure 3-5, 6.	Comparison of amplitudes of the cerebellar auditory potentials under monaural or binaural stimuli	110

Figure 3-7, 8. Comparison of amplitudes of the cortical auditory potentials under monaural or binaural stimuli 112

Figure 3-9. Auditory evoked potentials recorded from the cochlear nuclei on both sides correlated with the surface-recorded response from the occipital skull in midline 116

Figure 3-10. Auditory evoked potentials recorded from the contralateral inferior colliculus and the cerebellar dentate nucleus correlated with the surface-recorded response from the occipital skull in midline 117

Figure 3-11. AEPs recorded from the contralateral, midline and ipsilateral sides at different depths in the cerebellum 118

Figure 3-12. The depth profile in the amplitude of the cerebellar potentials 119

Figure 3-13. AEP recordings before and after intracerebellar injection of procaine 121

Figure 4-1. Clearance curve of MBP from the CSF circulation in 3 animals 140

Figure 4-2. Comparison of monitoring LPC-induced demyelination via cerebellar AEP recording and MBP detection in the CSF 141

Figure 4-3. (a) Acute focal demyelination in cerebellar white matter and (b) recovery of the lesions on day 15 with HE stain 142

Figure 4-4. Acute focal demyelination in cerebellar white matter with myelin stain 144

Figure 5-1. Changes of body weight (a), rectal temperature (b) and ataxia score (c) after TET intoxication 162

Figure 5-2. Decrease of body temperature under isoflurane anaesthesia and increase in effect of isoflurane after TET intoxication 163

Figure 5-3. Examples of AEP traces after TET intoxication 164

Figure 5-4. Changes in AEP latencies and the CCT after TET intoxication 165

Figure 5-5. Temperature dependence of impulse conduction along the normal and damaged auditory pathway 166

Figure 5-6. Changes of SEP recordings after TET intoxication 167

Figure 5-7. (a) TET induced spreading vacuolation in CNS white matter and (b) recovery of the lesions on day 15 with HE stain 168

GLOSSARY OF ABBREVIATIONS

AEP:	auditory evoked potential.
AETT:	acetyl ethyl tetramethyl tetralin, Tetralin.
AP:	anterio-posterior plate.
BBB:	blood-brain barrier.
CCT:	central conduction time.
cm:	centimetre(s).
cpm:	counts per minute
CPM:	central pontine myelinolysis
CNS:	central nervous system.
CSF:	cerebrospinal fluid.
CT:	computerised X-ray tomography.
A/D:	analogue/digital.
dB:	decibel.
DEET:	*N*,*N*-diethyl-*m*-toluamide.
DPM:	*N*,*N*-Dimethyl-2,2,-diphenylacetamide, diphenamid.
DV:	dorso-ventral plane.
EAE:	experimental allergic encephalomyelitis.
ENU:	Ethylnitrosourea.
EP:	evoked potential.
EPSP:	excitatory post-synaptic potential.
g:	gram(s).
HCP:	2,2'-methylene*bis*(3,4,6-trichlorophenol), Hexachlorophene.
Hz:	Hertz.
IgG:	immunoglobin G.
INH:	isonicotinic acid hydrazide, Isoniazid.
i.m.:	intramusclar injection.
i.p.:	intraperitoneal injection.
IPI:	inter-pulse interval.
IPL:	intraperiod line.
IPSP:	inhibitory post-synaptic potential.

i.v.:	intravenous injection.
kg:	kilogram(s).
LPC:	lysophosphatidyl choline, lysolecithin.
MAG:	myelin-associated glycoprotein.
MBq:	megaBecquerel.
MBP:	myelin basic protein.
mCi:	milliCurie.
MDL:	major dense line.
mg:	milligram(s).
min:	minute(s).
ml:	millilitre(s).
mm:	millimetre(s).
MRI:	magnetic resonance imaging.
mRNA:	messager ribonucleic acid.
ms:	millisecond(s).
MS:	multiple sclerosis.
mV:	millivolt(s).
ng:	nanogram(s).
nm:	nanometre(s).
O_2CT:	oxygen content in blood.
O_2SAT:	oxygen saturation in blood.
PCO_2:	partial pressure of carbon dioxide in blood.
PE10/50:	polyethylene 10/50 tubing.
PLP:	proteolipid protein.
PNS:	peripheral nervous system.
RIA:	radioimmunoassay.
s:	second(s).
SD:	standard diviation.
SEP:	somatosensory evoked potential.
S.E.M.:	standard error of the mean.
TET:	triethyltin.
TMT:	trimethyltin.

V:	Volt(s).
VEP:	visual evoked potential.
µl:	microlitre(s).
µV:	microvolt(s).

CHAPTER 1.

RESEARCH BACKGROUND

This Chapter presents an overall review of basic knowledge and previous investigations in the general field of this thesis. Sections strictly related to the experiments presented in this thesis are reviewed in detail, whilst others are only highlighted and provided with further references. Literature was obtained via both EMBASE and MEDLINE search engines to cover the widest possible range of publications in this field. In addition, a brief and more specific introduction to each group of experiments is also given in chapters 3, 4, and 5.

1.1. The question.

A great number of methods for studying the structure and function of neural conduction in both the central (CNS) and peripheral nervous system (PNS) have been already used to achieve the understanding of the ultrastructural, molecular biological and electrophysiological properties of myelin and myelinated nerve fibres at the systemic, cellular and molecular levels. At present, investigations of myelin and myelinated nerves have been widely extended to the processes of myelination, demyelination and remyelination. Nevertheless, the process of developing or evaluating repeatable and quantitative methods for *in vivo* monitoring demyelinating lesions in the CNS has continued in laboratory experiments to complement existing methods, and to continuously assess the progression of the lesions. Sensitivity and selectivity are important in such methods in order to acquire valuable information about the regional specificity or pathological status of the chemically-induced myelinopathies, *i.e.* various pathological conditions of myelin damage with or without demyelination. Those methods developed under experimental conditions could be useful and ultimately clinically applicable for diagnosing demyelinating disease or

demyelinating intoxication, monitoring its progression and recovery, and evaluating the effectiveness of therapy.

There are three potentially practicable approaches for *in vivo* monitoring of demyelinating lesions in the CNS. (1) Electrophysiological recording of evoked potentials, which is specific to the pathway being recorded from. (2) Immunochemical detection of myelin-specific markers, myelin breakdown products, in body fluid. (3) Computerized imaging of the nervous system. Two of these approaches were evaluated in the present investigation. Given that the cerebellum is a susceptible target for several demyelinating compounds, and that myelin basic protein (MBP) is liberated from myelin following demyelination, two methods of surface-recording cerebellar auditory evoked potential (AEP, action or field potential evoked by monaural or binaural auditory stimulation) and detecting MBP in the cerebrospinal fluid by radioimmunoassay were selected for exploration and evaluation in rat models of chemically-induced central myelinopathies. Several well-characterized myelin toxic compounds were administered by either systemic intoxication or focal injection in order to provide variations in the distribution pattern and pathological status of the induced lesions for evaluating the sensitivity and selectivity of the proposed *in vivo* monitoring methods.

1.2. Myelin and myelinated nerve fibres.

The nervous system is customarily divided into central and peripheral parts. The CNS consists of the brain and the spinal cord. The PNS includes the nerves of the body which convey the input and output information between the CNS and peripheral

structures of sensory receptors and muscles. The nervous system consists of neurones, surrounded by a framework of supporting cells. A 'classic' neurone has a cell body, an arbitrary number of small processes, dendrites, and a single long process, called the axon or nerve fibre. The axon of most neurones are 1-20 μm in diameter, and a few millimetres to a few meters long. The axon transmits information from the neurone to other cells, in a form of action potential, *i.e.* a transient biphasic potential across the stimulated membrane due to a transient opening of ion-channels. Most of the nerve fibres are myelinated by oligodendrocytes in the CNS or Schwann cells in the PNS. Myelination of CNS axons occurs when oligodendrocytes direct fragil-appearing extensions of their plasma membrane to target axons and proceed to envelop the axonal cylinder with a continuous wrapping of membrane until a complete circuit is accomplished and the extracellular faces adhere. The features of myelin and myelinated fibres in the CNS described here are its ultrastructure, molecular constituents and physiological properties. This description will be helpful in understanding pathological changes and the possible mechanisms of demyelination and in identifying markers for detecting demyelinating damage described later on in this thesis.

1.2.1. Ultrastructure of myelin and myelinated fibres. The basic ultrastructure of myelin was clearly revealed by several early studies using polarised light and X-ray diffraction (Schmitt, 1936; Finean, 1953). When viewed under the electron microscope in cross section, myelin is seen as highly regular and distinctive structure that consists of multiple tightly wrapped spirals of membrane that insulate axons. Two alternate hydrophilic layers are electron-dense. The wider one, named the major dense

line (MDL), represents apposition of the cytoplasmic aspects of plasma membranes, while the narrower one, named the intraperiod line (IPL), represents the outer surface of the plasma membranes (Robertson, 1962). Monuki and Lemke (1995) stated that "to understand the topology of the myelin sheath, it is useful to draw an analogy between this sheath and a rolled up sleeping bag. When a sleeping bag is rolled, two distinct surface appositions are created-one resulting from the interface between the inner surfaces of the sleeping bag, and another that results from the interface between its outer surfaces. Similarly, the spiral layering of myelin membrane results in apposition between either the intracellular or extracellular surfaces of membrane." In the CNS, oligodendrocytes both form and maintain myelin. Each oligodendrocyte myelinates more than one axon and each axon may be myelinated by several oligodendrocytes. The extension of the oligodendrocyte plasma membrane spirals many times around the axon with the uncompacted myelin. The cytoplasm between adjacent layers of membranes is extruded to form the major dense line. The extracellular faces of the membrane meet and form the double intraperiod line. The potential interlamellar space between the intraperiod line is sealed by the tight junctions. This type of junction between adjacent cellular membrane is sufficiently narrow to limit the free diffusion of water-soluble substances. Each internode is separated by the node of Ranvier, at which the axon is exposed. The inner, outer and terminal loops at nodes of Ranvier are the only places where cytoplasm remains.

1.2.2. Molecular constituents of myelin. Myelin consists of various highly regular and distinctive concentric lamellae of hydrophobic and hydrophilic components both in the CNS and PNS. The hydrophobic layers of myelin are constituted by the

hydrocarbon chains of fatty acids, cholesterol, and hydrophobic domains of proteins aligned radially. The hydrophilic layers consist of the polar parts of lipids and the hydrophilic domains of the various proteins aligned parallel to the axon. Not surprisingly, each individual molecular constituent of myelin plays important roles in forming and maintaining the structure of myelin sheath, and presents in various forms as the myelin breakdown products when demyelination occurs. The structural components of myelin, mainly myelin proteins, are briefly reviewed with emphasis on their roles in forming and maintaining myelin structure and as possible markers for detection of myelin damage, particularly the myelin basic protein.

The protein to lipid ratio is approximately 20:80 in myelin in contrast to the ratio of 60:40 in other mammalian cellular membranes. The total amount of protein in myelin is about 30% of the dry weight in both the central and peripheral nervous system. The proteins and lipids in myelin are made up of a number of molecular species, which have their own distinct chemical make-up and physical properties that contribute to the formation, maintenance of the myelin membrane, and possibly the pathogenesis of demyelination. Three different proteins account for 99% of the CNS myelin proteins. These are (1) the proteolipid protein (PLP) with a 24,000 molecular weight which comprises 50% of the total protein; (2) Myelin basic protein (MBP) with a molecular weight of 18,300 and comprising 30% of total protein in myelin preparations. and (3) the Wolfgramm protein with molecular weight of 45,000 - 55,000, comprising 2 to 5% of the total protein. The major myelin-associated glycoprotein (MAG) constitutes less than one percent of the CNS myelin protein (Whitaker and Snyder, 1982; Williams and Deber, 1993). In the CNS, myelin PLP positions mainly in the intraperiod line,

while MBP situates in the major dense line. In contrast to the above major myelin proteins, MAG is present in the non-compacted regions of myelin. These regions include the innermost layer, the outermost layer, and other regions such as the paranodal loops. Locations of the major myelin protein have functional meanings in which PLP is thought to be responsible for intraperiod line compaction; MBP is for major dense line compaction, and MAG is believed to function as an adhesion molecule that mediates axon-glial cell adhesion events that precede myelination (Bartsch, 1996). In addition to the major proteins of myelin, there are a number of soluble membrane proteins the are important in the formation and maintenance of the myelin sheath. For example, 2',3'-cyclic nucleotide 3'-phosphohydrolase, phosphatidylinositol-specific phospholipase C, and protein kinase C located in the myelin cytoplasm, are involved in posttranslational modifications during myelination and/or intracellular signal transduction (Morell, 1984). Some proteins are restricted specifically to oligodendrocytes and CNS myelin: they are the myelin/oligodendrocyte glycoprotein, oligodendrocyte/myelin glycoprotein, myelin/oligodendrocyte-specific protein, and myelin-associated/oligodendrocytic basic protein (Holz *et al.*, 1996), which may function in recognition and adhesion at the beginning of myelination and possibly remyelination.

Unlike the other major myelin proteins, MBP is not a transmembrane protein, but a cytoplasmic protein that is localized to and is responsible for compaction of the major dense line of myelin. Early studies shown (Carnegie and Moore, 1980) that MBP has a molecular weight of 18,300 and composed of approximately 170 amino acids. The primary sequence of MBP has been determined in a number of species including

human, mouse, guinea pig, cow, and chicken, (Martenson, 1992). In rats, mice, and related species there is a second, more abundant MBP. The second form of MBP shows an internal deletion of 40 amino acids from residues 116 - 155 of the large form. The amino acid sequences for human and bovine MBP and the small MBP of the rat have been determined. Recent study has shown that MBP is expressed in both oligodendrocytes and Schwann cells. At least six isoforms of MBP exits, ranging from 14 to 21 kD. A number of differences between MBP species have been described (Hudson, 1990; Monuki and Lemke, 1995). However, the functional significance of these different isoforms is unclear, and they generally are referred to collectively as 'MBP'.

1.2.3. Physiological properties of myelin and myelinated fibres. In myelinated nerve fibres, the inward membrane current during the rising phase of the action potential is generated only in the non-myelinated portion of the axon (e.g. Huxley and Stampfli, 1949) at the nodes of Ranvier, gaps in the myelin sheath between adjacent myelin cells and at where the axon is exposed. The segment between two adjacent nodes is called the internodal segment.. Because the internodal myelin sheath has a high electrical resistance, the inward current generated at each node is constrained to flow forward axially within the axoplasm to depolarise the axon membrane at the next node, while current returns externally to the fibre in the direction opposite to that of internal axial current flow via the next node to complete the current loop. Myelin thus restricts the membrane current to the successive nodal sites along the fibre. In a sense, therefore, the action potential can be said to jump from node to node. This mode of conduction is termed saltatory conduction. The saltatory conduction is also supported

by the heterogeneous distribution of Na^+ and K^+ channels. For example, Na^+ channels cluster in high density (approximately 1000/μm^2) in the axon membrane at the node. In contrast, the density of Na^+ channels in the internodal axon membrane, under the myelin sheath, is much lower (<25/μm^2), too low to support conduction in most axons (Ritchie and Rogart, 1977). The density of fast K^+ channels is maximal in the paranode, decreasing to 1/6 in the node and internode (Ritchie and Rogart, 1977; Chiu and Ritchie, 1980; 1981). The net velocity of saltatory conduction is fast and proportional to the outside diameter of the nerve, in which a thick myelin improves electrical insulation and hence reduces internodal losses of current across the cell membrane and thick axis cylinder reduces core resistance and thus improves the longitudinal spread of current. Another advantage of myelination is that, since ionic currents are confined to the nodal membrane, the amount of metabolic energy required for each nerve impulse is proportionally less, per unit length of the fibres, and less influenced by environmental changes. In comparison, the whole length of the fibre takes part in the action potential conducting process in non-myelinated nerves. This mode of conduction is called continuous conduction, which obviously requires more metabolic energy and is more susceptible to environmental influences. The velocity of continuous conduction is slow and approximately proportional to the square root of the diameter of the fibre.

1.3. Demyelination.

Demyelination could happen through a number of causes such as inflammation (Hughes, 1994), ischaemia/anoxia (Stys *et al.*, 1992), malnutrition (Adams *et al.*, 1959; Hillborn, 1984), traumatic injury (Povlishock, 1992), genetic deficit (Griffiths *et*

al., 1995), immune-mediated process (Zamvil and Steinman, 1990; Owen and Sriram, 1995.) and toxic poison (Le Quesne, 1993; Ludolph and Spencer, 1995). It is classified into primary and secondary demyelination. The former results from primary damage to the myelin sheath alone, or combined damage to both myelin and its related myelinating cells, and the latter occurs secondary to degeneration of the axon (namely Wallerian degeneration, a process whereby interruption of axonal continuity in peripheral nerve trunks leads to axonal and myelin breakdown and removal distal to the injury site). The final consequences of demyelination are reflected by changes in physiological functions (Rasminsky, 1980), biochemical properties (Cammer, 1980; Whitaker and Snyder, 1982) and ultrastructure (Lowenthal, 1991) of the myelinated nerve fibres which were described in several early reviews. Such changes are summarized in the early part of this section (see 1.3.1. - 1.3.3.). Although those changes induced by different demyelinating processes trigged by various causes have their own specific features (Banik, 1992; Cavanagh and Nolan, 1994; Tuohy, 1994; Maxwell, 1995; Miller *et al.*, 1995), there may be a common mechanism (or a segment of a common pathway), irrelevant to the specific cause of demyelinating lesions. This question has not been answered clearly yet, but some hypothetical key events seem to exist at the final stages of the development of several demyelinating lesions which are initially triggered by separate causes. These key events are highlighted later in this section (see 1.3.4.).

1.3.1. Physiological impairment. The normal conduction of impulses along the myelinated nerve fibre depends on the structural and functional integrity of the myelin sheath (see 1.2.3.). This conduction will be impaired even if the myelin sheath is only

partially damaged. The mechanism of demyelinating conduction of nerve impulses was studied in early animal experiments in which demyelination of the ventral root fibres was provoked by focal exposure to diphtheria toxin (McDonald, 1963; McDonald and Sears, 1970; Rasminsky and Sears, 1972; Bostock *et al.*, 1978), and later reviewed in great detail by (Rasminsky, 1980; Kaji and Kimura, 1991; Waxman *et al.*, 1994; Waxman *et al.*, 1995; Sharger, 1995).

Abnormal conduction of impulses. Impulses conducted with reduced velocity, loss of synchrony and, in the extreme case, complete conduction block are characteristics of abnormal conduction, and result from changes in the passive cable properties of the myelinated fibres by altering the mode of conduction along the demyelinated fibres. Such changes are substantially determined by the extent of demyelination. For instance, Rasminsky and Sears (1972) demonstrated that the internodal conduction time along the diphtheria-induced demyelinated fibre could be increased from approximately 20 ms in normal myelinated fibres to nearly 500 ms. Basically, the saltatory conduction (see 1.2.3.) characterising the myelinated fibre is changed into a mixture of saltatory and continuous conduction. When the myelin sheath is only partially damaged or has partially remyelinated, the excessive transverse current leakage crossing the damaged myelin sheath following the reduction in resistance, increase in capacitance and decrease in the overall insulation of the internodal myelin limits the amount of current flowing forward axially towards the next node. If the current delivered to the next node is insufficient to depolarise the axon to threshold for excitation, conduction block may occur. In addition, when the myelin is collapsed completely, conduction can only be maintained in the continuous mode. However the

current delivered to the bare axon is usually insufficient to depolarise it because of the low density of Na^+ channels in the internodal segments (Ritchie and Rogart, 1977; Waxman, 1977), and the exposed voltage-dependent K^+ channels interfere with conduction by holding the demyelinated membrane potential to the potassium equilibrium potential causing membrane hyperpolarization (Bostock *et al.*, 1981; Ritchie and Chiu, 1981). In focally demyelinated fibres, these conduction abnormalities are confined to the zone of demyelination, with regions proximal and distal to the demyelination behaving relatively normally. Temporal dispersion or loss of synchrony may occur because of the significant variation in internodal conduction time between normal and demyelinated segments in a nerve fibre or between neighbouring demyelinated fibres in a CNS tract, which may cause failure in functions that require synchronous discharge. Conduction block in the demyelinated fibres can also be frequency-related, with low-frequency action potential trains being conducted reliably and high-frequency impulse trains failing to propagate. The refractory period for repetitive impulse transmission of the demyelinated fibres is prolonged due to progressively decreased generation of inward membrane currents at nodes, which may in turn be a result of intracellular sodium accumulation during repetitive activity (McDonald, 1963; McDonald and Sears, 1970; Rasminsky and Sears, 1972). This increase of the refractory period of transmission is determined by the most severely affected part of the fibre rather than the average extent of demyelination along the length of the fibre.

Conduction abnormalities can also be due to hyperexicitabilities in demyelinated fibres, since abnormal currents may be generated in or around the demyelinated

segment of nerve fibres. These abnormalities can be described as (1) prolonged spontaneous activity (Eberstein *et al.*, 1975; Smith and McDonald, 1980), in which spontaneous activities of demyelinated fibres become hyperactive; (2) ultrasensitivity to mechanical stimuli which would normally not be sufficient to excite myelinated fibres (Howe *et al.*, 1976; Smith and McDonald, 1980); (3) abnormal transmission across fibres (Rasminsky, 1978); or (4) impulse reflection, in which antidromic impulses are reflected at sites of complete demyelination and interfere with the normal orthodromic conduction (Goldstein and Rall, 1974; Howe *et al.*, 1976). These hyperexcitabilities of demyelinated fibres are directly related to the change of permeability properties of the myelin sheath as the consequence of morphologic change, with or without a direct action of the demyelinating factor on the permeability of the axon membranes.

In addition, conduction in demyelinated nerve fibres is more sensitive to metabolic and pharmacological influences than in normal myelinated fibres. For instance, temperature decreases in the physiological range can cause complete blockage of conduction in a partially demyelinated fibre (Low and Mcleod, 1977). This is because ion channels, present in both the nodes and the demyelinated internodal segment of the axon and controlling both the current flowing forwards to the next node and the current leaking across the damaged myelin sheath, become more susceptible to metabolic and pharmacological manipulation. For instance, conduction block in demyelinated fibres can be reversed by even small increases in temperature as a result of the temperature dependent channel kinetics (Rasminsky 1973; Sears and Bostock, 1981). Changes in acid-base balance induced by intravenous bicarbonate or oral

phosphate or by hyperventilation can result in significant transient alterations of neurological status in MS patients (Becker *et al.*, 1974; Waxman and Geschwind, 1983). Application of fast K^+ channel-blocking agents in demyelinated nerve fibres has been demonstrated to effectively reverse conduction block (Bostock *et al.*, 1981; Targ and Kocsis, 1986; Blight, 1989; Davis *et al.*, 1990), and blockade of Na,K-ATPase has also been demonstrated to influence conduction block in demyelinated fibres (Kaji and Sumner, 1989; Kaji *et al.*, 1990; Kaji and Kimura, 1991).

1.3.2. Components of myelin breakdown products. Components of myelin breakdown products are mostly the degraded myelin constituents including lipid, proteins or enzymes released from the myelin sheath during demyelination into the extracellular space. Given the heterogeneous distribution of the myelin structural proteins in the intracellular and extracellular appositions of myelin sheath, the amount of specific degraded myelin proteins released can vary depending on the demyelinating patterns. As a consequence of breakdown of the myelin sheath, those myelin structural proteins, lipids or enzymes could be eventually released to the surrounding extracellular space. They may then pass to the cerebrospinal fluid, and then to other peripheral body fluids through the blood-brain barrier including the blood-brain, brain-CSF or CSF-blood barriers (Whitaker and Snyder, 1982).

The major myelin structural proteins of PLP and MBP may be present as intact protein, peptide fragments, or may be in a lipid, protein, or nucleic acid complex in the CSF. It is not clear how those proteins circulate across different compartments of the body fluid, including the cerebral extracellular space, CSF, blood plasma, and urine.

PLP (Trotter *et al.*, 1980), MBP (see 1.5.2.), cholesterol (Nicholas and Taylor, 1994) and Brain 2',3'-cyclic nucleotide 3'-phodphodiesterase (Sprinkle and Mckhann, 1978; Banik *et al.*, 1979) have been found in either the CSF, plasma or urine samples. Other products which are non-specific to demyelination, such as glial fibrillary acidic protein from astrocytes (Hayakawa *et al.*, 1979) and another glial marker S-100 (Michetti *et al.*, 1979) may appear in the CSF in acute bouts of demyelination.

In some chemically-induced central myelinopathies, fluid is accumulated within the myelin sheath. The composition of the intramyelinic fluid implies its origin is either plasma or CSF. However, in most instances, the fluid accumulated between myelin lamellae or in the places in myelin sheath where cytoplasm remains, *i.e.* inner, outer and paranodal loops of oligodendrocyte according to their locations, is not in contact with the extracellular space, and although the intraperiod line represents the external leaflets of the cell, it is sealed by the tight junctions at the inner, outer and paranodal loops (see 1.2.1.). This fluid is accumulated by either the dysfunction of the non-energy consuming chloride-hydroxyl ion and water exchange across the biological membranes or the increased membrane permeability induced by complement-dependent attack (see 1.2.4.).

1.3.3. Pathological features. Pathological studies of demyelination have been carried out in many demyelinating conditions. Although each specific demyelinating lesion has its own pathological pattern, the general features of demyelination are highlighted here. Two pathological core features are (1) the presence of myelin vacuolation and (2) loss of myelin sheath. Other commonly associated pathological features include

damage of myelinating cells and cellular infiltration; and degeneration of axon. Chemically-induced central demyelination is mainly reviewed here in comparison with the immune mediated central demyelination, which covers most of the features seen in demyelination resulting from other causes.

Demyelination can be induced by exposure to a wide variety of myelinotoxic compounds. These compounds cause demyelination by damage either directly to the myelin sheath, such as triethyltin and hexachlorophene, or to the myelin sheath and oligodendrocyte, such as cuprizone and lysolecithin (see 1.4.1.). The common features of chemically-induced demyelination are:

(1) Myelin disruption usually starts from the splitting of the myelin sheath, a process whereby the myelin sheath is separated along either the intraperiod or major dense lines by accumulation of fluid within the myelin sheath or a myelinlytic factor, which may proceed to demyelination. When the demyelinating factor acts from the extracellular space, the myelin splitting starts and spreads centripetally along the IDL, while demyelinating processes may begin in the MDL and spread centrifugally when the myelinolytic factor is located in the cytoplasm of the oligodendrocytes (Lowenthal, 1991; Wolman, 1992). Splitting of the myelin sheath reflects the loss of compaction in either the intraperiod line or the major dense line due to loss of myelin structural proteins of PLP or MBP, accompanied by accumulation of fluid within myelin lamellae in variant extent. Myelin sheath vacuolation usually occurs along the intraperiod line and in the loops of oligodendrocyte. Loss of myelin structural proteins and damage to the tight junctions at the inner, outer and paranodal loops would directly contribute this pathological process, and could also be considered as sensitive

non-specific indicators of oligodendrocyte malfunction (Verschoyle *et al.*, 1992). In some cases, vacuolation could be the only form of myelin disruption, which is usually reversible. In other situations such as cuprizone intoxication, vacuolation appears prior to, or accompanies, demyelination, i.e. actual loss of myelin sheath.

(2) Loss of myelin is usually presented as decrease in myelin density in an unit area or thinned myelin sheath accompanied with vacuolation and vesicular disintegration of myelin sheath. In the extreme case, the demyelinated area is described as status spongiosus of white matter (Lampert and Garrett, 1971) or myelinolysis (Adams *et al.*, 1959; Harris *et al.*, 1993). Loss of myelin sheath can also be determined by directly observing the broken myelin lamellae or bare fibres within the nerve trunk in most demyelinating lesions.

(3) Damage to oligodendrocytes can be typically found in cuprizone intoxication (Blakemore, 1972; 1982). At about the same time as myelin splitting at the intraperiod line, oligodendrocytes begin to be shrunken with degeneration of mitochondria, loss of ribosomes, condensed microtubules, cytoplasmic swelling of the inner loop. In some cases, although the morphological changes of oligodendrocytes are mild, the malfunction of those oligodendrocytes contributes to the process of breakdown of myelin sheaths.

(4) Infiltration of macrophages and astrocytes. Areas of active demyelination can be heavily invaded by macrophages and astrocytes. Macrophages take up the degenerating myelin sheath, which appears as extensive ruffling of peripheral cytoplasm. Myelin fragments are often taken up into small vesicles which will be quickly transformed to droplets of neutral fat. Astrocytes are also involved in the

removal of degenerating myelin sheaths, as shown by their hypertrophy at the time of myelin breakdown and the presence of droplets of neutral fat within their cytoplasm.

(5) Occasional axonal degeneration occurs in the demyelination induced by either lysolecithin or ethidium bromide. In comparison, the immune mediated demyelination, typically seen in the experimental allergic encephalomyelitis (EAE, an experimental model, induced by myelin-specific antigen and mediated via the cellular and humoral immune mechanisms, for simulating both the inflammatory and demyelinating processes that occur in multiple sclerosis), has variable perivascular demyelination and an additional of perivascular inflammation with mononuclear cells. Opening of the blood-brain barrier (BBB, powerful homeostatic mechanisms to stabilize the composition of the cerebral interstitial fluid against variations in composition including epithelial cells of cerebral capillaries, glial cells around the capillaries, and tight junctions between adjacent cells) is an early and significant event in acute EAE (Glynn and Linington, 1989; Owen and Sriram, 1995) and more responsible for the conductive dysfunction than demyelination.

1.3.4. A common mechanism of demyelination?

Demyelination can be induced by numerous causes (as listed in 1.3.), and the precise mechanism by which the myelin actually degraded is not always clear. Some key events have been proposed following work implicating various effective molecules in both experimental and clinical myelinopathies, and they are highlighted here.

(1) Proteolytic process. Proteolytic enzymes, e.g. neutral and acid proteases, are mainly associated with macrophages but also localized to glial cells present in the plaques of multiple sclerosis (MS, a chronic neurological disease of unknown

aetiology, characterized in its early phase by a cellular immune response and later by multiple areas of demyelination or plaques in the CNS white matter) brain samples, and also described in other demyelinating diseases (Banik, 1992). Myelin vesiculation or dissolution in the extracellular or cytoplasmic appositions may occur as consequences of the proteolysis of PLP or MBP, respectively. Dissociation of myelin sheath and axon may be caused by proteolysis of the MAG or MOG.

(2) Myelin attack complex (or terminal complement complex) produced by macrophages may directly damage membranes at the outermost lamellae or the loops, leading to extracellular proteolysis of PLP and MAG, and increases in membrane permeability. Thus, further intracellular damage can result from influx of extracellular proteases and calcium (Compston *et al.*, 1991). Similarly, if Ca^{+}-dependant phospholipase activities are activated at the cytoplasmic apposition in the myelin loop areas, then entry of extracellular fluid and calcium could also provoke dissolution of the lipid matrix from within. This could expose MBP sitting in the cytoplasmic apposition to the action of extracellular macrophage-derived proteases.

(3) Ions play important roles in demyelination, in which phospholipase activities damaging both the oligodendrocytes (Scolding *et al.*, 1992) and the myelin sheath (Smith and Hall, 1988; Maxwell *et al.*, 1995) are Ca^{+}-dependent. The oligodendrocyte carbonic anhydrase II is zinc-dependent enzyme. Specific binding of zinc to MBP is evident (Riccio *et al.*, 1995), and such binding may either co-ordinate binding between PLP and MBP (Earl, *et al.*, 1988), or facilitate the interaction of MBP with lipid and have a role in stabilizing the myelin sheath (Cavatorta *et al.*, 1991) or inhibit MBP proteolytic breakdown in the CNS (Liuzzi *et al.*, 1991). Zinc deficiency affects myelination (Liu *et al.*, 1992). Rapid correction of serum sodium levels is reported to

be responsible for central pontine myelinolysis (Adams *et al.*, 1959; Harris *et al.*, 1993).

(4) Oxygen radicals are well known to cause cell injury and thought to cause myelin breakdown via peroxidation of lipids (Griot *et al.*, 1990).

(5) Other proteins like γ-interferon (Olsson, 1992) and tumour necrosis factor (Selmaj *et al.,* 1991; Hershviz *et al.*, 1993) are thought to be involved in either central or peripheral demyelination as well.

1.4. Animal models of chemically-induced myelinopathy.

Intoxication by myelinotoxic compounds is an important cause of demyelination. Animal models of chemically-induced myelinopathy *in vivo* or *in vitro* continue to play important parts in investigating mechanisms (Cammer, 1980; Blakemore, 1982; Wolman, 1992; Ludolph and Spencer, 1995), validating diagnostic methods (Le Quesne, 1987; Nicholas and Taylor, 1994; Ford *et al.*, 1990; Dousset *et al.*, 1995), and evaluating the effectiveness of possible therapeutic intervention in demyelinating diseases (Blakemore *et al.*, 1994; Fressinaud and Vallat, 1994; Demura *et al.*, 1995; Schwab, 1995; Honmou *et al.*, 1996). An overview of demyelinating compounds is introduced in the early part of this section (see 1.4.1.), and followed by detailed reviews of four well characterized rat models of either the widespread or focal central myelinopathies induced by triethyltin, lysolecithin, cuprizone and diphenamid. Some of these animal models were reproduced and employed in the experiments presented in Chapter 4, 5, and Appendices.

Table 1-1. Classification of demyelinating toxins.

Chemicals which induce primarily damage the myelin sheath.

- Organotins (e.g. triethyl tin, TET; trimethyl tin, TMT *)
- Hexachlorophene (2,2'-methylenebis(3,4,6-trichlorophenol), HCP)
- Tetralin (acetyl ethyl tetramethyl tetralin, AETT)
- Isoniazid (isonicotinic acid hydrazide, INH)
- Salicylanilides
- Cyanate
- Ethylnitrosourea (ENU)

Chemicals which damage myelinating cells and myelin sheaths.

- Lysolecithin (lysophosphatidyl choline, LPC)
- Lead
- Tellurium
- Cuprizone (biscyclohexanone oxaldihydrazone)
- Diphenamid (N,N-Dimethyl-2,2-diphenylacetamide)
- Hypocholesteremic agents (20,25-diazacholesterol; AY-9944)
- Ethidium Bromide
- Diphtheria toxin
- Pyrithiamine
- Suramin
- Arsenic
- Nitrous oxide
- Cyanide*
- Carbon Monoxide*

(Based on Wendy Cammer. Toxic Demyelination: Biochemical studies and hypothetical mechanisms. Chapter 17. In: Experimental and Clinical Neurotoxicology, pp239-256, edited by P. S. Spencer and H. H. Schaumburg, Williams and Wilkins, Baltimore/London, 1980; and Ludwig Gutmann. Metabolic-toxic neuropathies. Current Opinion in Neurology and Neurosurgery 1991; 4:707-711.).

* mainly neurotoxic with minor demyelinating action.

Table 1-2. Myelinotoxic chemicals with effects on the CNS, PNS or both.

MYELINOTOXIC AGENTS	CNS	PNS
Hexachlorophene	+	+
Tetralin	+	+
Isoniazid	+	±
Salicylanilides	+	+
Cyanate	+	+
Lysolecithin*	+	+
Diphtheria toxin	+	+
Arsenic	+	+
Ethylnitrosourea	+	?
Pyrithiamine	+	?
Diphenamid	+	?
Organotins	+	-
Cuprizone	+	-
Hypocholesteremic agents	+	-
Ethidium Bromide	+	-
Cyanide	+	-
Carbon Monoxide	+	-
Tellurium	-	+
Lead	-	+
Suramin	-	+
Nitrous oxide	-	+

* not a systemic demyelinating toxin (local injection only).

1.4.1. Classification of demyelinating chemicals. Demyelinating chemicals can be classified into two categories according to their postulated primary site of damage: (1) Primarily damage to the myelin sheath without affecting the myelinating cell, and (2) damage to both the myelinating cell and myelin (Table 1-1). Those compounds are introduced into the nervous system either by direct injection or via systemic intoxication. In the latter case, chemicals have to go through the blood-brain barrier. If the compounds are small in molecular size and lipid soluble, they cross the BBB in a free diffusion fashion, and enter the nervous system without disturbing the blood-brain barrier. Table 1-2 shows the different chemicals with effects on the CNS, PNS or both. Systemic intoxication usually induces myelinopathies with a widespread pattern of damage in the nervous system. However, exceptions exist. For instance, orally dosed diphenamid in young female rats induces focally reversible myelinopathy limited in the cerebellum (see 1.4.5.).

1.4.2. Myelinopathies induced by TET. Some organotin compounds are widely used in agriculture, industry, and occasionally have been used in medical practice. Many of them are shown to be highly effective bactericides and antiparasiticides, mostly lower trialkyltin such as tributyl-, triphenyl- triethyl-, and trimethyl-tins. Despite extensive usage in the last century, their neurotoxic effects were only discovered following the poisoning of a large number of people in the 1950s, and were then studied in experimental animals. In 1954 a proprietary preparation contaminated with triethyltin was sold in France for treatment of staphylococcal skin infections. More than 200 people were poisoned, of whom 100 died. The most common symptom of poisoning was severe and persistent headache accompanied by raised intracranial pressure. A

striking oedema of the white matter of the brain was found at autopsy (Alajouanine *et al.*, 1958). In the laboratory, rats were the most common animals used to study the toxicity of TET *in vivo* in the past. Intoxication was produced by a number of routes, such as orally, intraperitoneally, intravenously, or intraventricularly. The toxic effects of TET are strongly dose-dependent, the actual amount accumulated in the brain being directly related to the dose (Leow *et al.*, 1979; Rose and Aldridge, 1968). Therefore, acute, subacute, and chronic myelin disruption may be produced by varying the dosage and the time period of dosing. Previous observations of TET intoxication in rats are reviewed here according to acute, subacute and chronic intoxication with emphasis on selecting the most suitable *in vivo* model for experimental evaluation of the proposed monitoring methods (see 1.1.).

Acute intoxication with TET. Most of the acute intoxication of TET was carried out by a intraperitoneal single-dose of up to 10 mg/ml (approximately 2 x LD50). Magee and his colleagues (1957) intraperitoneally injected 10 mg/kg body weight of TET sulphate dissolved in saline in rats, which produced a generalised progressive weakness from which the rat died within 5 days. Streicher (1962) administered 8 mg/kg of TET hydroxide to rats by a single intraperitoneal injection, and observed toxic signs (weakness of the hind limbs, dyspnea, and peripheral vasodilatation) in 30 minutes. Torack and associates (1970) injected TET sulphate at doses of 4, 7, 8, and 9 mg/kg. At a 9 mg dose, the rats became severely ill and did not survive past 18 hours. With a 4 mg dosage, rats failed to manifest any functional abnormalities up to 24 hours. At 7 and 8 mg dosages, the rats showed biphasic symptoms: first, they became lethargic within 15 - 30 minutes, they revived after 3 hours, but at 12 hours, they again

became lethargic, developing weakness of the hindlimbs, and finally lapped into a stupor. Ruppert *et al.* (1983) dosed rats by single intraperitoneal injection of TET bromide at doses 0, 3, 6, or 9 mg/kg, there were no treatment-related deaths at doses of 0, 3, or 6 mg/kg. However, the overall mortality was 52% in the group of 9 mg/kg, and the majority of deaths occurred 8 - 11 days after injection. There was no sex difference in mortality. Pluta and Ostrowska (1987) demonstrated that 12 hours after intraperitoneal injection of triethyltin at 2.5 mg/kg, slowness of movement was noted in the rats. At 48 hours, the clinical state of these animals approached normal. In the animals receiving triethyltin at 9 mg/kg, additional symptoms of drowsiness were noted. Strong, painful stimuli (pinching of the ear) caused short-term, delayed, and lethargic motor reactions, and finally they died with severe brain symptoms, intensified paresis, and *paralysis* of the hind legs. In comparison with single *i.p.* dose, Studer *et al.* (1973) administered TET bromide intraperitoneally at dose rate of 1.25 mg/kg, daily, for seven days. 9 of 34 animals (29%) died. Leow *et al.* (1980) reported that at dose rate of 10 mg/kg body weight, *i.v.* injection of TET chloride via the tail vein produced immediate collapse, muscle weakness and flaccid paralysis (hindlimbs worse than fore). Although the rats recovered slightly at 3 hours, thereafter their condition deteriorated and they died within 2 - 3 days. Jacobs and co-workers (1977) injected rats intravenously at dose rates of 10 mg/kg and 20 mg/kg TET sulphate in normal saline. Immediately after the injection, respiration of the rats became very rapid, the rats usually remaining still or becoming almost comatose; however, when prodded they were able to move about slowly. Another dosing route of intraventricular injection of TET chloride at dose rate of 100 - 200 μg/kg was reported by Leow *et al.* (1980). The most common neurological sign of paralysis of the hind limbs did not

appear at 30 - 60 minutes after the injection when the rats recovered from the light anaesthesia with ether.

The systemic and neurological effects of the acute intoxication of TET were highly dose-dependent (Leow, *et al.*, 1980; Torack, *et al.*, 1970; Howell, 1982; Pluta and Ostrowska, 1987). Systemic blood pressure rapidly declined mainly because TET directly dilated the peripheral vessels. At a dose rate of 10 mg/kg *i.v.* injection, blood pressure fell to 60 mm Hg followed by a recovery to normal within 0.25 - 0.5 hour and heart rate also fell from 200 to 110 beats per minute for 2 - 5 minutes. The body temperature, after *i.v.* injection of TET at a dose of 5 mg/kg fell 2 - 3 °C, then remained stable for some hours but eventually returned to normal within 24 hours; at a dose of 10 mg/kg, body temperature fell between 5 and 6°C within 120 minutes and then remained stable at this reduced temperature until the rat died. Rats were unable to shiver during the first hour. Rapid respiration and dyspnea occurred within 30 minutes. Pluta and Ostrowka (1987) found that TET at 2.5mg/kg caused systemic hyposia and acidosis at 12-48 hours and a 30% fall in cerebral blood flow at 12-24 hours. At 9mg/kg these effects were seen at 12-24 hours. Neurologically, weakness of the hind limbs was a leading sign at low dosage intoxication. When the *i.p.* or *i.v.* dosages were at the range of 9 - 20 mg/kg, immediate paralysis of most muscles (Magee, *et al.*, 1957) appeared, and coma (Jacobs, *et al.*, 1977), or convulsions (Leow, *et al.*, 1980) also occurred at high dose. Pathological observations shown that small numbers of intramyelin vacuoles formed by splitting of myelin at the intraperiod line, were seen 2 hours after an *i.p.* dose of 10 mg/kg and from 1 hour after 20 mg/kg. there was a progressive increase in the number and size of the vacuoles over the time

interval. Vacuoles were found in all parts of the brain and spinal cord containing white matter. Longitudinal sections of optic nerve at 6 hours after TET showed the myelin vacuoles to occupy only a small proportion of the internodal length. The greatest increase in myelin vacuole area took place between 6 and 15 hours. No intramyelinic vacuoles were found in peripheral nerve fibres coursing through the 5th nerve ganglion, or in the associated Schwann cell-covered root fibres at any time interval after intravenous injection of TET; neither were any changes seen in the retina of rats 42 hours after injection (Jacobs *et al.* 1977). Leow *et al.* (1979) observed that vacuoles were present in the optic nerve 3 hours after *i.v.* injection, and between 3 and 12 hours the number and size of vacuoles increased. At 48 hours, most vacuoles had become very large and counts of the number of axons in a fixed area of optic nerve showed the treated nerve contained less than half the number of axons than a control nerve. The water content of the brain tissue increased linearly between 6 and 24 hours after injection. During the first 6 hours, only the forebrain showed a small gain in water content. On the other hand, the medulla and spinal cord gained twice as much water (per gram of tissue) as the forebrain over 48 hours. A rapid transient increase in the CSF pressure occurred immediately after *i.v.* injection of TET. The pressure was increased by 50 mm of water and this increase lasted for about 2 - 5 minutes before returning to normal for the remaining 2 hours of the recording. No cellular damage or axon degeneration was found.

Subacute intoxication with TET. Oral administration of TET added to animal's diet or drinking water for a short period of a few weeks produce less dramatic and more reversible effects compared with *i.p.* or *i.v.* injection. Magee *et al.* (1957)

administrated TET hydroxide, dissolved in arachis oil and added to the powdered diet. The first effect of adding 20 parts per million (p.p.m.) TET hydroxide to the diet was a reduction in the amount of food eaten. The first neurological symptom was that the rats had difficulty manipulating their hind limbs and this appeared after 7 - 9 days on the diet. By this time, the rat had consumed about 1.0 mg TET hydroxide per 100g initial body weight. The initial weakness of hind limbs was progressive, until after 14 days the hind limbs were dragged motionless as the rat moved about the cage with the aid of its fore limbs. By this time, the total amount of TET hydroxide consumed was about 12mg/kg initial body weight. The feet were usually pink and the hind limbs would be withdrawn if pinched. The condition of the rat then deteriorated rapidly. The paresis extended to the forelimbs and finally the rat lay on its side unable to move. If the rats were kept on this diet containing 20 p.p.m. TET hydroxide about two thirds of them died during the third week. The survivors began to recover a few days after changing to 10 p.p.m. TET. They ate better; their general and neurological condition improved with the increase in weight. After about 6 weeks, although still on a diet containing 10 p.p.m. TET hydroxide, the rats appeared remarkably normal. Bakay (1965) treated rats with 20 p.p.m. of water as drinking water plus TET mixed with their food. The rats were killed and fixed during 10 - 18 days on diet. The first neurological signs developed 7 - 10 days after the beginning of TET feeding, similar to those described by Magee *et al.* (1957), and were characterized by weakness of the hindlegs. General symptoms included loss of weight, diarrhoea, and in the more advanced and terminal state, protrusion of the eyeballs and frothing at the mouth. Interruption of TET-feeding and return to a normal diet was compatible with complete clinical recovery within 3 days, even in animals that were severely paralysed, no

neurological abnormality could be found eventually. Graham *et al.* (1973), Amochaev *et al.* (1979), and Magos *et al.* (1986) gave their rats drinking water containing 20 mg of TET sulphate per litre. All of the animals showed evidence of motor dysfunction between the 10 - 17 days of intoxication. Some of them became too incapacitated to feed or take water before day 22. A slightly higher dose of TET bromide, 30 mg/litre in drinking water and food, was employed by Richman and Birkamper (1984) for their histological study. Hindleg weakness was observed by 1 week; by 3 week hind legs had become paralysed. Distension of the urinary bladder was noted in some treated animals after 3 weeks. Recovery at the end of 3 weeks dosing appeared grossly. Smith and co-worker (1960) administrated TET hydroxide to rats at the higher dosage of 40 p.p.m. and 80 p.p.m. in drinking water. The animals became quadriplegic and died between 10 and 14 days. Functional recovery of survivors occurred when the TET was removed. Lee and Bakay (1965) used 40 p.p.m. of aqueous TET hydroxide in the drinking water; it was also spinkled on food. Paraplegia developed on day 7, quadriplegia on the day 9, and somnolence, emaciation and death on the day 15 - 17. When TET feeding was discontinued and a normal diet resumed, functional recovery was completed in five days. Squibb *et al.* (1980) dosed the rats by lavage twice per week with 15% ethanol containing TET bromide at dose levels of 1.0, 2.0, or 3.0 mg/kg. Severe toxic signs had appeared in the 3.0 mg/kg dose animals after second dose of TET. After the third dose of TET these toxic signs appeared to a lesser degree in the 2.0 mg/kg dose group. No toxic signs were seen in the 1.0mg/kg dose animals. One of the most obvious general symptoms of rats with subacute intoxication of TET was the progressive loss of body weight caused by the toxic effect of losing appetite and, to a greater extent, by loss of eating ability as a consequence of muscular

weakness. Neurologically, the rats developed hindlimbs weakness, followed by quadriplegia, tremor, or terminal convulsions. However, the above symptoms were reversible if TET feeding was discontinued and a normal diet resumed. Functional recovery could be completed within a few days later (Magee *et al.*, 1957; Bakay 1965; Smith *et al.*, 1960; Lee and Bakay 1965).

Chronic intoxication with TET compounds. If the TET intoxication is maintained for more than 8 weeks, this enables the toxic lesion to become fully developed and irreversible. Magee and colleagues (1957) had rats on a diet containing 20 p.p.m. TET for 2 weeks followed by 6 weeks on a diet with 10 p.p.m. and found that, after this period, no further clinical improvement could be obtained by restoring them to the normal diet. Eto and co-workers (1971) administered TET to rats in drinking water at 5 p.p.m. for initial 15 days, and then a dose rate of 10 p.p.m. for following 15 days. From day 30, the concentrations of 5 and 10 p.p.m. were altered at 5-day intervals to prevent death. The paralysis of rats started on day 12, and progressed slowly thereafter.

In summary, the most common pathological features of TET intoxication are that oedema fluid accumulates between myelin lamellae which splits along the intraperiod line (a very early event) and that vacuoles begin to appear to begin in the outer lamellae of the sheath and move inwards towards the axon with time. Oedema distributes to wide regions of the brain, brainstem, cerebellum and spinal cord with a high dose, the brainstem being the most vulnerable area. No preceding changes could be found in either type of glial cell or in the extracellular space. The mechanism by

which myelin becomes vacuolated in TET intoxication remains obscure, Direct application of TET by either intracerebral injection or adding the compound to cultures of mouse spinal cord suggested that it acts directly on myelin and, in the latter case, indicated that TET is the neurotoxic agent and not a metabolite.

Several possible mechanisms of TET intoxication have been proposed:

(1) It is a result of the non-energy-consuming catalytic process of chloride-hydroxyl *ion exchange* across the biological membranes with accompanying inflow of water molecules. This is supported by the complete absence of any consistent ultrastructural mitochondrial changes in the presence of intense vacuolation (Aldridge *et al.*, 1977; Brown *et al.*, 1979; 1984).

(2) It results from the uncoupling or inhibition of mitochondrial oxidative phosphorylation required by the energy-requiring pumps to maintain fluid and electrolyte gradients across cell membranes (Aldridge, 1976; Aldridge and Street, 1976).

(3) There is direct binding of TET to a component of the ATP synthase complex of the cellular respiratory chain (Snoeij *et al.*, 1987).

Is there myelin breakdown in acute TET-induced myelinopathy? The answer is most likely no because there is no evidence of any detectable myelin breakdown products in either the intramyelinic or extracellular fluid. However, the loss of myelin lipid in the damaged tissue is only moderate, while the total amount of myelin is reduced (Eto *et al.*, 1971). In addition, myelin isolated from oedematous tissue separates into a normal and a "floating" fraction. The latter is presumed to be partially deproteinated myelin

(Smith, 1973). There is evidence of increased synthesis of the three myelin structural proteins: basic, proteolipid protein and Wolfgram protein (Smith, 1973), which may imply that this increased synthesis of myelin components is a response to the breakdown, a suggestion supported by evidence of increased expression of MBP-mRNA response to the TET intoxication (Veronesi *et al.*, 1991).

In conclusion, the acute *i.p.* injection of TET in the rat induces severe systemic and neurological symptoms and myelinopathies in wide regions of the brain which, at lower doses (≤ 8mg/kg), are reversible, but at higher doses (> 8mg/kg), may produce death. In contrast, chronic intoxication of TET over period of more than 8 or 10 weeks leads to mild but irreversible neurological deficits and axon degeneration. In between, subacute TET intoxication induces less severe symptoms, and the neurological deficits can be reversed after withdrawal of TET. The acute TET intoxication produced by a single *i.p.* injection at a dosage of 8 mg/kg which would induce a severe but reversible myelinopathy in wide regions of the white matter involving the brainstem and cerebellum seemed an ideal model for the present study.

1.4.3. Acute focal demyelination induced by LPC. It has been well demonstrated that focal acute demyelination in both the peripheral and central nervous systems in a number of species, including mouse (Hall and Gregson, 1971; Hall, 1972), rat (Blakemore, 1976), cat (Blakemore *et al.*, 1977), rabbit (Blakemore, 1978; Foster *et al.*, 1980), and primates (Dousset *et al.*, 1996), can be effectively induced by local injection of microlitre qualities of lysolecithin (lysophosphatidyl choline, LPC) which has a strongly myelinolytic action. Unlike many of the other myelinotoxic agents, LPC

disrupts the myelin sheath without producing intramyelinic oedema. The myelinolytic activity of LPC has also been demonstrated in a wide range of nervous structures in both the peripheral and the central systems. Microinjection of LPC into the sciatic nerve, in addition to the tibial and sural nerve (Sedal *et al.*, 1992), is a commonly used PNS model (Hall and Gregson, 1972; Low *et al.*, 1983; Griffin *et al.*, 1989). In addition to a number of studies in which focal demyelinating lesions were induced by LPC in the dorsal column of the spinal cord (Hall, 1972; Blakemore, 1976; Gilson and Blakemore, 1993; Jeffery and Blakemore, 1995), such lesions were also satisfactorily induced in several other locations within the CNS, such as the corpus callosum (Foster *et al.*, 1980), the internal capsule (Ford *et al.*, 1990), the fimbria (Payne *et al.*, 1991), and the centrum semiovale (Dousset *et al.*, 1996). Limited variance among different locations in time course of progression and pathological features of demyelinating lesion induced by LPC injection is evident from those studies. This demyelinating model was applied to study primary demyelination (Hall, 1972; Blakemore, 1976; Ford *et al.*, 1990; Payne *et al.*, 1991) and the subsequent natural remyelination processes (Blakemore *et al.*, 1977; Gilson and Blakemore, 1993; Jeffery and Blakemore, 1995). Recently, studies based on this local demyelinating model were extended to investigations of remyelinating and migratory potential of transplanted glial cells (Duncan *et al.*, 1981; Vignais *et al.*, 1993; Blakemore *et al.*, 1994) and of *in vivo* monitoring using magnetic resonance imaging (Ford *et al.*, 1990; Dousset *et al.*, 1996). Examples of the previous observations of focal demyelination in the CNS induced by LPC injection are reviewed in detail here with emphasis on selecting the most suitable *in vivo* model for experimental evaluation of the proposed monitoring methods (see 1.1.).

In Hall's (1972) experiment of injecting 0.2 µl, 1% LPC into the dorsal white matter of the adult mouse spinal cord, pathological examination after injection showed that there was little initial change in the lamellar pattern of the myelin sheath in the early period. The earliest response of the sheath, occurring within 30 minutes of injection of LPC, was a loss of the previously compact myelin structure, resulting from the splitting of the intraperiod lines. However, by 48 hours, there was some splitting of the sheath, generally along the intraperiod lines, frequently accompanied by the collapse of loops and whorls of 10-nm repeat material into a dilated periaxonal space. Over 72 hours, much of this material disappeared from the extracellular space: the various lamellar forms of degenerating myelin and the membranous elements of disrupted glial cells were all seen within vacuoles in the cytoplasm of macrophages which were present in the area after 24 hours. Further degradation of the components of the sheath was indicated by the large lipid droplets, some of which were membrane-bound, present in these macrophages by the third day. Small whorls of lamellar debris, predominantly 4 - 6 nm repeat material, were also observed infrequently in the cytoplasm of both astrocytes and oligodendrocytes. The axons remained apparently undamaged throughout the period of demyelination, although in many cases, the increased density of axoplasmic organelles, and the irregular axonal outline were indicative of some degree of shrinkage. By day 5, the lesion was sharply delineated, and was bordered by normal myelinated fibres. Extended observation of remyelination by Jeffery and Blakemore (1995) following 2.0µl of 1% LPC injection into the spinal cord showed that demyelination was rapidly followed by remyelination which was first evident at 7 days as a small number of axons in the damaged area were surrounded by very thin myelin sheath. At 10 days clear evidence of both peripheral

and central remyelination, was found in all cords. Oligodendrocyte-type remyelination predominated, and cells with the characteristics of Schwann cells were also found. At 13 and 23 days, myelin sheaths were thicker and only occasional naked axons were detected.

In summary, focal acute demyelination can be induced by injection of a few microlitres of LPC in a number species and locations in both the CNS and PNS. In such demyelinating lesions, both myelin sheath and membrane of myelinating cells were destroyed with prominent astrocytosis but no apparent myelin oedema. Axon degeneration was rare. Demyelination was followed by a spontaneous repair process of remyelination predominantly by oligodendrocytes and Schwann cells. Thus, a rat model of acute, focal, and reversible demyelination induced by LPC of 1% in the cerebellar white matter would provide a suitable model of primary demyelination. Furthermore, together with the model of TET intoxication (reviewed in 1.4.2.), these two models would provide variations in (1) intoxication route (systemic/focal dosing), lesion pattern (wide-spread/focal lesion), pathological status (myelin oedema/myelin breakdown), and recovery process (absorption of oedema/remyelination) for evaluating the sensitivity and selectivity of the proposed *in vivo* monitoring methods of recording the cerebellar AEP and detecting MBP in the CSF (see 1.1.).

1.4.4. Chronic demyelination induced by cuprizone.

Cuprizone (biscyclohexanone oxaldihydrazone) has limited industrial use as a chelating agent in the detection of copper in food products. There are no reports of accidental human or animal intoxication; however, experimental studies have shown it

to be toxic and to result in both CNS and hepatic pathology. Chronic intoxication with cuprizone in mice induces oligodendrocyte degeneration. The extensive demyelination which cuprizone produces in certain areas of the brain has been the subject of considerable interest, and experimental studies have provided much information both on CNS demyelination and the ability of the CNS to be remyelinated because in cuprizone demyelination the axons are all left intact and in place even after a year of intoxication, and consists of relatively mild gliosis between axons (Ludwin, 1994). Most of the studies of cuprizone intoxication were carried in mice (Cammer, 1980), and to a much lesser extent in rats (Carlton 1969; Love 1988 and Purves *et al.* 1991). The previous observations of cuprizone intoxication, well established in mice, are reviewed here with a discussion of the possibility that similar lesions could be produced in a larger animal, the rat, so that lesions could be monitored *in vivo* by implanted CSF cannulae and evoked potential recording electrodes.

Carlton (1966) administered α-benzoinoxime, sodium diethyldithiocarbamate, and cuprizone incorporated into chicken mash diets, each at levels of 0.1 % and 0.5 %, to three groups of mice. The results showed that the α-benzoinoxime and sodium diethyldithiocarbamate were non-toxic even at a level of 0.5 % of the diet and did not induce lesions in the brain. In contrast, cuprizone was found to be extremely toxic when fed as 0.5 % of the diet. Oedema with demyelination, especially prominent in the cerebellar white matter, was observed at both the 0.1 % and 0.5 % levels, but hydrocephalus was restricted to the group of fed 0.5 % of this compound. Pathological and biochemical changes produced by cuprizone in mice have been investigated in some early studies (Suzuki and Kikkiwa, 1969; Kesterson and Carlton, 1971; Hemm

and Carlton, 1971; Blakemore, 1972; 1973a; 1973b; Ludwin, 1978; 1979; 1980; Ludwin and Johnson, 1981; Johnson and Ludwin, 1981) and summarized by Cammer (1980). Gross changes in the mouse brains included hydrocephalus and status spongiosus of cerebellar white matter and the brain stem. Blakemore (1972) identified the demyelinating/remyelinating nature of the lesion seen in cuprizone toxicity. The first microscopic change to be noted in the brain is astrocytic hypertrophy and hyperplasia. Shortly thereafter, the first evidence of degeneration of oligodendrocytes begins (Blakemore, 1972; 1973a) with degeneration of mitochondria, loss of ribosomes, increased microtubules, cytoplasmic swelling, and inner tongue abnormalities. At about the same time, vacuolation of myelin begins with myelin splitting at the intraperiod line. Demyelination is seen between 3 and 4 weeks. Vacuolated myelin is removed and phagocytosed by microglial cells or by a variety of other means. By 5 weeks, almost all axons in the superior cerebellar peduncles are demyelinated. During the course of intoxication, remyelination is rare, but if cuprizone is terminated, remyelination occurs rapidly and by 4 weeks after termination of dosing, almost all axons are re-sheathed (Blakemore, 1973b). Ludwin (1979) carried out an electron microscopic autoradiographic study in cuprizone-intoxicated mice. He discovered that immature glial cells divided 5 to 6 weeks after demyelination and those cells were marked with myelin-oligodendrocyte glycoprotein, MOG and carbonic anhydrase, which distinguished them as oligodendrocytes (Ludwin, 1994). In chronic cuprizone intoxication, however, the initial phase of remyelination after termination of dosing would have disappeared and with continued poisoning of oligodendrocytes, few of these cells or their precursors would be available to commence remyelination when intoxication was stopped (Ludwin, 1980). Once

remyelination has occurred, demyelination can occur again if a cuprizone is added to the diet although the second bout of demyelination is protracted, unlike the first (Ludwin and Johnson, 1981; Johnson and Ludwin, 1981). In this situation, degeneration of oligodendrocytes appears to start within the inner cytoplasmic tongue and it has been suggested that this may indicate a "dying-back" gliopathy, *i.e.,* the most distal part of the oligodendrocyte is most susceptible.

Possible mechanism of cuprizone intoxication: The mechanism of cuprizone-induced demyelination is far from clear. Damage of oligodendrocytes occurred well before demyelination was demonstrated morphologically by some early studies (Blakemore 1972; Ludwin 1978), and then the mechanism of oligodendrocyte damage directly from a loss of oligodendrocyte carbonic anhydrase activity in the affected areas was proposed by Komoly *et al* (1987). In their study, both immunohistochemical and biochemical evidence showed that cuprizone caused a loss or inhibition of oligodendrocyte carbonic anhydrase II (CA II) activity even earlier. They suggested that the reduction in CA II activity in the brain could be due to removal of the zinc ion from the zinc enzyme CA by cuprizone chelating effect. Chelating intracellular zinc, an inhibitor of MBP cleavage (Liuzzi *et al.*, 1991), of the oligodendrocyte by cuprizone may also enhance the proteolytic breakdown of myelin proteins. In addition, involvement of other molecular components, such as MAG and insulin-like growth factor I, have been suggested to play important role in the cuprizone-induced demyelination. Fujita *et al.*, (1990) demonstrated that both forms of myelin-associated glycoprotein (MAG) mRNA decreased markedly during the demyelinating stage and, when feeding with cuprizone was stopped, MAG mRNA began to increase. Komoly *et*

al., (1992) found that high levels of IGF-T during demyelination and IGF-I mRNA during recovery were expressed by astrocytes in the area of demyelination.

Intoxication of cuprizone in rats. Carlton administrated cuprizone at the concentration of 0.5 % which reduced weight gains by about half and 4 of 10 animals died during the experimental period of 8 weeks. At concentration of 1.0 and 1.5%, cuprizone was extremely toxic; the animals did not grow and half of the rats of each group had died by 3 and 4 weeks of dosing. Other signs of toxicity in addition to failure to gain weight included an unkempt fur, but signs of neurological disturbance were not observed. Pathological alterations were very mild in the 0.1 % fed animals, consisting of scattered vacuole formation around the nuclei of the cerebellar white matter. Lesions were most severe in the animals fed 0.5 % cuprizone. Sites of predilection for the lesion extended from the level of the telecephalon to the medulla oblongata and the cerebellum. The site with the most consistent and severe alterations was the white matter around the nuclei of the cerebellar white matter. In the medulla oblongata of a few rats, tissue changes involved the vestibular regions and the descending root of the trigeminal nerve. Lesions were not observed in the cerebral cortex or corpus striatum. In severely affected brains, the tissue changes were consistent with a severe oedema creating a status spongiosus characterised by vacuolar changes in both white and grey matter. With the Kuluver-Barrera preparation for observing myelin, the spongy tissue boarding the cerebellar nuclei and the white matter above dentate nucleus of the rat cerebellum showed reduced staining suggestive of demyelination in those areas. No hydrocephalus was found in experimental animals. In agreement with the above results, recent observations (Love, 1988; Purves *et al.*,

1991) also showed that cuprizone induced myelin damages in rats were very limited. Thus, rats are relatively insensitive to cuprizone intoxication, resistance to which may be enhanced by greater maturity of the brain (Carlton, 1969) as older mice are less sensitive than younger ones to cuprizone. High doses of cuprizone (>0.5% in diet) may be required to induce myelin damage, with the disadvantage that the majority or all of the intoxicated animals may be lost during the initial few weeks because of non-neurological damages.

In summary, chronic intoxication of cuprizone in mice induces extensive demyelination accompanied by oligodendrocyte degeneration, astrocytosis, and status spongiosus in certain areas of the brain. It is a good model for experimental studies on CNS demyelination and the ability of the CNS to be remyelinated. Rats are relatively insensitive to the neurotoxic effects of cuprizone. Only high doses of cuprizone intoxication can induce myelin damage in rats with much more lethal non-neurological damages.

1.4.5. Focal myelinopathy induced by oral intoxication of diphenamid.

The herbicide diphenamid (*N,N*-Dimethyl-2,2,-diphenylacetamide, DPM) is one of a number of dialkylamides which have neuropathological potential. It produces myelinopathy similar to that produced by the insect repellent, *N,N*-diethyl-*m*-toluamide (DEET) but with only moderate CNS hyperexcitability (Verschoyle, *et al.*, 1992). Young female rats are more susceptible. Previous studies (e.g. McMahon and Sullivan, 1965) have showed that, in rats, one or two days after being dosed with diphenamid, oedema fluid accumulates in the inner myelin loop and bilaterally

symmetrical vacuolation of myelinated fibres in the cerebellar roof nuclei occurs with splitting at the intraperiod line, as seen under the light microscope. Similar vacuolation involves the vestibular nuclei and also the reticular formation in some rats, but less severely. Less severe vacuolation is also found in the cerebellar roof nuclei six days after dosing suggesting that the lesions are reversible. No reactive glial or secondary neuronal changes are found in the myelin damaged area at the early stage. A few necrotic neurones with shrunken eosinophilic cytoplasm are seen in the region later.

The mechanism of diphenamid-induced focal myelinopathy is unclear. Diphenamid undergoes N-dealkylation by cytochrome P450 linked microsmal systems, and therefore, it is possible that regional variations in the brain P450 isozyme spectrum may be responsible for its regional selectivity. It is possible that the myelin oedema in the inner loop may be due to the inner loops in the myelin sheaths being the most distal parts of the oligodendrocytes and thus the most susceptible.

In summary, oral intoxication of diphenamid induces fluid accumulation in the inner myelin loop and bilaterally symmetrical vacuolation of myelinated fibres in rat cerebellar roof nuclei. It proves useful as an animal model of localized reversible conductive abnormalities due to myelin oedema in the CNS, but has limited value for monitoring such lesions by detection of myelin breakdown products.

1.5. Monitoring central demyelination *in vivo*.

The CNS is shielded from the outside world by anatomical or functional barriers (e.g. skull or blood-brain barrier, respectively); however, central demyelinating lesions can

be detected outside the barriers by using either a myelin-related signal conducted through the barriers or molecular markers 'leaked' across the barriers broken by the demyelination in the peripheral compartments of the body. Repeated measures of demyelination in the CNS are needed to assess the current status of demyelinating lesions in order to monitor their course including onset, progression, and recovery. Studies in animal experiments are useful in identifying and validating of such monitoring methods, and may complement existing methods which may be ultimately applicable in clinical practice. Three practical approaches of electrophysiological, molecular biological and morphological monitoring can be pursued based on the effect of demyelination on the corresponding properties of myelin and myelinated nerve fibres (see 1.3.). Previous investigations and applications of monitoring demyelinating lesions *in vivo* are reviewed here along with these three approaches, with emphasis on evoked potential recording and detection of myelin breakdown product. The surface-recorded cerebellar AEP, i.e. the evoked potentials recorded from cerebellar surface following auditory stimulus, and radioimmunoassay of released MBP in the CSF were used in this study for monitoring TET or LPC-induced myelinopathies.

1.5.1. Evoked potential recordings. Neural (nerve) pathways can be tested by recording evoked potentials following stimulation of either the peripheral sensors or a group of neurones centrally. The measurement of evoked potentials has established itself as a valuable technique in evaluating neurological disorders or neurotoxicity affecting central pathway transmission (Seppäläinen, 1988; Chiappa, 1990; Jones 1995). Compound action potentials conducted along the nerve, post-synaptic potentials and evoked potentials generated by the receiving neurones or muscles (for

axonal conduction and synaptic transmission, see 1.2.3.) may all be recorded directly by electrodes inserted into the nervous system, and corresponding surface potentials may also be recorded. An understanding of the relationship between neuronal responses and surface field potentials is required for interpreting the surface-recorded evoked potential. This question was extensively addressed in the 1930s and 1940s, while the origin of surface evoked potentials has more recently been reviewed in detail (Mauguière and Binnie 1995). The obvious advantages of surface recording field potential are that the method is (1) non-invasive, (2) easy to repeat in order to follow up the progression of a disorder with low cost, (3) quantitative, and (4) specific to the modality recorded from.

Some special recording techniques of evoked potential are stated here (see Cooper and Binnie, 1995, for a thorough review): (1) Because field potentials are relatively small compared to the superimposed spontaneous activities of the brain and other background signals, the technique of averaging is often applied. In averaging, a computer is used to add the signals produced successively following repeated presentations of the stimulus. The potential evoked by the stimulus is thus increased many times relative to the spontaneous background activity which, not being synchronised to the stimulus, tends to cancel out. The 'signal-to-noise ratio' is increased by the square root of the number of recordings averaged. (2) Field potentials generated along a multisynaptic pathway are usually presented as a superimposed complex of multiple components with different frequencies. In order to highlight the component which is of interest, the technique of signal filtering can be helpful. For instance, the background noise, which has frequency components above and below

frequency range of interest, may be reduced by using filtering. (3) Indices may be selected in evoked potential recording to represent possible conductive dysfunction of the tested neural pathway. Such indices include a decrease in amplitude of one or more components, in which amplitude is presented as the value of either three-point measurement (or baseline to peak) for a monophasic peak, or peak-peak measurement (from the peak of one polarity to the immediately following peak of the opposite polarity) for a biphasic peak. A decrease in amplitude mainly reflects a reduction in excitability of the tested pathway. Another index is the delay in latency of one or more components, in which latency measured from the onset of the stimulus to either the onset (onset latency) or the peak (peak latency) of the wave. Such delay mainly reflects a reduction in conductivity of the tested pathway. A change in latency of an early component indicates a reduction in conductivity in the peripheral stage of the tested pathway. A further index is the prolongation in signal conduction time along a given pathway, which can be calculated by subtracting the latency of an early component from that of a late component as an inter-peak interval. For instance, the central conduction time (CCT, the time interval for nerve impulses to travel along a transmission pathway within the CNS) can be used as a special index for the overall conductivity in a central pathway.

In summary, the evoked potential may reflect changes in both excitability and conductivity of the tested neural pathway. It may also provide further information about which part of the pathway being affected once the origin of each component of the evoked potential has been identified.

Sensory evoked potential measurements. Sensory evoked potentials have been used for many years as a means of estimating development of sensory pathways (e.g. Jewett and Romano, 1972), as a method of diagnosis helping to reveal the cause of neurological defects (e.g. Stockard and Rossiter, 1977; Robinson and Rudge, 1975), and as a means of monitoring the effect of drugs, chemicals, surgery or other influences upon the sensory mechanism (Johnson, 1980; Fox, *et al.*, 1980; Le Quesne, 1982; 1987; Kaji *et al.*, 1990; Chiappa, 1990; Davis *et al.*, 1990). The potentials can be classified, according to the nature of the stimulation applied and the pathway tested, as auditory, visual and somatosensory evoked potentials (Cooper *et al.*, 1995). As far as the CNS is concerned, the SEP reflects not only the conduction of the somatosensory pathway within the cerebral hemisphere but the spinal cord as well (Le Quesne, 1982; 1987). The VEP and AEP have been used to test conduction along the visual and auditory pathways, the AEP having particular application for studying conduction within the brainstem (Jewett, 1970; Shah, *et al.,* 1978; Fabiani *et al.*, 1979; Shaw, 1987; 1992; 1995). The auditory afferents to the cerebellum and the corresponding evoked potential inside or on the surface of the cerebellum are reviewed later in 1.6. with emphasis on the possibility of using the surface-recorded cerebellar AEP as a functional index of cerebellar conduction.

1.5.2. Detection of myelin breakdown products in body fluids. Studies have been performed on detecting myelin breakdown products , i.e. forms of myelin constituents such as MBP, PLP, lipids and 2',3'-cyclic nucleotide 3'-phosphodiesterase, to determine if these substances are present in the CSF, serum or urine and whether their concentrations correlate with massive myelin injury. Among the above biochemical

markers, MBP-like materials derived from MBP are the most sensitive, selective and well characterized marker (Carnegie and Moore, 1980; Cohen, *et al.,* 1980; Whitaker and Snyder, 1982; Williams and Deber, 1993).

Detection of MBP in body fluids. The MBP may be present as intact protein, peptide fragments, or may be in a lipid, protein, or nucleic acid complex in the CSF. How the MBP is released into the CSF through the extracellular space and ependyma, whether and how much of it will appear in a CSF sample taken from a certain region of the CSF circulation, and the magnitude of the clearance and turnover rates of MBP in the CSF circulation are still not completely clear. Among the early studies of MBP, work by Whitaker and his colleagues focused particularly on the development of an immunoassay for detecting MBP and are summarized in their review chapter (Whitaker and Snyder, 1982). Although the sequence of MBP is conserved across species, there is limited immunochemical cross-reactivity for some anti-MBP antibodies which may be of importance when developing antisera for immunoassays to detect MBP in human and different experimental animal models for studying demyelination. Success has been archived in many laboratories using the appearance of MBP-like materials in CSF or other body fluids an index of immune-mediated but not yet chemically-induced demyelinating lesions. The features of MBP-like materials in the CSF are summarized by Whitaker and Snyder (1982) as follows:

1. Index of CNS myelin damage
2. Level related to volume and time of myelin damage
3. Not disease specific
4. Unrelated to the CSF protein or IgG concentration

5. Probably exists as a fragment of basic protein
6. Rapidly becomes undetectable.

Immunoassays employing a carefully selected anti-MBP antibody or antibody to peptides derived from MBP and appropriate radioligands for detection of MBP-like materials in body fluids have been progressively improved in both aspects of selectivity and sensitivity (Whitaker, *et al.*, 1980; Whitaker and Snyder; 1982; Barry, *et al.*, 1990; Whitaker, *et al.*, 1993; Whitaker, *et al.*, 1994) and applied clinically. Application of such a method, however, has been focused on the conditions in which massive demyelinating lesions occurred such as traumatic brain injury (Thomas, 1978), stroke and multiple sclerosis (Whitaker, *et al.*, 1993). Experimentally, it has been applied to detect MBP-like materials in the animal model of the experimental allergic encephalomyelitis (Maugh, 1977; Glynn and Linington, 1989) in which there is a massive immune-mediated demyelination on the surface of the brain and spinal cord. However, it has not been used to detect chemically-induced demyelinating lesions, and there is a major concern that the MBP-like materials released from the immune-mediated and chemically-induced demyelination may be in different formats because of they are produced probably by different demyelinating mechanisms (inflammatory and non-inflammatory) and the cellular processing and paths of degradation process of such products may be different. They could also have different immunoreactivities so that they may not cross-react with the anti-MBP antibody. This is just the gap which the present study was designed to fill in by applying a radioimmunoassay which has been proved to be effective to the immune-mediated demyelination (Barry, *et al.*, 1990) to detect the released MBP-like materials in experimental models of chemically-induced myelinopathies.

Detection of other myelin breakdown products. Other myelin breakdown products or myelin-related markers have been detected from the CSF or urine, which are less specific and sensitive compared to MBP, and are briefly pointed out here. For general descriptions of biochemical CSF analysis, see also reviews by Lowenthal (1991) and Thompson (1995). PLP, another major myelin structural protein positioned at the intraperiod line, has been found in the CSF or serum of approximately 50 per cent of persons with acute-phase MS, but it is neither disease-specific nor consistently associated with myelin damage as the level of MBP-like materials (Trotter *et al.*, 1980), and also has some difficulties in its detection procedure. Antibodies against myelin oligodendrocytes glycoprotein and glycosphingolipid appeared in the CSF from patients with MS (Xiao *et al.*, 1991; Miyatani *et al.*, 1990). Urinary cholesterol metabolites were used to determine the rate of central demyelination with limited specific and selective (Nicholas and Taylor, 1994). Brain 2',3'-cyclic nucleotide 3'-phodphodiesterase is a myelin-related enzyme. Its activity correlates with the appearance of myelin and with the level of MBP. It is hardly detectable in normal CSF, while the CSF from persons with myelin damage, irrespective of cause, frequently has increased enzyme activity (Sprinkle and Mckhann, 1978; Banik *et al.*, 1979). However, this detection is less specificity and sensitivity than the quantitation of MBP for myelin damage. Tumour necrosis factor alpha (TNF alpha) was suggested as an index of demyelination in MS (Maimone *et al.*, 1991), but only found in the CSF of 23% of MS patients. Glial fibrillary acidic protein is from astrocytes, which may appear in the CSF in acute bouts of demyelination. However, it could also be found in CSF samples with brain tumours and strokes (Hayakawa *et al.*, 1979). S-100 is another glial marker. Similar to the glial fibrillary acidic protein, it may provide

information about nervous system damage, but is not specific to myelin injury (Michetti *et al.*, 1979; Nagamatsu *et al.*, 1995).

1.5.3. Computerized imaging systems. Such systems provide the possibility to observe non-invasively the gross morphological changes of brain tissue *in vivo.* Computerised X-ray tomography (CT) or magnetic resonance imaging (MRI), which allows part of the body to be examined by digitally reconstructed images, are currently available methods in clinical practice (e.g. Lee *et al.*, 1991). Compared with methods of recording evoked potentials and detecting myelin breakdown products (see 1.5.1. and 1.5.2.), imaging systems have an obvious disadvantage of high cost.

Computerised X-ray tomography. Demyelination in the CNS can be detected as a low-density lesion by CT images. CT does show the site and size of lesions, which is particularly helpful in case of diagnosing multiple lesions. Enhanced CT imaging with contrast media provides information about possible damage of the BBB. However, it has been replaced to a large extent by MRI in diagnosis of demyelinating disorders because the CT images lack specificity (demyelinating lesions are usually confused with oedema, brain tumours, or even infectious lesions).

Magnetic resonance imaging. MRI provides the most sensitive method for *in vivo* observation of demyelinating lesions in the CNS (Young *et al.*, 1981; Filippi *et al.*, 1995a, b). With a high magnetic field, lesions as small as a few millimetres in diameter may be detected. The acute demyelinating lesion appears as high signal areas in T_2-weighted images, usually associated with oedema components. Myelin lipid can

be detected by using chemical-shift imaging to suppress lipid signals. The high lipid signal, typically bright in T_1-weighted images, disappears several days after the onset of an induced acute demyelination because of clearance of breakdown lipid by macrophages and astrocytes. In gadolinium-enhanced imaging, active demyelination with BBB disruption may be distinguished by enhancement in T_1-weighted images (Offenbacher *et al.*, 1993). Imaging in well-characterized experimental animal models has also been carried out in order to improve imaging techniques (Ray *et al*, 1996), to identify more specific and quantitative parameters for demyelinating lesions and accompanying pathological process, such as changes in the molecular composition or involvement of BBB breakdown (Ford *et al.*, 1990; Dousset *et al.*, 1996).

1.6. The surface cerebellar AEP: An index of cerebellar conduction?

It has been known for more than half a century that the cerebellum receives a variety of sensory afferent signals. The peripheral auditory projection to the cerebellum has been demonstrated in a variety of mammals by depth-recording of single unit activity in the cerebellar cortex (Shofer, 1969; Aitkin & Boyd; 1975) and recording the fine field potentials on the surface of the cerebellar cortex (Snider & Stowell, 1944; Morin, *et al.*, 1957; Highstein & Coleman, 1968; Wolfe, 1972; Lorenzo, *et al.*, 1977). In subdural recordings with fine electrodes, which provides a good spatial resolution of the field potential, the regions responsive to auditory stimuli in cat cerebellum have been identified (Snider & Stowell, 1944; Gilman *et al.*, 1981). More recently, field responses were recorded in rats by placing a gross screw electrode in the skull over the cerebellum (Shaw, 1992). The practical questions still remain whether the surface-recorded cerebellar AEP is an index of conductivity of the cerebellar fibres which are

susceptible targets of several demyelinating agents, and whether this potential could be employed for monitoring myelinopathies involving cerebellar white matter. Some doubts exist. Firstly, as a result of attenuation of field potentials by the high electrical impedance of the dura and the large size of recording electrode, less spatial resolution would be expected in field potentials recorded in the skull with gross surface electrodes than if those recorded subdurally. In addition, such less spatially defined potentials may represent the summation of activities contributed by multiple electrical dipoles of varying size, orientation and depth under the recording electrode within the cerebellum or even from locations in wider range of brain structures along the cerebellar auditory pathway. Secondly, since the cerebellar AEP has not been studied as intensively as either the brainstem or neocortical AEPs, the identity and location of possible generators contributing the gross surface potential are not clear, nor is the precise trajectory of the auditory cerebellar projecting pathway. However, despite all the above doubts, evidence previously obtained by my colleagues (Verschoyle *et al.*, 1992) demonstrated that changes in cerebellar conduction following diphenamid-induced focal myelin oedema in the area of the cerebellar deep nuclei could be detected by recording the cerebellar AEP, which provides the justification for exploring and validating the surface-recorded cerebellar AEP further as an index of impulse conduction in the cerebellum and applying it to the monitoring of both LPC and TET-induced myelin damages in the present study.

1.7. Hypotheses and protocols of the present investigation.

(1) Changes in the surface-recorded AEP provide an index of conductive dysfunction in the cerebellum and will occur following the progression of chemically-induced

myelinopathies involving the cerebellum, although the precise identity of the generator and afferent pathway of auditory input to the cerebellum is still unclear.

(2) Appearance of the released MBP in the CSF following myelin collapse would be detectable by radioimmunoassay even though the nature of the MBP-like materials released from the myelin sheaths following the chemical insult was unidentified, the quantity of myelin released would be smaller than in autoimmune demyelination models, and the CSF samples obtained in small animal experiments are limited in quantity. In addition, information about the effectiveness, selectivity and sensitivity of both quantitative methods could be obtained by comparing the results from two models with lesions varying in location, size and pathological status. If successful, both methods could then usefully be extended to clinical applications provided the corresponding component of the cerebellar AEP and sufficient CSF samples were obtainable from human patients.

In the present series of experiments, the techniques to record the cerebellar AEP from the skull were firstly explored by a number of electrophysiological manipulations (presented as Chapter 3). A previously developed radioimmunoassay for detection of immune mediated demyelination was applied in a rat model of chemically-induced myelin damage. A CSF sampling method was modified (presented in Chapter 2) to increase the long term patency rate of the cannula implanted into the subarachnoid space (the space between the arachnoid mater and the pia mater membranes covering the brain and spinal cord and in communication with the cerebral ventricles, in which the CSF circulates), and the clearance rate of MBP from the CSF circulation determined by injecting MBP of into the normal CSF circulation followed by

measurement of MBP concentration in CSF samples at different time points (in Chapter 4); (2) Rat models of focal demyelination (bilaterally intracerebellar injection of 1% LPC, 2.5μl × 2) and acute wide-spread myelinopathies (intraperitoneal intoxication with TET, 8mg/kg) were reproduced; (3) The LPC (as Chapter 4) and TET (as Chapter 5) induced demyelinating lesions were monitored in surgically prepared animals by observing the systemic and neurological symptoms, repeatedly recording the surface cerebellar AEP and, in some experiments, the surface neocortical SEP, and detecting the appearance of MBP in the CSF by radioimmunoassay. (4) Some pathological data on those lesions were collected. The conclusions drawn from the present investigation and pointers for further studies are finally summarized in Chapter 6.

CHAPTER 2.

EXPERIMENTAL METHODS

This chapter provides a general description of animals, materials, equipment, previously and currently developed experimental techniques, including implantation of cannulae for repeated CSF sampling in small animals, radioimmunoassay of MBP, evoked potential recording, and histopathological and statistical methods used in the experiments described in the present thesis. In addition, specific detailed description of experimental methods is also given, with cross-references, in each chapter.

2.1. Animals: A total of 118 rats were used in the entire study. Among them, 30 male Fisher/344 rats, body weight of 250 - 300 grams were used in the experiments for developing cannula implantation into the cisterna magna for repeated CSF sampling and measuring the clearance rate of MBP from the CSF circulation. Another 24 rats of the same strain and similar body weight were used in the experiments for identifying the surface-recorded cerebellar AEP. 40 more rats of the same strain and similar body weight were used in experiments for monitoring LPC-induced demyelination and TET-induced myelinopathy. 12 male Fisher/344 rats, 90 - 110 grams were used in the experiments with cuprizone intoxication. 12 female Lac:P Wistar derived rats, 150 - 170 grams were used in the experiments of diphenamid intoxication. All animals were bred for experimental purposes and kept in either purpose-built animal rooms or positive-pressure isolators at an environmental temperature of 21±2°C and relative humidity of between 40 - 60%. All animals, except those used in the experiments of cuprizone and diphenamid intoxication, were given free access to food (41B diet) and water (tap water). All experimental procedures applied in the animal experiments were covered by the project licence on "evaluation of mechanisms in neurotoxicology"

(PPL90/00025) and personal licence (PIL 70/08816) granted by the Secretary of State, Home Office, under the ANIMALS (SCIENTIFIC PROCEDURES) ACT 1986.

2.2. Toxic chemicals: LPC, Gamma-O-hexadecyl L-α-lysophosphatidyl choline was obtained from Sigma Chemical Co. (L5016, Dorset, UK), and prepared, in a similar way to that previously reported by Payne, *et al.*, (1990), as micelles in normal saline by sonication at the concentration of 1% (10 mg/ml). The LPC was dissolved in chloroform-methanol, dried with nitrogen gas, and taken up in isotonic saline. This mixture was sonicated for 2 min × 4 with 5 min intervals between sonications to allow for cooling, then stored at 4°C, and resonicated before injection. TET, triethyltin bromide was obtained from chemical stock in MRC Toxicology Unit (Leicester, UK), and dissolved in sterilized saline to make 8 mg/ml solution. The single intraperitoneal dosage of 8mg/kg could be easily carried out by an injection with a dosing volume of 1ml/kg. Diphenamid, *N,N*-Dimethyl-2,2-diphenylacetamide was obtained from the British Greyhound (Birkenhead, Merseyside, UK), and freshly prepared as a 100 or 150 mg/ml solution in glycerinformal. Cuprizone, biscyslohexanone oxalyldihydrazone was obtained from Sigma Chemical Co. (C-9012, Dorset, UK), and mixed in a fume-cupboard with standard rat diet in powder to make 0.5 % and 1.0 % toxic diets.

2.3. Experimental anaesthesia in rats. Several forms of general anaesthesia were carried out in rat experiments covered by this thesis. Each of them was selected based on the requirement of each experiment under specific situation. A general description of anaesthetics, dosage and administration route is summarized here as (1) recoverable

general anaesthesia and (2) terminal general anaesthesia. Anaesthetics used in the experiments were:

1. Halothane, used for AEP recordings in the experiments for monitoring LPC-induced focal demyelination (Chapter 4). It is easy to vaporize, and induction and recovery are rapid (a few minutes). After induction with a 3% concentration, a minimum level of anaesthesia can be maintained by less than 1.5%. However, it has a depressant effect on the cardio-vascular system.
2. Isoflurane, used for AEP recordings in the experiment of monitoring TET toxicity (Chapter 5). Compared with halothane, it has less interference in drug metabolism since there is little effect on liver enzymes, but it is much more expensive. More importantly from the neurophysiological point of view, none of these two anaesthetic agents in low dose affects the AEP recording significantly.
3. Sagatal (sodium pentobarbitone, 60-70 mg kg^{-1}, *i.p.*), used mainly for the surgical procedures of electrode and cannula implantation. It induces a satisfactory surgical level of anaesthesia lasting 30-45 minutes by a single *i.p.* dose. The calculated amount of Sagatal for *i.p.* injection is close to the lethal dose, and thus occasional mortality (a few percent) may occur. Repeated dosing (top-up) is even more difficult to control, which is avoided and replaced by a short period of inhalation of either Halothane or Isoflurane in low concentration.
4. Urethane (1.4 g kg^{-1}, *i.p.*), used mainly for the acute and terminal experiments of cerebellar AEP exploration (Chapter 3) and brain perfusion afterwards. It produces long-lasting (8-10 hours) terminal anaesthesia with little cardio-respiratory system depression. Care should be taken in handling urethane since it is carcinogenic.

5. Ether (10-20% induction, and 4% for maintenance), used for the short-period terminal anaesthesia during the surgery in which animals used for histological examination were perfused with fixative.

For a recent and more detailed reference about anaesthesia in laboratory animals, see Laboratory Animal Anaesthesia (Flecknell, 1996).

2.4. Surgical implantation of cannulae and repeated sampling CSF in rats. CSF sampling has been extensively used in the human for clinical diagnoses and monitoring diseases. Similar procedures were, therefore, required to be developed in experimental animal models to simulate the clinical situations for studying the unknown mechanism of disorders. Considering the sensitivity of the method used for detecting specific CSF elements and the available volume of CSF, most of the repeated sampling CSF techniques were previously developed in fairly big animals, such as non-human primates, dogs, and cats. With the advantage of more sensitive detecting methods, the application of similar methods to the much smaller volumes of CSF available from small animals has been possible (Sarna, *et al.*, 1983). Repeated sampling of as small a quantity as a few microlitres from the conscious rat offers a method for experimentally studying cerebral metabolism in the small animal and thus repeatedly monitoring changes in specific elements of the brain. However, in my experience, the previously reported method (Sarna, *et al.*, 1983) had several obvious disadvantages. The first is a low long-term patency rate (only a few percent), which makes the method unsuitable for chronic experiments lasting for weeks. Secondly, the cannula has to be inserted into the cisterna magna blindly using a metal wire pushed

down inside. This may damage the surface vessels of the brain and cause intracranial bleeding. In addition, the cannula has to travel subdurally all the way from the vertex to the cisterna magna thus occupying a large volume of the intracranial space which may be crucial for animal survival if cerebral oedema is induced afterwards. I therefore modified the method by implanting a polyethylene tube in the rat cisterna magna via an opened occipital transcranial approach in order to obtain a better view of the cistern to avoid damage to the surface vessels during implantation. The intracranial segment of the approach, leading to the cisterna magna, was only a few millimetres in length and the intracranial space occupied by the implanted cannula was thus minimised. Accurate placement of the cannula into the subarachnoid space increased its long-term patency rate so that the cannula became suitable for experiments lasting for weeks.

The surgical details are as follows: The cannula (with spare ones), surgical instruments and other materials including glass container and pipettes for mixing dental acrylic were sterilized by either 15 min steaming in a boiler or heating in an oven at 100°C overnight (standard procedure for sterile surgery). The animal was anaesthetized by injecting Sagatal (60 mg/kg, *i.p.*) and placed in a small-animal stereotaxic frame. A midline incision was made between the lambda and the external occipital crest. Skin and underlying tissues were retracted to expose the dorsal skull, and a burr hole was drilled for the placement of a stainless steel screw (which was also used as a gross superficial electrode for EP recording) for securing the implanted cannula later on. The middle part of the occipital muscles were dissected from the skull down to the upper bony edge of the foramen magnum, and retracted caudally to expose the back of

the skull. Under a low-power surgical microscope, another bigger burr hole (1 × 2 mm) was made in the midline, 2 mm from the bony edge of the foramen magnum, with care being taken to keep the dura intact. The subarachnoid space was opened with the tip of a sharp 30G needle. A 'J - shape' 6 - 8 cm PE10 polyethylene tube (Portex Ltd, Kent) held by a manipulator was implanted into the cisterna magna. Correct placement of the cannula was indicated by the ability to withdrawing the CSF gently via the cannula without any difficulty. After surrounding area had been dried, the cannula and stainless steel screw were secured in place with dental acrylic (Austenal Dental Products Ltd, Harrow), and a few stitches finally inserted as necessary around the incision. After a short period of training, one could expect to complete such surgery within 30-40 minutes, during which adequate surgical anaesthesia was maintained by original single *i.p.* injection of Sagatal. The tail of the catheter was then cut to a length of approximately 4 cm, and its free end covered by a 0.5 cm long, heat-sealed PE50 tube (Fig. 2-1). After 2 days' recovery, the animals invariably appeared to be in good health. A few more samples of 50μl were taken by a small syringe with 30G needle inserted into the PE10 cannula within the next a few days to clear any CSF possibly contaminated by the surgical procedure.

Further repeated samplings of 50μl were achieved via the cannula by connecting a 30G needle and a 50μl syringe at the same time as the AEP was recorded. A volume of CSF sample of 50μl (approximate 10% of total CSF volume in a rat) was considered as the maximal practical volume that could be withdrawn safely without significantly affecting the physiological condition of the CSF circulation or causing bleeding from the superficial vessels of the brain due to a change in the intracranial

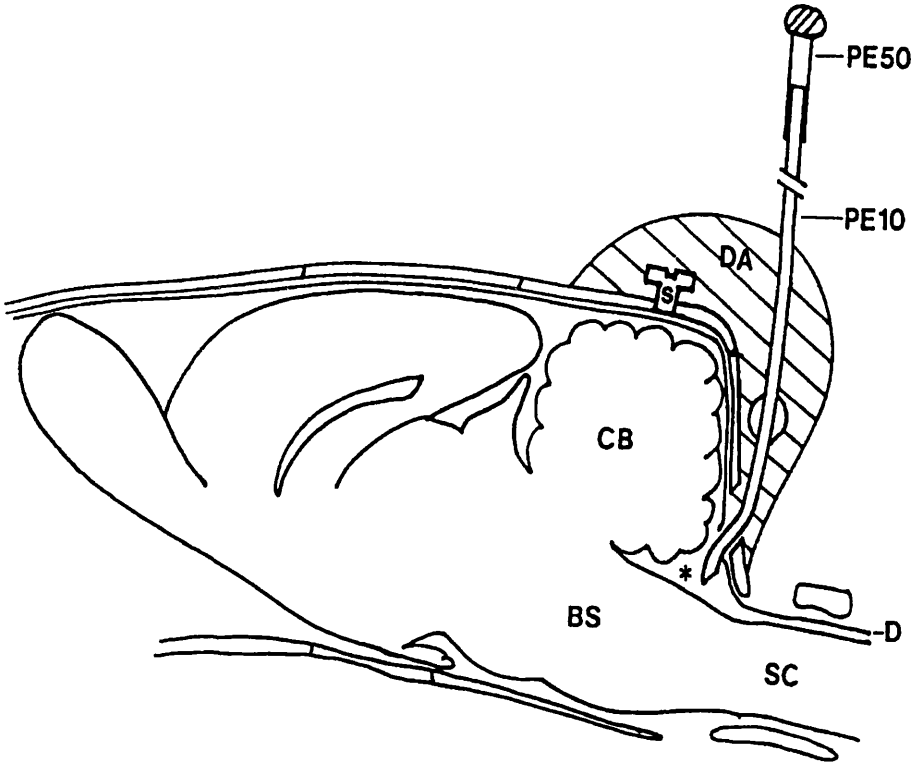

Fig 2-1. Chronic implantation of a cannula into the cisterna magna for repeated CSF sampling in rats. *: cisterna magna; BS: brainstem; CB: cerebellum; D: dura; DA: dental acrylic; PE10: implanted polyethylene size 10 tube; PE50: heat-sealed polyethylene size 50 tube; S: supporting screw; SC: spinal cord.

pressure locally around the cannula.

Of 30 cannulae placed using this modified implantation, a 100% patency rate was obtained at 24 hours post implantation, and 50% remained patent for 2 - 4 weeks. The most common reasons for later failures are as follows. (1) Misplacement of the cannula in the epidural rather than the subarachnoid space. Since the arachnoid mater is thin and transparent, it is difficult to identify it correctly, even under the surgical microscope, while it is covered by the CSF after the subarachnoid space is opened. (2) Blockage of the open-tip of the cannula because the subarachnoid space is significantly reduced of due to cerebral oedema following intoxication. A few cannulae became blocked at 7-9 days after TET intoxication, and among those, one became patent again after a few days of the peak effect of TET-induced cerebral oedema. (3) Blood contamination of the CSF due to intracranial bleeding during sampling increases the possibility of catheter block.

The above method was demonstrated at the Physiological Society Meeting (Liu and Ray, 1993, see appendices).

2.5. Estimation of clearance rate of MBP from CSF circulation: Injection was carried out by using the 'replacement method' in three animals: Before the injection, 30µl CSF was gently withdrawn by using a 50µl syringe with a 30G needle connected to the implanted PE10 tube. After 10µl of known purified MBP (170 µg/ml) was taken by using the same syringe, the front 30µl fluid in the syringe, including 10µl purified MBP and the following 20µl CSF, was then slowly injected back into the cisterna

magna via the cannula. The change of the regional CSF pressure and the flow of the CSF following the injected MBP would have facilitated the MBP to diffuse within the subarachnoid space and ventricular system (Bakay, 1951). Thirty minutes after injection, the first sample was taken via the implanted cannula, and sampling was repeated at time points of 1, 2, 4, and 24 hours. A few microlitres more CSF than the final volume of each sample, 50µl, was taken at each sampling in order to subtract the CSF remaining in the dead space of the cannula. All samples were diluted one in two with buffer A (0.05 M phosphate buffer pH 7 containing 1.2% (w/v) sodium chloride, 0.05% (v/v) Tween 80 and 0.5 mg/ml calf thymus histones) and frozen at -40°C until assayed.

Samples of CSF were assayed to measure the MBP concentration, and two clearance curves were then plotted with the values of remaining MBP concentration in the CSF against time. In the first plot, the actual values detected in the experiments were used, while the second plot used the detected values plus 10% compensation due to the artificial withdrawal of 50µl CSF (about 10% of total CSF) at each sampling point.

2.6. Radioimmunoassay for detecting MBP in the CSF. The essential reagents of synthetic ligand and the rabbit antiserum to human MBP used in the current studies were previously developed and kindly provided by Dr. Nigel Groome's group at Brookes University, Oxford. Details of developing the assay were previously reported (Barry, *et al.*, 1990) and are summarized as follows: The synthetic peptide (34T) had an artificial sequence of NH2·TYR-LYS-THR-HIS-GLY-LYS-THR-GLN-ASP-GLU-ASN-PRO-VAL-VAL-HIS-PHE·COOH corresponding to the sequences within the 75

- 89 region of human MBP with an amino terminal tyrosine and conservative amino acid substitutions at two positions: serine is switched to threonine at position 76 and arginine is switched to lysine at position 79, which was intended to restrict the antisera to epitopes in 80-89 whilst hopefully not changing the confirmation of this region too drastically. The antiserum was prepared using an immunogen of purified human MBP, coupled to ovalbumin with carbodimide (Groome, *et al.*, 1986). Female New Zealand White rabbits were immunised by subcutaneous injections (500 μg of MBP-ovalbumin conjugate) at 0, 7, 11, 23 and 45 weeks. The antiserum was obtained from the rabbits 3 weeks after the final boost.

2.6.1. Preparation of rat MBP: Rat MBP was needed as a standard for the radioimmunoassay in later experiments. Adult Fisher/344 rats were killed, and their brains placed in a chilled container. To reduce degradation of basic proteins by brain acid proteinases, defatting was performed by gradually adding chloroform-methanol (2:1, v/v) previously chilled to -10°C to the fresh tissue (19 ml/g tissue) and homogenising in an ultramix blender for 5 min. The suspension was then filtered under vacuum using a sintered glass funnel. The defatted tissue was homogenised for a further 5 min with cold water (2 ml/g original tissue) and the pH carefully decreased to 3 by adding additional of 1M HCl. This pH was maintained by the further addition of HCl while stirring on ice for 30 min and the suspension was then filtered through a sintered glass funnel and dialysed against three changes of 5 litres distilled water over night at 4°C and then freeze dried. This rat MBP preparation was then calibrated with human purified MBP of known concentration as standard.

2.6.2. Preparation of CSF samples: All CSF samples without contamination of blood were stored at -20°C until assayed. Prior to use, each CSF sample was diluted 1 in 2 - 4 in buffer A (composition described in 2.5.) and heated in a boiling water bath for 5 minutes. After centrifugation, the supernatant was used for assay.

2.6.3. Protocol of labelling the peptide 34T for RIA. Preparing 1 - 10 ml of the following solutions in PBS or TBS (pH 7.0 - 7.4) were prepared just before use:

1. chloramine-T, 5 mg/ml.
2. Na-metabisulphite, 12 mg/ml.
3. NaI 10 mg/ml.
4. 20 ml 10 mM HCl containing histone (0.5 mg/ml).

Sephadex-G10 swollen in 10 mM HCl was packed into a plastic pipette to make a 3 ml bed column. (NB. Set up in fume-cupboard in a hot-room as NaI^{125} plus chloramine-T may transiently generate small amounts of volatile I^{125} vapour. Wear gloves, badge and lab coat. Monitor area before, during and after procedure. Do not remove anything from fume-cupboard before monitoring.)

1. Pipette 10µl 34T (100 µg/ml stock, i.e. 1µg = 0.5nM) into Eppendorf tube.
2. Using designated Hamilton syringe withdraw 10µl NaI^{125} (= 1mCi = 37mbq = 0.5 nM) and add to tube.
3. Add 10µl chloramine-T and vortex to mix.
4. After 60s, add 10µl Na-metabisulphite; vortex to mix.
5. Add 10µl NaI solution; vortex to mix. (NB. Do not add NaI before Na-metabisulphite !)

6. Add 0.45ml histones/HCl; vortex to mix, then transfer whole reaction mix to 3 ml Sephadex G-10 column.
7. Collect load in Eppendorf tube, then collect another five 0.5 ml fractions eluting with 0.5ml aliquots of histones/HCl.
8. Count 10µl aliquots of fractions 1 - 6. Labelled 34T (calculate 5 - 8 million cpm/10 µl) should elute in fraction 4 or 5.
9. Store the Eppendorf of the right fraction in freezer in hot-lab.
10. Dispose of all hot solid waste (G-10 column, pipette tips, tissues, etc.) in appropriate bin. Rinse out hot Hamilton, first with NaI solution and then with distilled water.

2.6.4. RIA procedures: MBP was assayed by a three-day procedure which is summarized as follows. The ligand peptide was radioiodinated to a specific activity of 100 µCi/µg using iodogen catalysis (see the above section). An initial titration was carried out to determine the concentrations of antisera needed to bind 10 - 25% of the radiolabel, which indicated that the best concentration was a 1/10,000 dilution. All dilutions were made in buffer A. In the non-equilibrium RIAs all incubation stages were at 4°C. On day 1, each tube of three independent series received 100µl of antibody dilution followed by 50µl of either purified rat MBP (for standard), buffer A only (for the bound counts obtained at 0 concentration of unlabelled MBP, Bo), or diluted samples. The non-specific binding tubes received 150µl of buffer only. All tubes were well mixed. On day 2 each tube received 10,000 cpm of radiolabelled peptide in buffer and were vortexed. Finally on day 3, 50µl of second antibody (SacCel anti-rabbit IgG, Wellcome) was added and the tubes were vortex mixed and

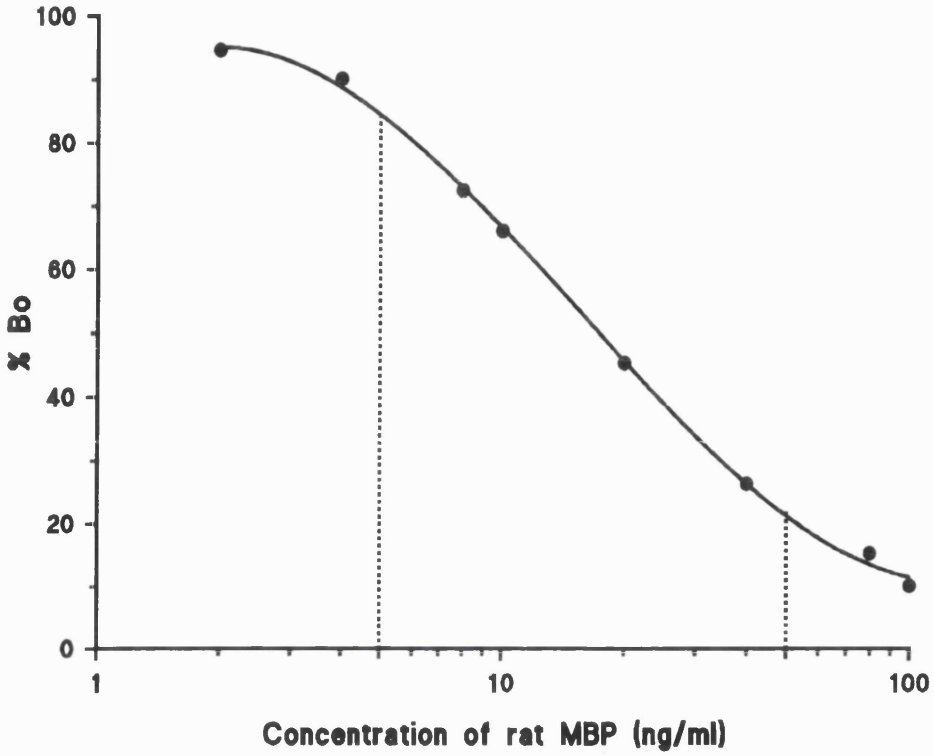

Fig. 2-2. Standard curve of radioimmunoassay used for the detection of rat MBP. Fifty percent inhibition of tracer binding corresponded to 15.3ng/ml of rat MBP standard, and the limit of detection (10% inhibition) in CSF was 5ng/ml.

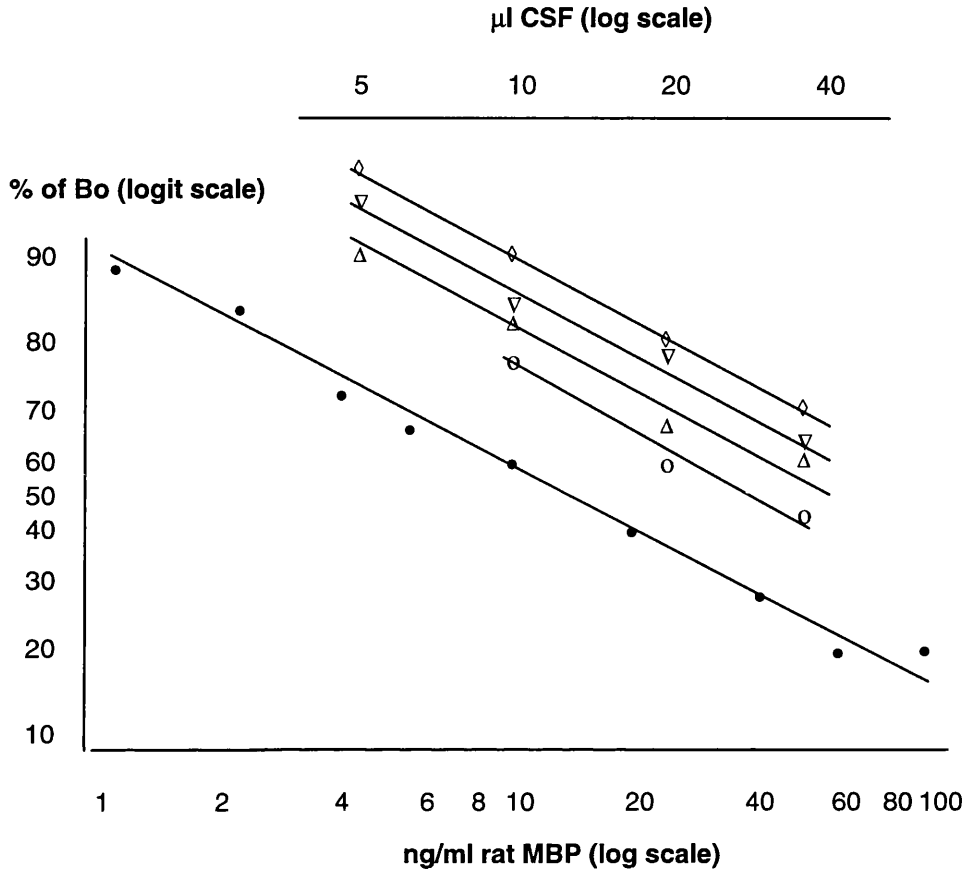

Fig. 2-3. Parallelism tests for CSF samples from four rats using logit-log plot. The standard MBP (•) and the CSF samples (o, Δ, ∇, ◊) are shown with an x-axis of ng/ml.

left to stand for 30 minutes, after which 1.5ml of cold water was added and the tubes centrifuged. The supernatants were aspirated and the bound radioactivity counted in a gamma counter (Packard Instrument Co., Inc.).

2.6.5. Standard curve of rat MBP and parallelism test of rat CSF samples. The standard curve (Fig. 2-2) was obtained by using calibrated rat MBP preparation (see 2.6.1). Fifty percent inhibition of tracer binding corresponded to 15.3 ng/ml of rat MBP standard, which gives limit of detection (10 % inhibition) of 5ng/ml. CSF samples from 4 animals were diluted by a factor of 2 - 6 and assayed. A logit-log plot was constructed from the results (Figure 2-3). There was a linear relationship observed in each case between the relative amounts of immunoreactive material calculated from the known dilution factors and measured in serial dilution of samples. Parallel responses were also observed between standard and samples indicating an indistinguishable dose-response between them within the accurate region of the inhibition profile corresponding to 20-80% of Bo. Both the linear relationship and the parallelism are important factors of validating the current assay of using anti-human MBP antibody for detection rat MBP in the CSF.

2.7. Recording AEP. The AEP was first explored under acute experimental conditions and then repeatedly recorded using surface electrodes as an electrophysiological index for monitoring conductive abnormalities induced by myelinotoxins upon the auditory pathway. General methods of evoked potential recording and analysis are described in this section. In addition, details of electrophysiological exploration of the surface-recorded cerebellar AEP and surface

recording methods in other toxicological experiments are also specifically addressed in Chapter 3, 4 and 5, respectively.

2.7.1. Surface-recording of AEP. AEPs were superficially recorded either from the skull over the cerebellum or neocortex, allowing repeated recordings for *in vivo* monitoring. The basic method of implantation of surface electrodes in the present experiments is similar to that in the previous experiments carried out in this laboratory (Ray, 1980; Verschoyle, *et al.*, 1992). The recording electrodes were 1 mm diameter stainless steel screws placed epidurally at different positions on the skull. Changes were made in the number and location of electrodes, and also by replacing the Ag/AgCl reference electrode with a screw because a large DC potential enough to block the amplifier was generated between the steel and AgCl electrodes. AEP recordings for the chronic toxicological studies were made via electrodes implanted together with the CSF cannula while the rats were under Sagatal anaesthesia (60 - 70 mg/kg, *i.p.*), 4 - 7 days prior to dosing of any toxic compound. The arrangement of the electrodes was as follows. The reference was placed in the skull over the olfactory bulbs, between the eyes in the midline. One recording electrode was placed over the vermis (midline, 1 mm from the rear edge of the dorsal skull) for the cerebellar AEP recording, and another over the auditory cortex for cortical AEP recording. A fourth electrode was placed in the parietal region as a ground (Figure 2-4). The electrodes were soldered to an four pin strip connector and this was embedded, together with electrodes, in dental acrylic. Recordings were achieved via an overhead lead which was plugged into the connector while animals were lightly anaesthetized by either

Isoflurane or Halothane (< 1.5%) and kept on a heating blanket with a rectal probe in place to monitor and control the body temperature themostatically.

In a series of acute experiments (see Chapter 3), up to 12 screw electrodes were placed over the dorsal skull in rats under urethane anaesthesia (1.4 g kg $^{-1}$, *i.p.*) in order to determine the surface spatial distribution of the cerebellar AEP. Two of these electrodes were placed over the auditory cortices on both sides, and nine were placed in three rows of three at 2 mm apart, thus covering most regions of the dorsal skull. The reference was at the same position as in the chronic experiments (Fig. 2-5).

2.7.2. Depth-recording of AEP. Glass-coated platinum electrodes (ϕ 0.250 mm) were used in combination with the surface electrodes. The purpose of such experiments was to investigate the contribution of deep structures in the brainstem, inferior colliculus and cerebellum to the surface recorded cerebellar AEP by either recording the compound action potentials along the auditory pathway and spatio-temporally correlating such potentials to the surface recording, or obtaining the depth profile of the field potentials while the recording electrode was gradually inserted into the brain. Various structures were targeted stereotaxically at positions (Table 2-1) calculated according to the atlas by Paxinos and Watson (1986). The reference electrode was placed in the same position as in other experiments for surface recordings (i.e. in the skull between the eyes).

2.7.3. Calibration and application of sound stimulus. A sound intensity over the range 40 - 120 dB SPL referenced to a sound pressure of 2 x 10^{-4} μbar was applied for

either open field binaural or closed field monaural stimuli, and separately calibrated using a Brüel and Kjaer type 4135 measuring microphone at the level of the animal's ears (Fig. 2-6). The background noise level in the laboratory was about 60 dB SPL, mostly in the <100 Hz range. The sound stimuli were 1 ms tone bursts of 40 kHz produced by a stimulus generator (Model 2100, A-M SYSTEMS), delivered at 1 - 40 Hz and triggered by another generator (Model 2100, A-M SYSTEMS) via a tuned ultrasonic transmitter (RS Component, No. 307-351). The speaker was either placed 34 cm directly above the animal's head, so that sound was binaurally conducted through an open field with matched timing and intensity, or attached to a hollow earbar of the stereotaxic frame via a sealed truncated plastic cone to produce closed field monaural stimulation. In addition, monaural stimulation was restricted further by blocking the other ear canal with an earbar to avoid possible contralateral sound conduction through the open field.

2.7.4. Recording parameters. Responses were amplified (Lectromed MT8P) with filter bandwidth of 3 - 5,000 Hz, and averaged 512 - 2048 times (for signal averaging and filtering techniques, see 1.5.1.) synchronized to sound stimuli by a common trigger. Single or averaged potentials were selectively displayed with either a 20 ms sweep for the cerebellar AEP or a 100 ms sweep for neocortical AEP on a monitor via an A/D converter (DIGIDATA 1200 Interface, AXON Instruments, Inc.). Data were stored on a PC hard disk.

2.7.5. Analyses of AEP. The surface-recorded cerebellar AEP has several distinguishable vertex-positive waves shown in Figure 2-5. Peak 2 was not consistent,

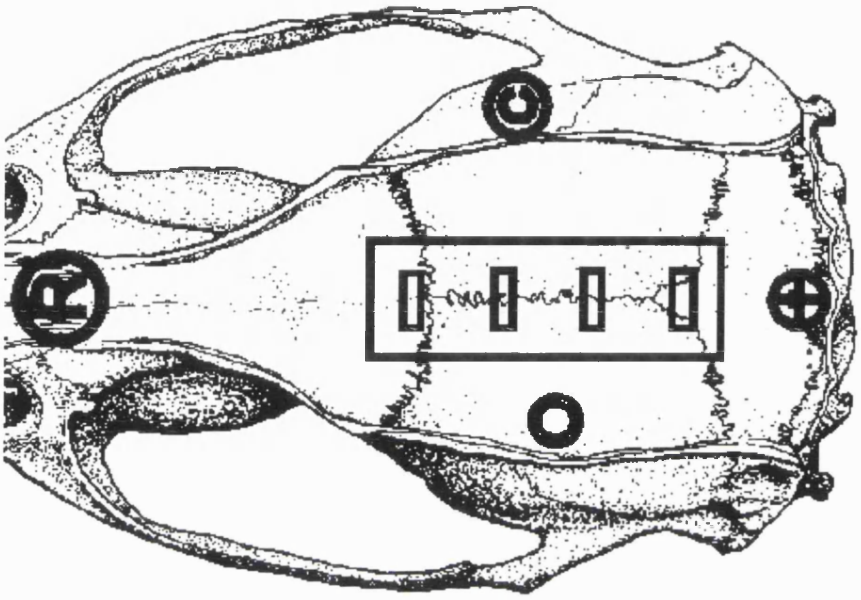

Fig 2-4. Position of pre-implanted surface electrodes in the dorsal skull for repeated neocortical and cerebellar AEP recordings in the toxicological experiments. Electrodes were soldered onto a four-pin connector and secured by dental acrylic on the skull. ®: reference electrode; ©: neocortical recording electrode; ⊕: cerebellar recording electrode; and ○: ground electrode.

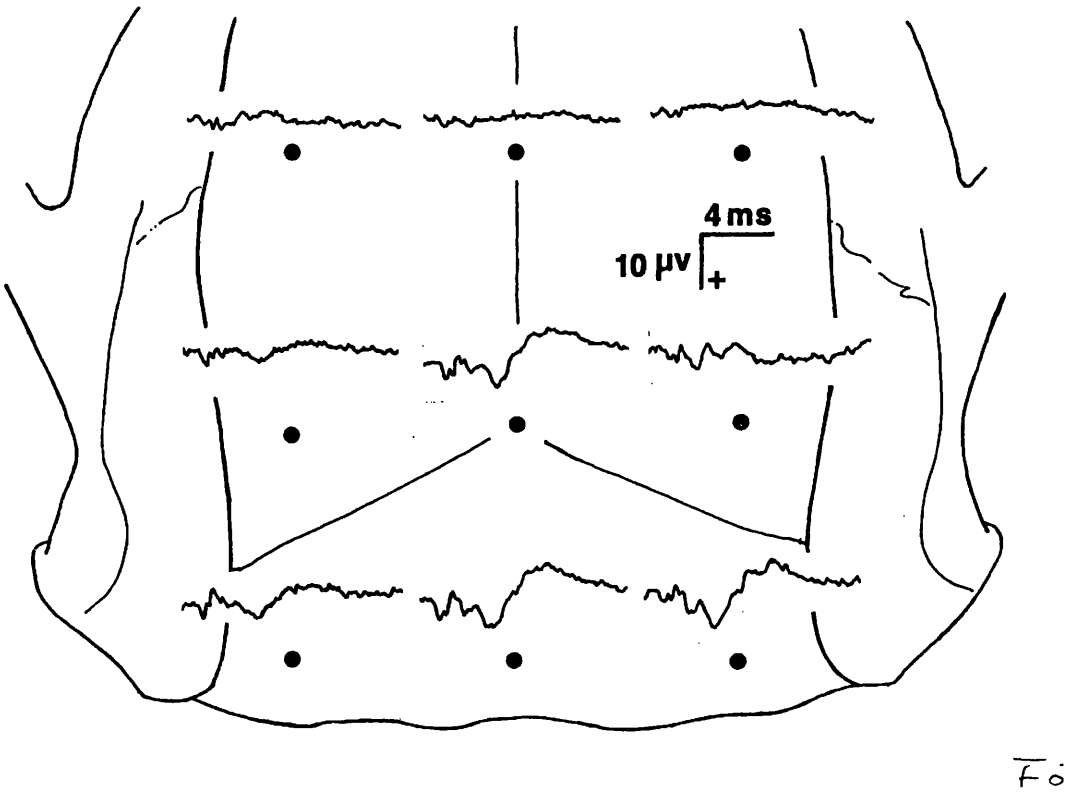

Fig 2-5. Position of the superficial electrodes placed in the dorsal skull, superimposed with corresponding AEP traces from one experiment present an example of spatial distribution of the surface-recorded AEP following monaural stimulation via a hollow earbar to the left ear with the right ear blocked. Positions of recording electrodes are indicated by " • "; the reference electrode was placed in the skull between animal's eyes at the midline.

Table 2-1. Stereotaxic positions of varies brain structures.

	AP	DV	LR
		(Interaural, mm)	
Cochlear nuclei	- 2.3	3.0	± 3.2
Inferior colliculus	- 0.2	5.6	± 1.8
Cerebellar nuclei	- 2.3	4.2	± 3.2

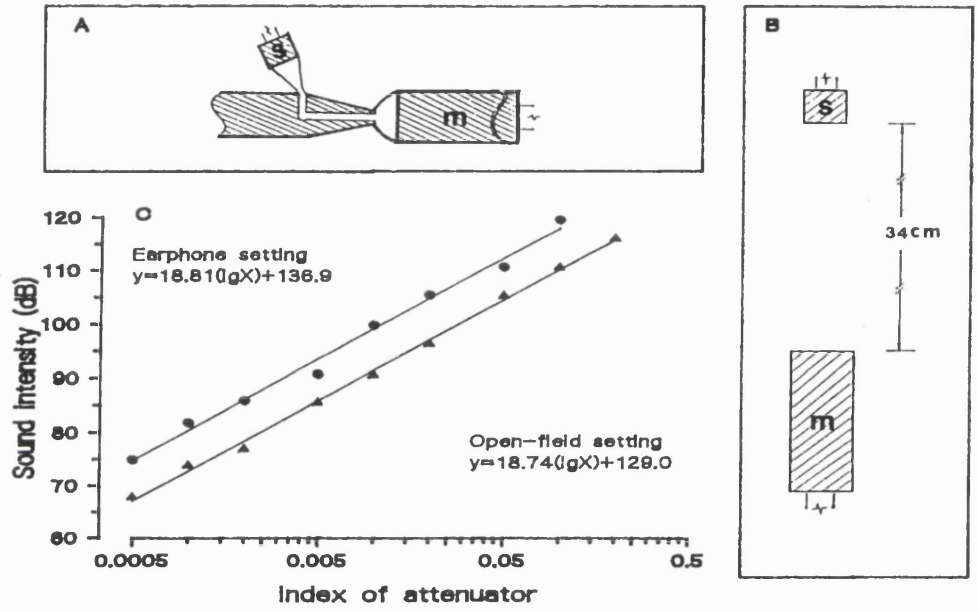

Fig. 2-6. A: A speaker was attached to a hollow earbar of a stereotaxic frame via a truncated-cone-shape plastic tubing for monaural stimulation. B: A speaker was placed 34 cm straight above the animal's head, by which sound was binaurally conducted through the open-field at the same time and with matched intensity. C: Calibration curves of sound intensities for monaural (•) and binaural (▲) stimuli. s: speaker; m: microphone. dB = 20 × lg (K × mV) + 1; K = 1241.26.

appearing in only about 50% of recordings, and it is, therefore, not included in the analyses. Peak latencies were measured from the onset of stimulus, and the central conduction time was calculated by subtracting the peak latency of wave 1a, most likely generated by the cochlear nuclei, from that of the wave 4, generated by the cerebellum. The amplitude of each component was estimated by using a three-point analysis. The inflexions used for measuring are indicated in Figure 2-7. The neocortical AEP has P1-N1-P2-N2 waveform. Peak latencies of P1 and P2 were measured from the onset of stimulus, and amplitudes were with peak-peak values. (The principles of evoked potential analysis as used in these experiments are described in Section 1.5.1.)

2.8. SEP recording. Part of the central auditory pathway parallels the somatosensory pathway at the level above the upper brainstem, whilst somatosensory afferents also traverse the lower brainstem and spinal cord. In the experiments of monitoring TET-induced myelinopathy (Chapter 5), the cortical SEP evoked by stimulating the median nerve was also recorded and used to confirm the conductive abnormalities detected by the AEP recordings. Electrical stimuli were 0.1ms square waves, generated by a stimulator (Model 2100, A-M SYSTEMS) as used in AEP recording, and delivered at 1 Hz via a stainless steel needle over the median nerve at the wrist (cathode). Intensity (usually in the range of 4 - 10 volts) was determined as up to 3 times above the threshold intensity producing thumb twitch. The anode was subcutaneously placed 1.5 cm from the stimulating electrode. The recording electrode was placed in the skull over the contralateral sensory cortex 2 mm posterior to the frontal suture and 3 mm from the midline. This position was previously identified electrophysiologically as the place from which the maximum SEP could be recorded. Responses were collected via

an amplifier with filter bandwidth of 0.3 - 5,000 Hz, averaged 16 - 64 times, and displayed with a 100 ms sweeps on a monitor. Data were stored on a PC. The waveform of the cortical SEP was P1-N1-P2-N2 as shown in Figure 2-8. Peak latencies were measured from the onset of the stimulus, and peak-peak measurement was used to estimate amplitudes.

2.9. Histopathological methods. Histology sections of 10 cerebella were obtained following the acute experiments of exploring the cerebellar AEP. Animals were killed after AEP recording under deep urethane by perfusion of fixative (10% formalin, 2% acetic acid) through the left ventricle into the aorta. Two days later, the cerebella were dissected and sliced as serial 100μm vibritome sections. Sections were stained with fast blue, and either electrode tracks or India ink markers were examined under the light microscope for confirmation of electrode or injection positions. Pathological evidence at the light microscope level was obtained in the experiments of LPC, TET and cuprizone intoxication. Animals were killed under deep ether anaesthesia by perfusion of fixative (10% formalin, 2% acetic acid) through the left ventricle into the aorta at survival times from 24 hours to 15 days after intoxication of TET or LPC, and 8 weeks after cuprizone intoxication. Following delayed removal (2 days at 4°C, to allow the brain to shrink slightly and avoid dark cell artefact), the cerebella were sliced coronally for step-serial sectioning (2 in 20) and 7μm sections stained with Hematoxylin and Eosin, or stained with solochrome cyanin for myelin. Electronic prints of those sections presented in this thesis were directly photographed by an electronic camera attached to the microscope, or transformed to an electronic image by scanning the conventional photograph.

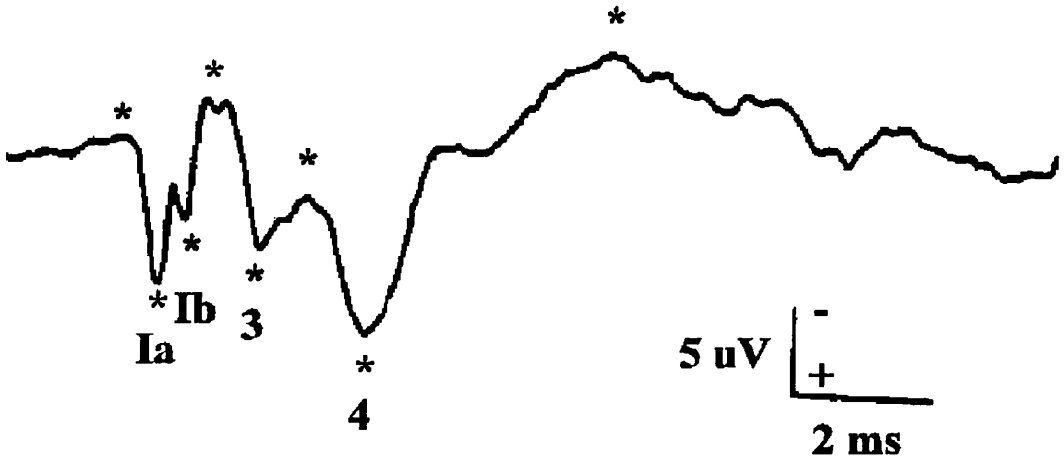

Fig. 2-7. Analysis of the surface-recorded cerebellar AEP. The surface-recorded cerebellar AEP is a vertex-positive peak marked as peak 4. There are also several early components marked as peaks Ia, Ib, and 3 which are generated from the proximal stages of the auditory pathway. The peak latencies were measured from the onset of stimuli; amplitudes were measured by three-point assessment with the inflexion points are marked as "*"; and the central conduction time was calculated as interpeak interval of peak Ia - 4.

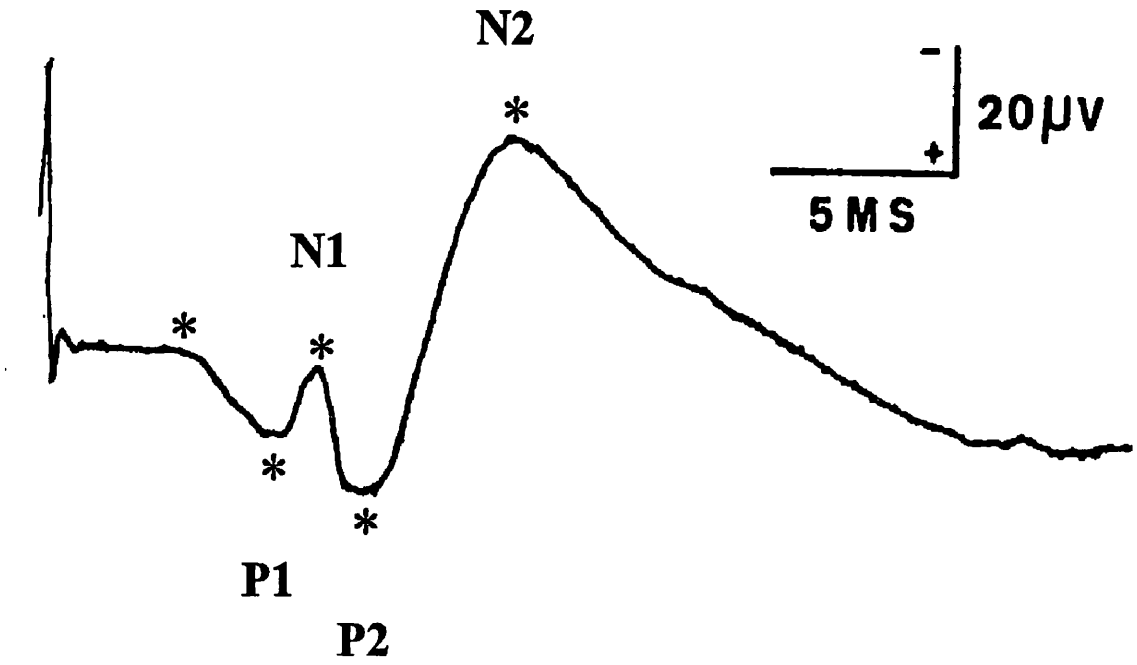

Fig. 2-8. Analysis of the surface-recorded neocortical SEP. The typical SEP consists of two vertex-positive peaks marked as P1 and P2. The latency of those peaks was measured from the onset of stimuli; amplitude was measured by three-point assessment with the inflexion points marked as "*".

2.10. Statistical analysis of data: Data are presented as either mean ± SD or mean ± S.E.M. together with the number of animals from which values were obtained. The mean values of measurement before and after treatments were statistically compared using paired or unpaired t-tests (Robert and James, 1987). Significance is indicated at either $p<0.05$ or $p<0.01$.

CHAPTER 3.

AUDITORY AFFERENTS TO THE CEREBELLUM: THE SURFACE-RECORDED CEREBELLAR AUDITORY EVOKED POTENTIALS IN ANAESTHETIZED RATS

3.1. Summary

Experiments were carried out in urethane-anaesthetized rats to investigate the auditory afferents to the cerebellum generating the field potentials evoked by either monaural or binaural auditory stimulation using simultaneous recording from multiple surface electrodes. In addition, monopolar depth responses were recorded from different sites of the auditory pathway, including the cochlear nuclei, the inferior colliculus, and the cerebellum, to evaluate the possible generators contributing to the surface potential. The effect of temporary blockade of cerebellar fibres induced by injection of procaine on the surface potential was also investigated. Our results indicate that cerebellar auditory responses can be detected by superficial field potential recording, appearing as a complex of multiple fast and slow components distributing caudally and medially but symmetrical to the midline following binaural stimulation. Auditory input is possibly projected via a ponto-cerebellar pathway, and conducted by the mossy fibres to both cerebellar nuclei and cortex. Auditory responses are not, however, generated exclusively by the cerebellar cortex. Surface-recorded auditory potentials can be used as an index for monitoring conductive dysfunction in the auditory cerebellar pathway.

Some of these results were orally presented in the Physiological Society Meetings (Liu & Ray, 1994; 1995a).

3.2. Introduction

The cerebellum receives a variety of sensory afferent signals. The peripheral auditory projection to the cerebellum has been demonstrated in mammals by recording unit discharges in the cerebellar cortex (Shofer, 1969; Aitkin & Boyd; 1975) and potentials

on the surface of the cerebellar cortex (Snider & Stowell, 1944; Morin *et al.*, 1957; Highstein & Coleman, 1968; Wolfe, 1972; Lorenzo *et al.*, 1977). More recently, responses have been recorded in rats by placing a gross screw electrode in the skull over the cerebellum (Shaw, 1992). Using subdural electrodes which provide good spatial resolution of the field potential, the regions in cat cerebellum responsive to auditory stimuli have been identified (Snider & Stowell, 1944; Gilman *et al.*, 1981). However, such potentials may represent the summation of activity from multiple dipoles of varying size, orientation and depth under the electrode within the cerebellum or even from different locations in wider range of brain structures. The identity and location of possible generators contributing the gross surface potential are far from clear, and so is the precise course of the auditory cerebellar projection pathway. In addition, as a result of attenuation of potentials by the high electrical impedance of the dura, less spatial resolution would be expected in the field potentials recorded by gross electrodes in the skull. Evidence, however, suggested (Verschoyle *et al.*, 1992) that the surface-recorded cerebellar AEP may be a practical index for detection of conductive dysfunction in the cerebellum.

Experiments were therefore carried out to investigate the spatial distribution of the cerebellar AEP recorded using screw electrodes in the skull. Depth responses were simultaneously recorded with the surface potentials from different sites of the auditory pathway, including the cochlear nuclei, inferior colliculus, and cerebellum, and a depth profile of the cerebellar surface potential was obtained from which identification of the possible generators contributing to the surface potential was attempted. The effect of temporary blockade of cerebellar fibres induced by injection of procaine on the surface

potential was also investigated. The spatial and temporal relationship between the cerebellar, collicular and cochlear AEPs, and the practical implication of such a surface-recorded potential for detecting cerebellar damage *in vivo* are discussed below.

3.3. Materials and methods

34 Adult male Fisher/344 rats, 250 - 300 grams body weight, were used in this study. Auditory evoked potentials were recorded under anaesthesia (urethane, 1.4 g kg^{-1}, *i.p.*). (A general description of study methods can also be seen in Chapter 2).

Electrode arrangements for surface and depth AEPs recordings: Three types of electrode arrangements were employed for recording AEP: (1) In a group of 4 animals, up to 12 stainless steel screw electrodes of 1.2 mm diameter were placed epidurally on the dorsal skull in order to study the spatial distribution of the evoked potential. Two electrodes were placed over the primary auditory cortices on both sides, nine were placed in three rows of three at 2 mm apart, thus covering most regions of the dorsal skull. The reference electrode was placed in the skull over the olfactory bulbs in the midline. Animal was grounded via a silver plate under the abdomen; (2) In a total of 15 acute experiments of combining surface and depth recordings, three screw electrodes were used: a recording electrode was placed in the skull over the vermis (midline, 1 mm from the rear edge of the dorsal skull) for the cerebellar AEP recording, a common reference electrode for both surface and depth recordings was placed in the skull over the olfactory bulbs, and a third electrode was planted in the parietal region for grounding; (3) Glass-coated platinum electrodes (ϕ 0.250 mm) were used for depth recordings in combination with the surface electrodes to investigate the

possible contribution of deep structures in the cochlear nuclei, inferior colliculus and cerebellum to the surface recorded evoked potential. Those brain structures were targeted stereotaxically according to the atlas of Paxinos and Watson, (1986), and electrode placement was confirmed morphologically afterwards.

Auditory evoked potential recordings: Sound intensity over range of 40 - 120 dB SPL were applied for either open field binaural or closed field monaural stimuli. The background noise level in the laboratory was about 60 dB SPL, mostly in the <100 Hz range. The sound stimuli were 1 ms tone bursts of 40 kHz generated and delivered at 1 - 40 Hz by two stimulus generators via a tuned ultrasonic transmitter which was either placed 34 cm directly above the animal's head so that sound was binaurally conducted through an open field with matched timing and intensity, or attached to a hollow earbar of the stereotaxic frame via a sealed truncated plastic cone to produce closed field monaural stimulation. The responses were amplified with filter bandwidth of 3 - 5,000 Hz, averaged 512 - 2048 times, displayed with a 20 - 100 ms sweeps on a monitor via a D/A converter. Data was stored on a PC.

Intracerebellar injection of procaine: Temporary inactivation of the cerebellar fibres was carried out in 5 animals by making local injections of procaine (2.5µl 4% procaine in saline with Indian ink) into the central cerebellar white matter between the deep nuclei and the cortices on each side using a 5µl micro-syringe with a 30G needle. AEPs were recorded before and after injections, and the site of injection was checked histologically.

Data analyses: The surface-recorded cerebellar AEP has several distinguishable vertex-positive waves, as shown in Fig. 3-2. Peak 2 was not always present, appearing in only about 50% of recordings, and it is, therefore, not included in the analyses. Peak latencies were measured from the onset of the stimulus, and the CCT was calculated by subtracting the peak latency of wave 1a from that of the wave 4. The amplitude of each component was estimated by using a three-point analysis. The inflexions used for measuring are indicated in Fig. 3-2. Data were presented as mean ± SD, and a paired t-test was used to make comparison of the potentials recorded before and after injection of procaine.

3.4. Results

3.4.1. Spatial distribution of the surface-recorded AEP. In 4 experiments, the surface-recorded AEPs were epidurally recorded via gross screw electrodes over the parietal and occipital regions. The spatial distribution of such field potentials can be illustrated by superimposing each recorded trace over the position of the corresponding recording electrode (Fig. 2-3). Simultaneous recordings showed that, following monaural stimulation, the spatial distribution of the field potentials over the dorsal skull was contralateral and caudal, whereas the potentials were caudal but symmetrical to the midline following binaural stimulation (Fig. 3-1). There was only insignificant variance in potential amplitude at each location between different animals, but the general waveform and distribution patterns were similar.

3.4.2. Effects of changing stimulating and recording parameters on the cerebellar AEP. Settings of stimulus and recording parameters affecting on the cerebellar AEP

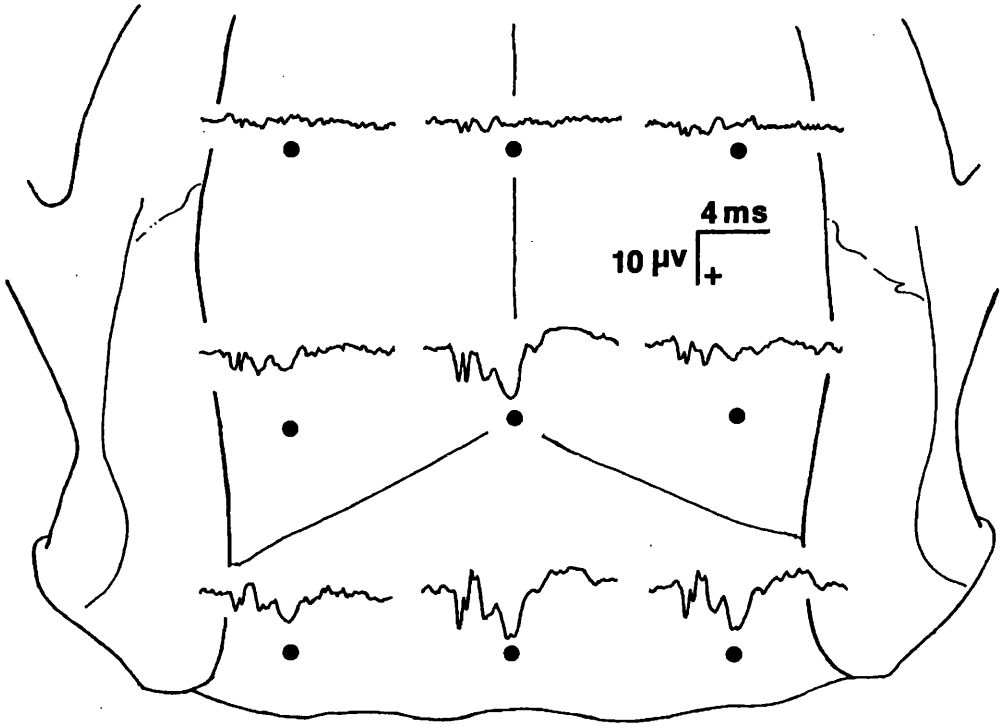

Fig. 3-1. Spatial distribution of the surface-recorded field potentials over the dorsal skull, following binaural stimulation, was caudal but symmetrical to the midline. The best positions for the surface-recorded cerebellar auditory potential are at the midline. Position of recording electrodes is indicated by "•". Reference electrode was placed in the skull between the animal's eyes.

included stimulus intensity, frequency of stimulus delivery and band-width of the recording amplifier.

Stimulus intensity. There is a linear positive correlation between the potential amplitudes and the sound intensity both applied monaurally and binaurally. An example of the cerebellar AEP evoked by binaural stimuli over the stimulus intensity range of 82 - 112 dB SPL is illustrated in Figure 3-2. When the sound intensity increased, the latencies of the response shortened.

Stimulus frequency. As with the neocortically generated evoked response, the cerebellar AEP was remarkably affected by stimulus repetition rate, *i.e.* when the frequency increased, the potential amplitudes decreased (Fig. 3-3). In contrast to the later major cerebellar component, the early far-field components which were thought to be generated from more peripheral stations of the central auditory pathway involving fewer synaptic transmission were affected much less.

Filter settings of the recording amplifier. The surface-recorded AEP is a complex of multiple fast and slow components, and, therefore, the band-width setting on the recording amplifier will affect the signals differentially. The major cerebellar component is a low frequency wave, whereas the earlier far-field components are fast waves, and these waves are superimposed. One has to be aware that use of a low pass filter to emphasis a slow component causes some artificial changes including loss of fast components, decrease in amplitude and delay in peak latency of the component displayed (Fig. 3-4).

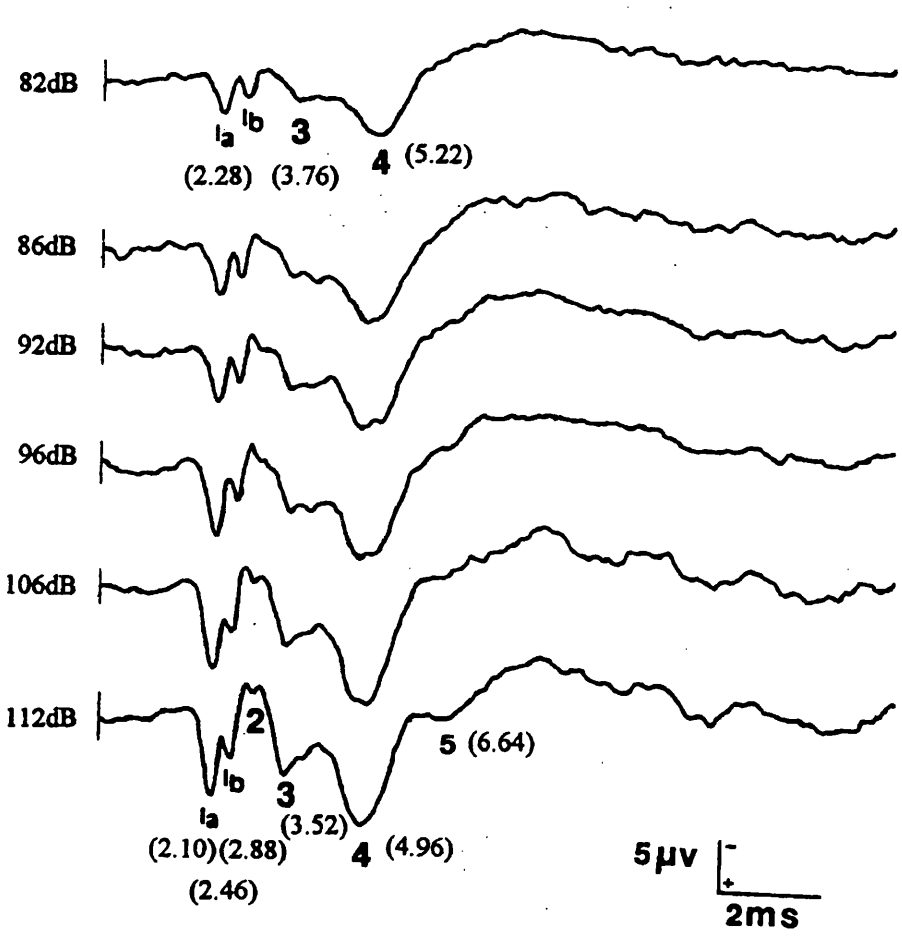

Fig. 3-2. The cerebellar AEP recorded from the skull over the vermis following binaural stimulation. As sound intensity increases (labelled at left to each trace), amplitude of components increases and latency shortens. Actual latencies (ms) are indicated in parentheses.

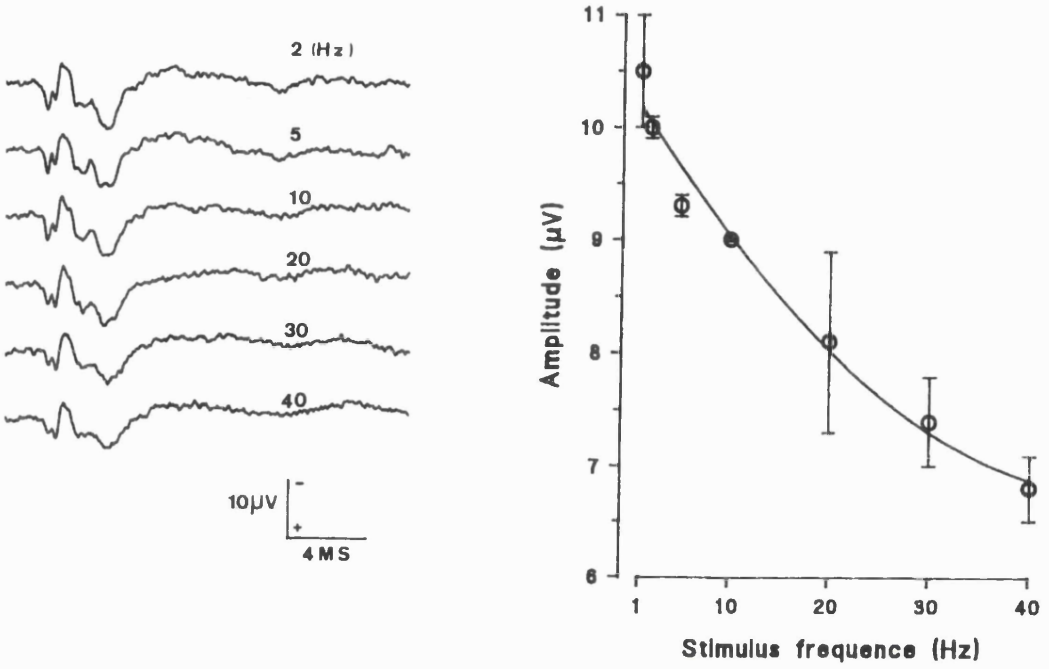

Fig. 3-3. Recording traces of the surface-recorded cerebellar AEP following increase in the delivery frequency of the sound stimuli (left half, the delivery frequency of sound stimuli is labelled above each trace). As the frequency increased, the amplitude of the P4 component decreased (right half, data are presented as mean ± SD, n=3), while the early far-field components were affected much less.

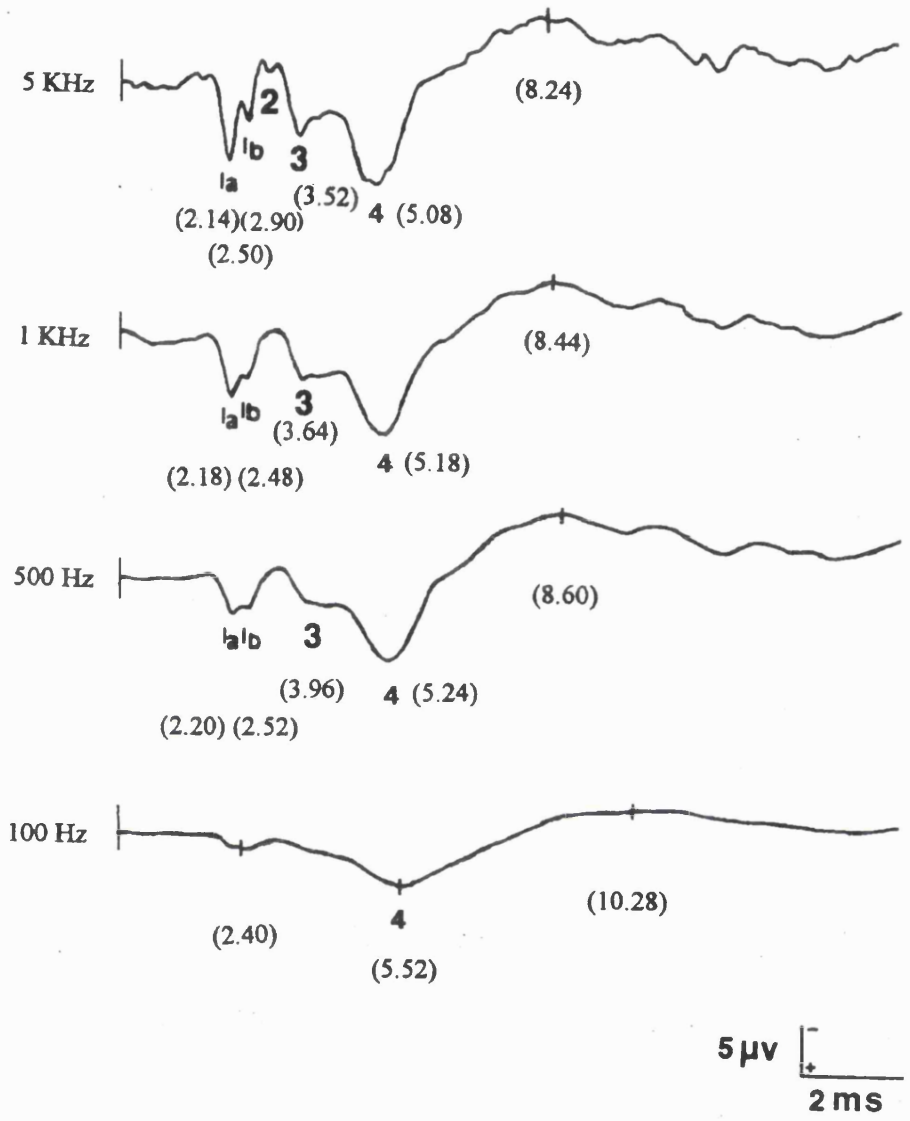

Fig. 3-4. As the cut-off of the low-pass filter stepped down (labelled at left to each trace), the amplitudes decreased and latencies increased with fast components being filtered out. Actual latency of some components is indicated in parentheses (ms).

3.4.3. Binaural interaction of the cerebellar and neocortical AEPs. Despite the similarity of the general waveform and peak latencies of the surface-recorded AEP to left or right ear stimuli, the binaural interaction of the auditory input in the cerebellar and the primary cortical receiving areas was remarkable in terms of altered spatial distribution and amplitude of the response. Following monaural stimulation, simultaneous recordings showed that the spatial distribution of the field potentials over the dorsal skull was contralateral and caudal, whereas the potentials were symmetrical to the midline and larger caudally following the binaural stimulation (Fig. 2-3, 3-1), as described previously (see 3.4.1.).

The early components of the cerebellar AEP. In five experiments, with matched stimulus intensities of 100 dB SPL, the amplitude of the early component (1.2 ms in latency) to binaural stimuli was 5.3 ± 0.75 μV, which is 185 ± 11 % of that (2.9 ± 0.43 μV) to monaural stimuli (Fig. 3-5, 6).

The late components of the cerebellar AEP. The comparable value for the late component (4.1 ms in latency) was 11.1 ± 1.52 μV to binaural stimuli, which is 129 ± 5 % of that (8.6 ± 1.14 μV) to the monaural stimuli (Fig. 3-5, 6).

The responses recorded over the primary auditory cortex. In contrast to the cerebellar AEP, the near-field cortical AEP (P2) to monaural stimuli were asymmetrical with values of 31.9 ± 3.42 μV (considered as 100 %) contralaterally and 5.7 ± 0.55 μV (18.7 %) ipsilaterally (Fig. 3-7, 8); whereas to binaural stimuli, they

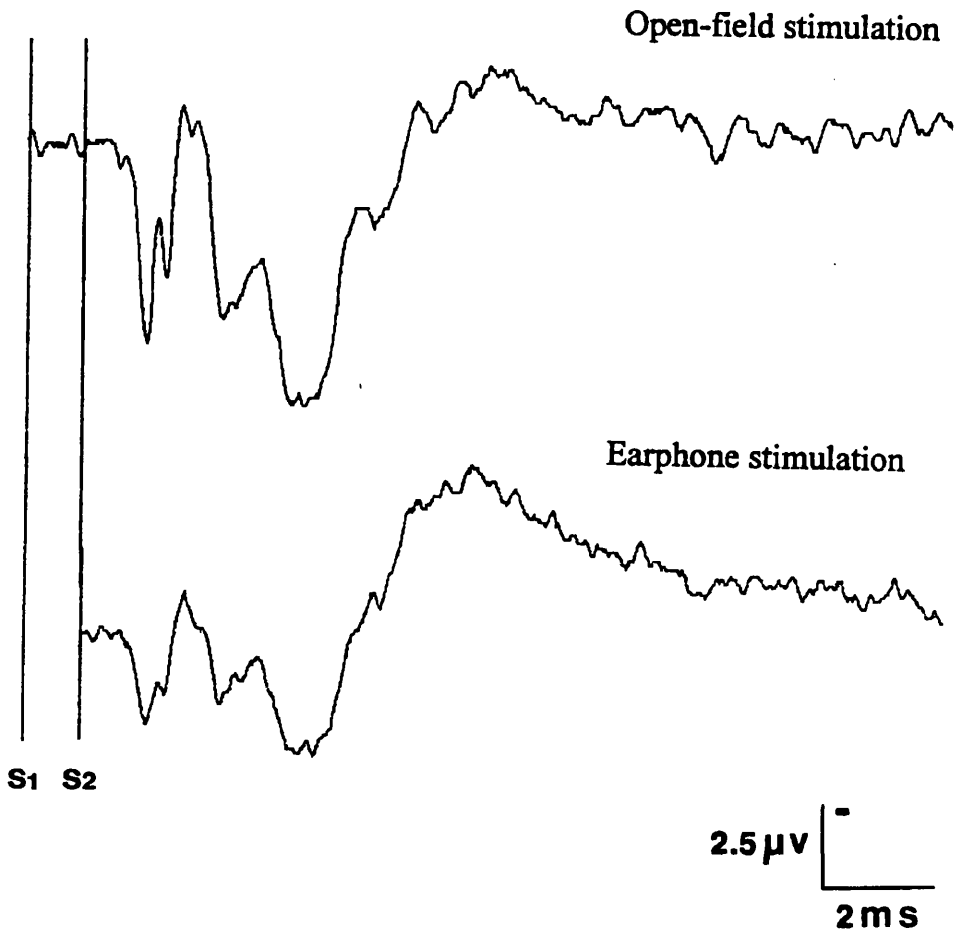

Fig. 3-5. Comparison of the surface-recorded cerebellar AEP following binaural (open-field) and monaural (earphone) stimuli with matched intensities of 100 dB SPL. S1 and S2 indicate the onset of the binaural and the monaural stimuli, respectively. There is a delay of one ms in the upper trace for the sound conducting from the speaker to ears (34 cm).

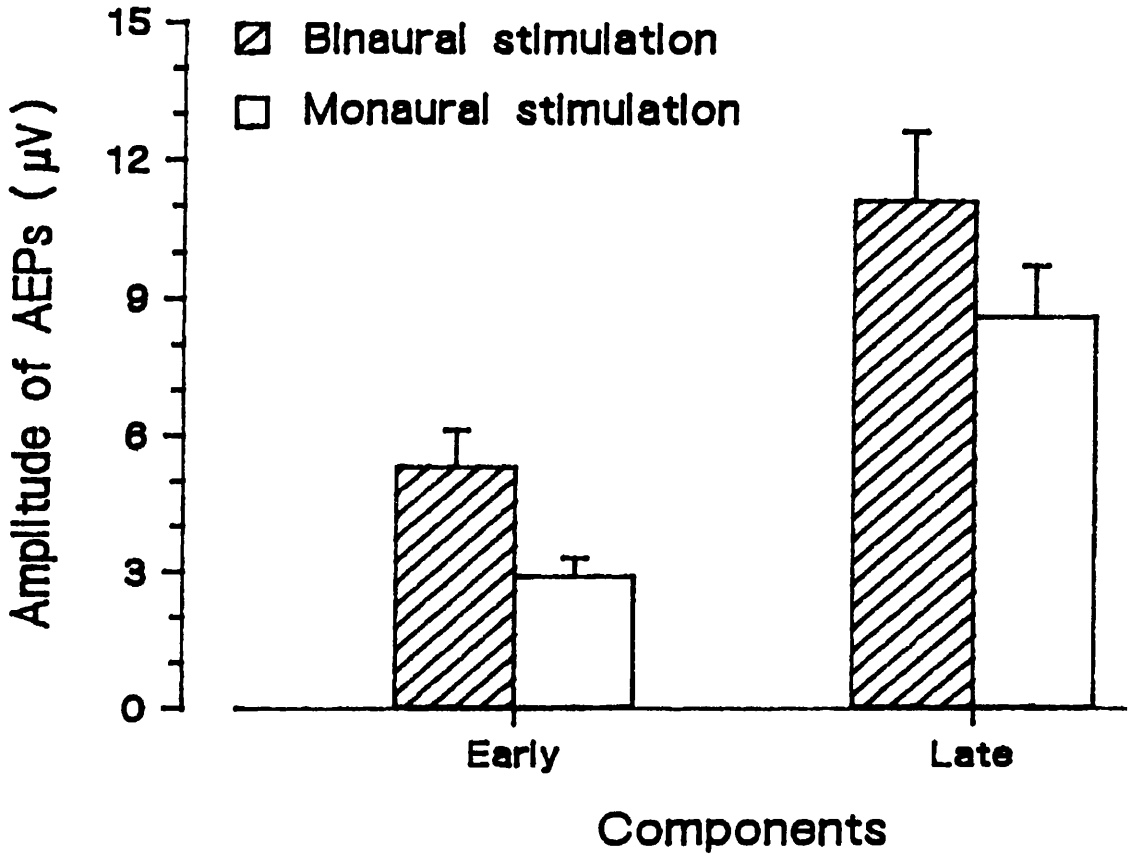

Fig. 3-6. The amplitude of the early (1.2 ms) component of the cerebellar AEP to binaural (■) stimuli was 185 ± 11 % of that to the intensity-matched monaural (□) stimuli, but the comparable value for the late (4.1 ms) component was 129 ± 5 %. Data are presented as Mean ± S.E.M.; n = 5.

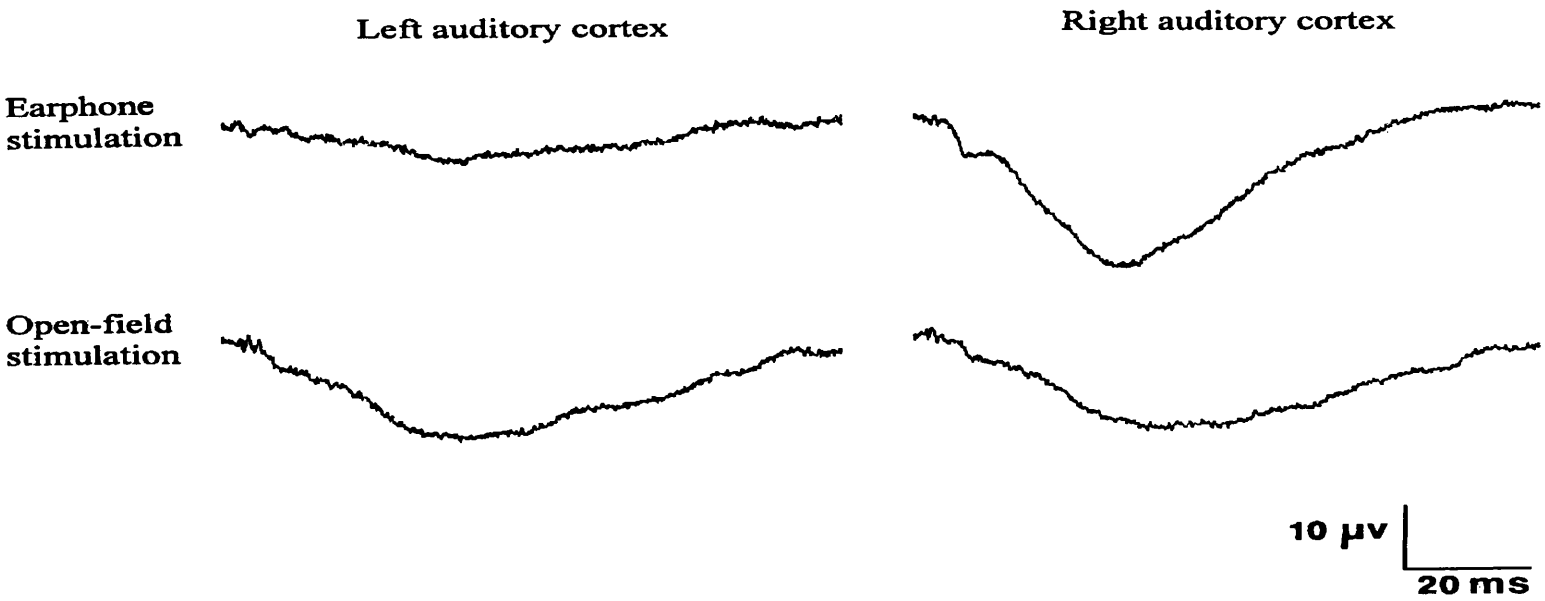

Fig. 3-7. Comparison of the surface-recorded neocortical AEPs following binaural (open-field) and monaural (earphone) stimuli to the left ear with matched intensities of 100 dB SPL. There is a delay of one ms in the upper trace for the sound conducting from the speaker to ears (34 cm).

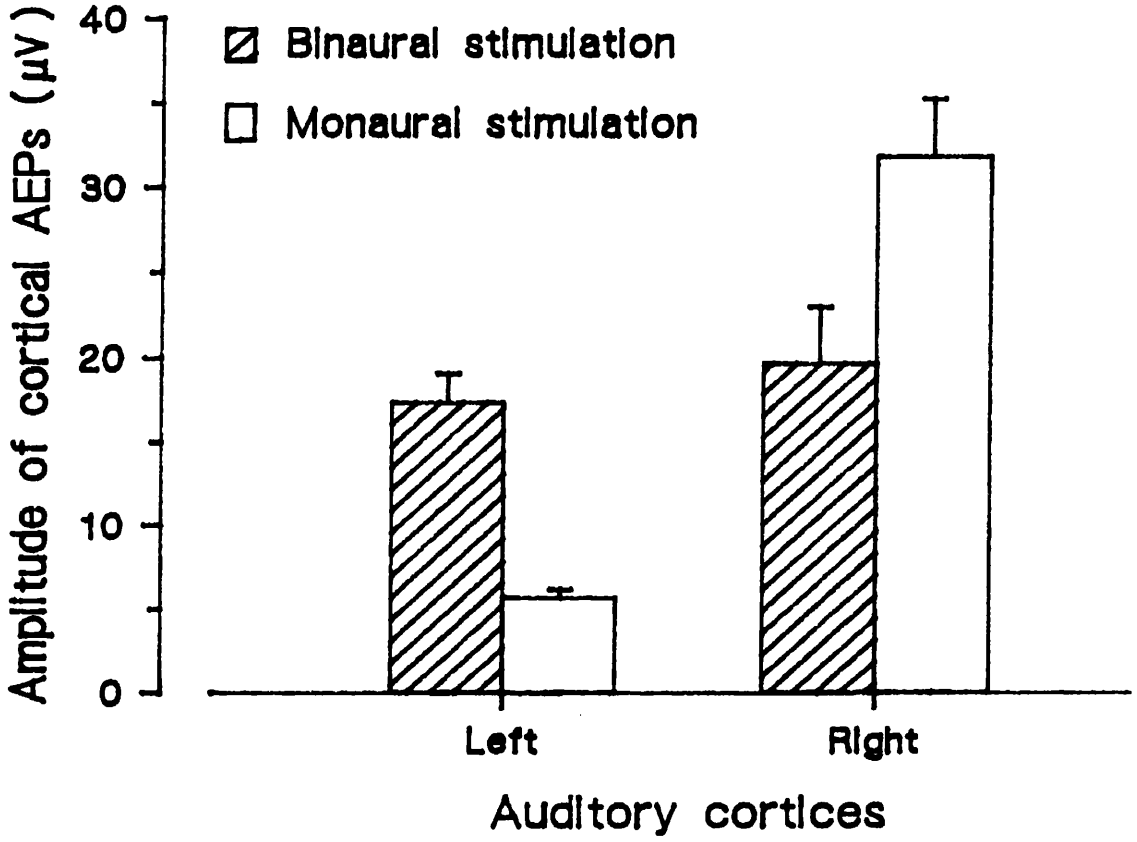

Fig. 3-8. The amplitude of the neocortical AEPs responsive to binaural (■) stimuli was 59 ± 4 % of that to intensity-matched contralateral monaural (□) stimuli. Data are presented as Mean ± S.E.M.; n=5.

were almost symmetrical with values of 17.4 ± 1.68 μV (55.8 ± 0.05 %) and 19.7 ± 3.29 μV (62.1 ± 0.09 %).

3.4.4. Monopolar depth recordings of AEP at different levels of the auditory pathway. Monopolar glass coated platinum electrodes were stereotaxically inserted into the different stages of the auditory pathway to identify possible generators contributing to the surface-recorded response. Stimuli were monaurally delivered via a hollow earbar of a stereotaxic frame via a closed truncated-cone-shape plastic tubing with intensity of 90 dB SPL.

AEP generated by the cochlear nuclei. Depth electrodes were stereotaxically inserted to target the dorsal cochlear nuclei (AP: -2.3 mm, DV: 3.0 mm; Lateral: 3.2 mm) in both sides with a surface screw electrode in the skull over the vermis and a common reference electrode over the nose on the midline. Simultaneous recordings showed that the component having the same onset latency as the Ia component of the surface-recorded response is bigger in the ipsilateral cochlear nucleus than that at the surface, and almost non-existent on the contralateral side. In contrast, the first component recorded at the contralateral cochlear nucleus not only has the same onset latency as, but has a similar waveform to, the Ib component of the surface-recorded response (Fig. 3-9).

AEP generated by the inferior colliculus. Depth electrodes were stereotaxically inserted to target the contralateral central nucleus of the inferior colliculus (AP: -0.2 mm, DV: 5.6 mm, Lateral: 1.8 mm) and the contralateral cerebellar dentate nucleus (AP: 2.3 mm, DV: 4.2 mm; Lateral: 3.2 mm) with a surface screw electrode in the

skull over vermis and a common reference electrode over the nose in midline. Simultaneous recordings showed that the major late component of the inferior colliculus response not only had a vertex-negative polarity, but was also 0.3 ms later in peak latency than the corresponding component of the both depth and superficial cerebellar responses which had vertex-positive polarity and the same overall waveform (Fig. 3-10).

Depth profile of the cerebellar AEP. In three experiments, depth electrodes were stereotaxically inserted to target the cerebellar hemispheres bilaterally (AP: 2.3 mm and Lateral: 3.2 mm) and the midline structure at the same AP plane with a reference electrode over the nose at the midline. Simultaneous recordings made at different depths while the electrodes entered the cerebellum from the surface showed that the general waveform of the responses was similar from all three electrodes. More interesting are the changes in amplitude of the major cerebellar component. At the surface, the biggest response was obtained at the central electrode as the electrodes penetrated the cerebellum, all responses increased, but at different rates, and the contralateral response clearly became the biggest in amplitude when the electrodes reached the level of interaural 5.0 mm. With deeper penetration this increase in amplitude still continued on in the contralateral side, whereas a decrease in amplitude appeared on both the midline and ipsilateral sides until the electrodes reached the level of interaural 4.0 mm; and finally the general waveform changed as the electrodes penetrated further (Fig.3-11). The measurements of the changes in amplitude from one experiment are presented in Figure 3-12.

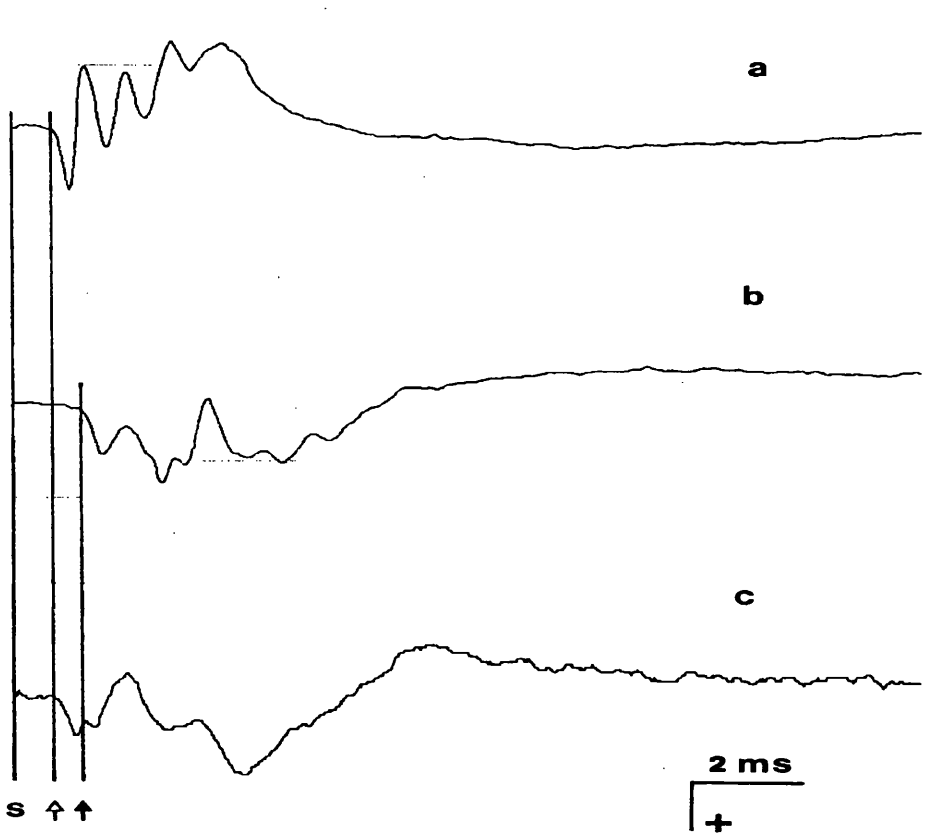

Fig. 3-9. The AEPs recorded from the ipsilateral (a) and the contralateral (b) cochlear nuclei, correlated to the simultaneously surface-recorded cerebellar AEP (c) with sound intensity of 90 dB SPL. Reference electrode was placed in the skull between eyes. The onsets of the stimuli, the ipsilateral and the contralateral responses are indicated by S, open arrow and solid arrow, respectively. The unit bar for the measurements of amplitude is 20 μV for the cochlear responses (a and b) and 5 μV for the surface response (c).

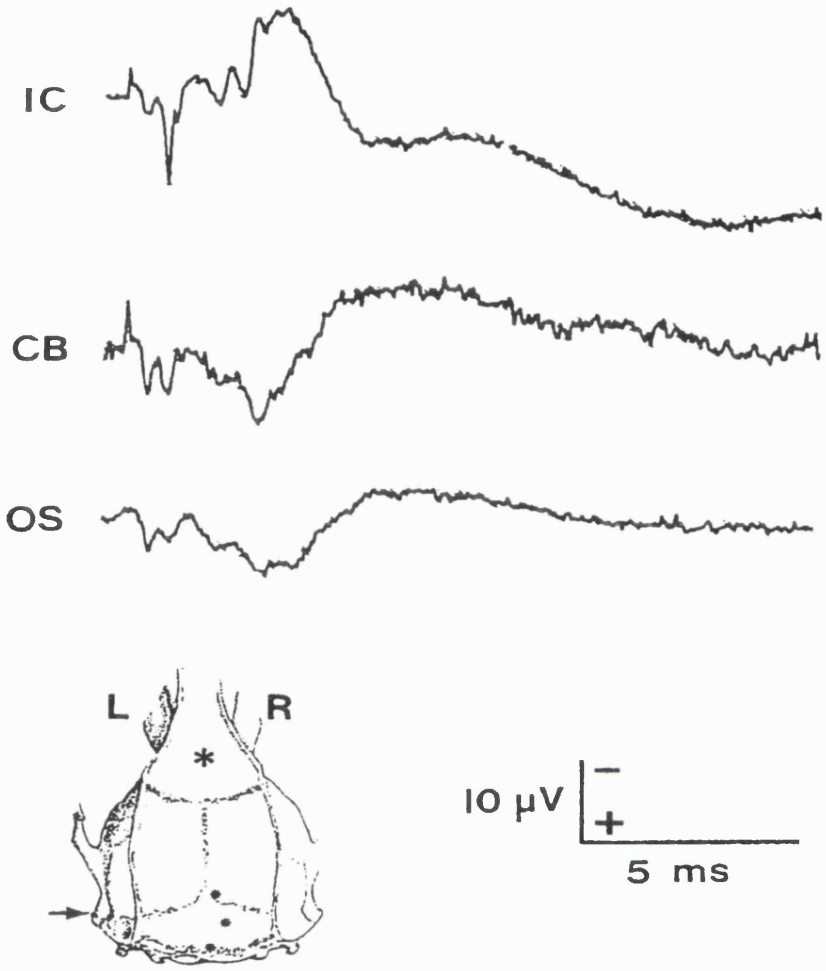

Fig. 3-10. Comparison of AEP traces recorded from the contralateral inferior colliculus (IC), the cerebellum (CB) and the occipital skull (OS) at the midline. The major late component of the inferior colliculus response was not only vertex-negative, but also 0.3 ms later in peak latency than the corresponding component of the both depth and superficial cerebellar responses which had vertex-positive polarity. L: left; R: right; *: positions of reference and recording electrodes.

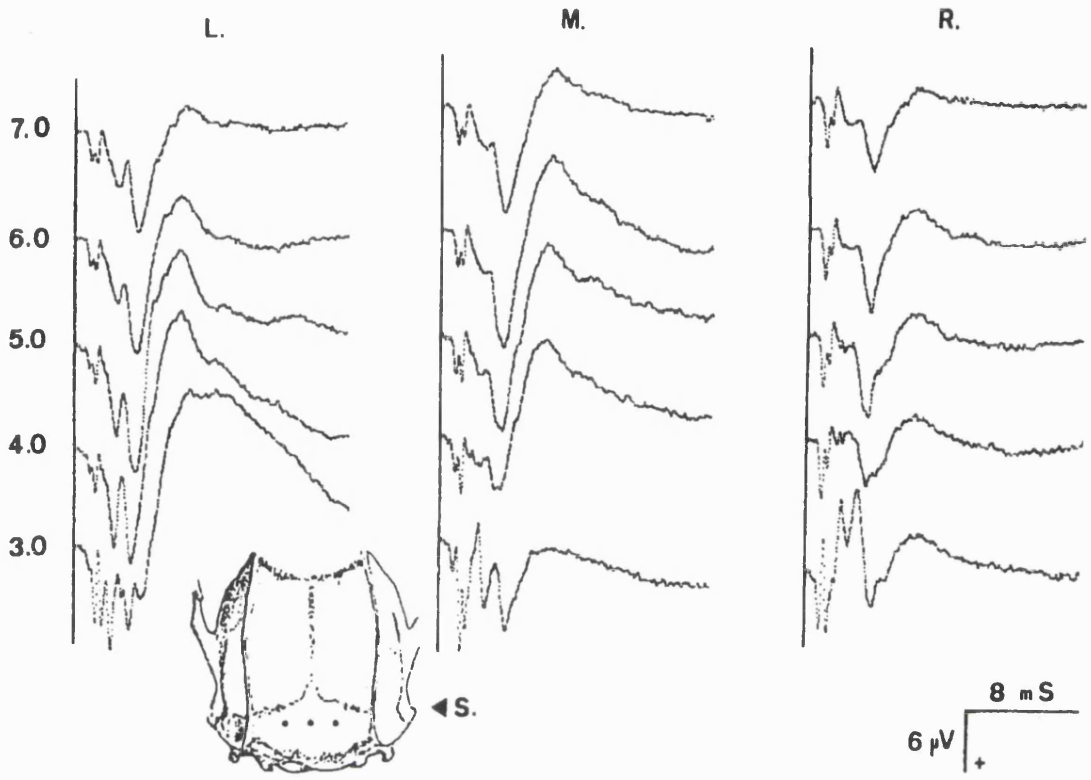

Fig. 3-11. Depth profile of the cerebellar AEP. Traces were simultaneously recorded from the cerebellum by monopolar glass-coated platinum electrodes. ←S: Stimuli of 94 dB SPL were delivered via an earphone to the right ear. *: Recording positions were: AP -2.5; LR 2.2, 0, -2.2; and depth is indicated by the numbers at the left side of each trace (interaural, mm). Reference electrode was placed in the skull between eyes. L.: Left; M.: Middle; R.: Right.

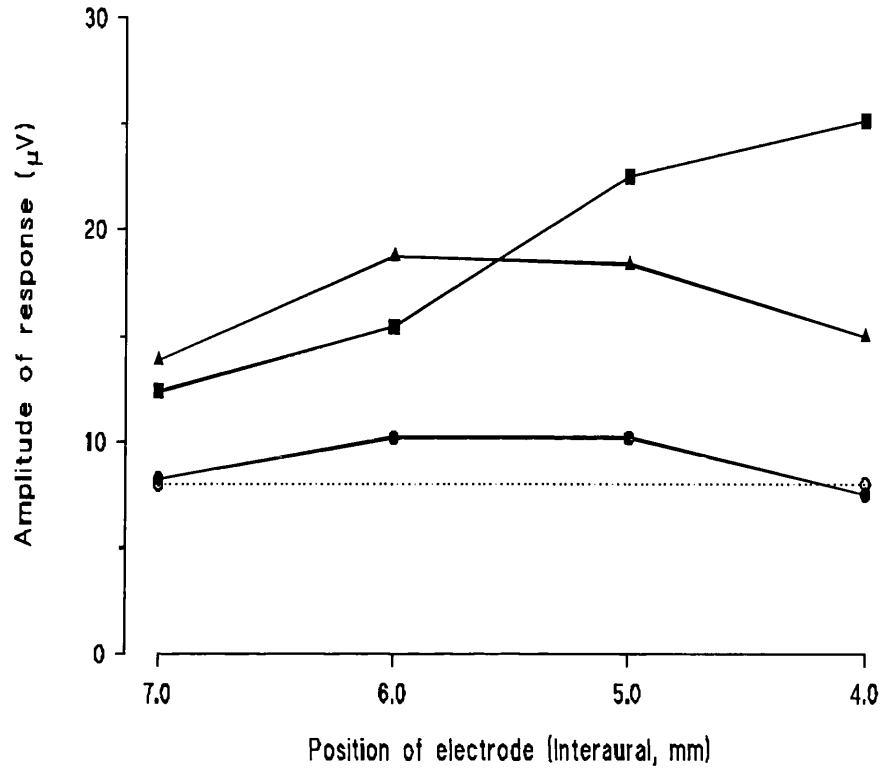

Fig. 3-12. Comparison in P4 amplitude of the cerebellar auditory evoked potentials simultaneously recorded at different depth of the contralateral (■), ipsilateral cerebellar hemispheres (●) and the vermis at the midline (▲) by glass-coated electrode with the response surface-recorded by gross-screw electrode (O).

3.4.5. Effects of intracerebellar injection of procaine on the cerebellar AEP. Five acute experiments were carried out in order to find out more about the afferent pathway and generators within the cerebellum and to test whether this surface-recorded AEP could be used as a functional index of the cerebellum. Procaine (2.5μl 4% procaine in saline) was injected into the central cerebellar white matter between the deep nuclei and the cortices on each side, and AEPs were recorded before and after injections. Figure 3-13 shows the comparison of AEP recordings before and after procaine injection from two different animals. There were clearly decreases in amplitude and delays in latency. Averaged results from five animals showed that the peak latency of the response was delayed from 4.98 ± 0.05 to 5.22 ± 0.16 ms ($p<0.05$, $n=5$), wholly due to an increase in central conduction time (2.79 ± 0.06 to 3.04 ± 0.15 ms, $p<0.05$). Amplitude decreased from 9.27 ± 0.77 to 8.22 ± 0.94 μV ($p<0.05$, Table 3-1.), while the early far-field components were unchanged in both amplitude and latency.

3.5. Discussion

We examined auditory afferents to the cerebellum by recording the auditory evoked field potential via multiple surface and depth electrodes to illustrate the spatial distribution and depth profile of the surface-recorded cerebellar AEP. The surface cerebellar AEP is a complex field potential of multiple components and may represent the summation of activity from multiple dipoles of varying size, orientation and depth under the electrode or even from different locations in a wide range of brain structures. Attempts were therefore made to identify the possible cerebellar generators contributing to the surface potential along the auditory pathway. Evidence for the

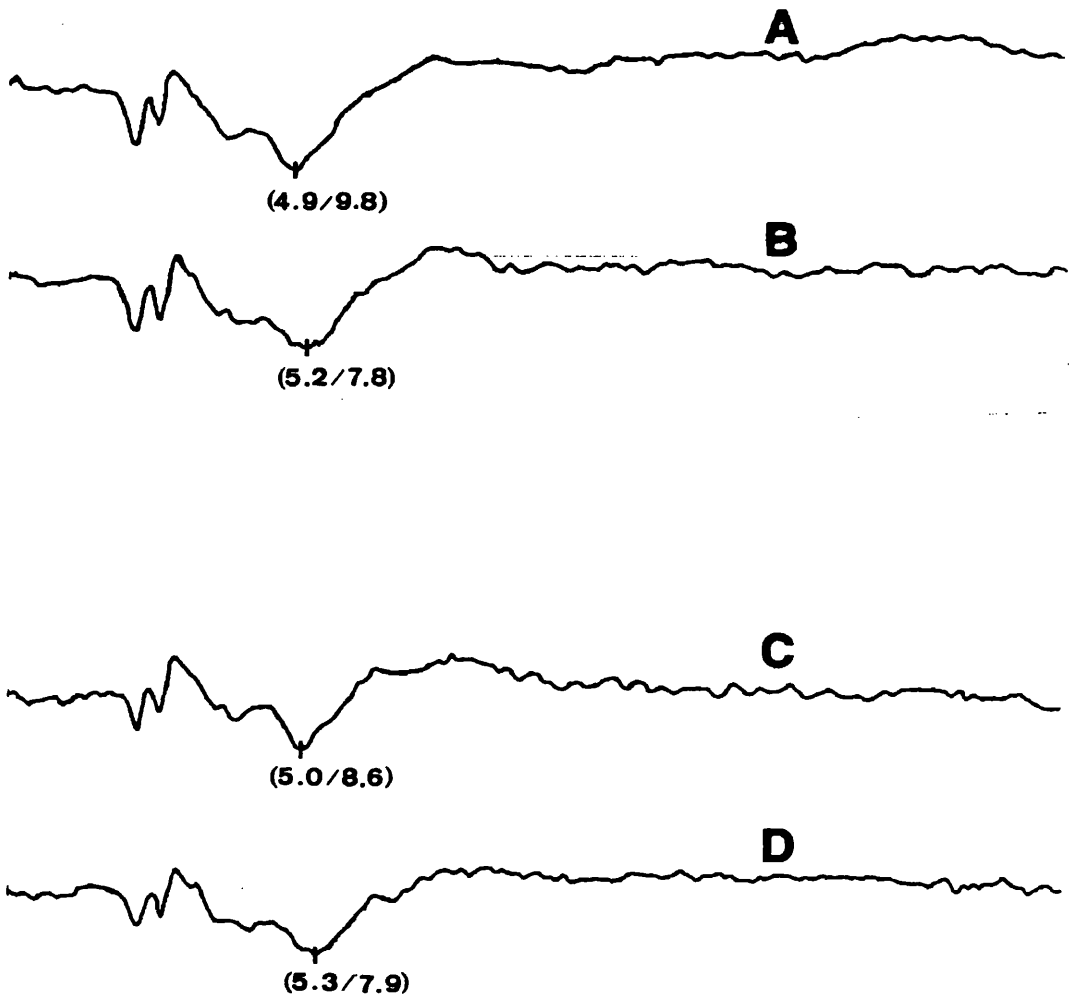

Fig. 3-13. Two examples of the cerebellar AEP altered by the bilateral injection of procaine (4% solution, 2 x 2.5μl) into the cerebellar white matter. The AEPs were recorded over the vermis referring to the electrode placed in the skull between eyes. Actual peak latencies and amplitudes are indicated in parentheses (ms/μV). A, C: Pre-injection recordings; B, D: Post-injection recordings. *: Three-points assessment of peak amplitude.

Table 3-1. Alteration of the surface-recorded cerebellar AEP following intracerebellar injection of procaine.

	Pre-injection	Post-injection	Paired T-test
Latency (ms)	4.98 ± 0.05	5.22 ± 0.16	$P < 0.05$
Conduction Time (ms)	2.79 ± 0.06	3.04 ± 0.15	$P < 0.05$
Amplitude (μv)	9.27 ± 0.77	8.24 ± 0.94	$P < 0.05$

Data are presented as mean ± SD, n=5.

cerebellar origin of P4 is provided by (1) its spatial distribution, which is limited to the occipital region over the cerebellum, (2) its close correlation with the corresponding component recorded within the cerebellum, and (3) its diminution following inactivation of cerebellar fibres. In addition, simultaneous depth recordings of both the collicular and cerebellar responses with a common reference electrode in the present study provide further evidence in support of the theory that cerebellar auditory potentials are genuine and not simply far field reflections of activity generated in the inferior colliculus. Our results clearly differentiate these two responses by the facts that (1) there is neither a spatial nor a temporal relationship, as previously demonstrated by surface recordings (Shaw, 1992), between these two potentials, and a vertex-positive polarity of the cerebellar potential opposes to a vertex-negativity of the collicular potential. These findings provide further evidence to support the theory of Shaw (1995) that the tracts and nuclei of the central auditory system generate a succession of slow overlapping waves of varying polarity with a frequency content which denotes a post-synaptic origin. In the present study, the investigation of the possible generators has also been extended to the early components. The correlation between responses recorded from the cochlear nuclei and early components of the surface potential indicates that the early components P1a and 1b of the surface-recorded cerebellar potential are possibly the distant projections contributed by the cochlear nuclei.

Previous laminar analysis of the focal cerebellar cortical potential indicated that apart from the initial positivity (P_1), the later components (N_1 and P_2) of the surface potential are depth-related within the cerebellar cortex (Shofer, 1969). The amplitude

progressively increased down to a depth of 300 microns below the surface and then became smaller at greater depths with superimposed unit discharges. The unit responses were classified on the basis of latency of unit firing relative to the peak of N_1 (type I) and P_2 (type II) components of the surface response, respectively. At the depths corresponding to the location of Purkinje cells, more type II than type I responses were evoked, and the more deeply situated Golgi and granule cells which receive direct mossy fibre projections were expected to be among the type I units, firing before or at the onset of N_1. The majority of positively identified Purkinje units were little influenced by tones (Altman, *et al.*, 1976), and the surface conditioning stimuli which affect the excitation of the parallel fibres produced predominantly inhibitory effects on auditory activity (Aitkin & Boyd, 1975). The superficial auditory response is, therefore, considered to be generated within the cortex and mediated mostly by the mossy fibres, which activate the granule cells and convey the excitation via their parallel fibres in the molecular layer to the dendritic fields along their pathway, i.e. those of Purkinje, Golgi, basket and outer satellite cells. In the present investigation further examination of the depth profile of the cerebellar response showed that a large peak, at a latency similar to that of the surface response, increased amplitude in contralateral as the recording electrode was seen at the level of the cerebellar nuclei (4.2 mm), while the general waveform of the potential suddenly changed when the electrode moved deeper. Thus, much of the surface-recorded response appears not to be generated exclusively in the cerebellar cortex and it perhaps contains contributions from the deep cerebellar nuclei as well as projections from the colliculi. The field potential of the activated neurones within the cerebellar nuclei would have a close temporal relationship to the cortical response and could contribute,

via volume conduction (conduction within a volume of an electrical conductor including nervous structures which generate the currents and non-nervous structures such as CSF or bone), to the field potential picked up at the surface of the cerebellar cortex or the skull. Morphological evidence for this hypothesis was provided by other investigators (Gilman, *et al.*, 1981; for a recent review, see Voodg, 1995), who showed that many mossy fibre projections terminate not only in the granular layer of the cerebellar cortex but also in the cerebellar nuclei. The mossy afferents from those various extracerebellar sources that terminate in the cerebellar nuclei produce excitatory effects.

Although the cerebellum receives auditory impulses after only a few synapses, as indicated by the short latency of the cerebellar potential, the identification of the afferent pathway is still unclear. On the basis of previous studies, at least four afferent routes have been proposed:

(1) A possible tectopontocerebellar or a tectocerebellar pathway involves the sensory signal being conveyed to the cerebellum via the inferior colliculus and possibly the pons (Highstein & Coleman, 1968; Aitkin & Boyd, 1975). The evidence to support this is the disappearance of the potentials after destruction of the inferior colliculus (Snider & Stowell, 1944). In this case, the auditory afferents project to the contralateral inferior colliculus before the ipsilateral pontine nuclei and then via the pontocerebellar tract to the auditory area of the cerebellum. This hypothesis predicts that the cerebellum should not be activated by auditory stimuli prior to any collicular activity. However, this is contradicted by the fact that the peak latency of the

cerebellar response is shorter than the latency of the collicular response, as demonstrated by the present study and those of others (Lorenzo, 1977; Shaw, 1992).

(2) A second, more direct, projection from the cochlear nucleus to the cerebellum has also been suggested (Highstein and Coleman, 1968; Wolfer, 1972; Aitkin & Boyd, 1975). However, the latency of the activity proceeding along such a pathway would be expected to be earlier than 4 ms.

(3) A third reticulocerebellar pathway has been proposed, in which the cerebellar potentials are produced by crossed afferents from the pontine reticular formation (Shofer, 1969; Lorenzo, 1977). The difficulty with such a multisynaptic route is that a cerebellar potential would most likely have a much longer latency and would be markedly affected by barbiturate anaesthesia, in contrast to the known stability of the major component of the cerebellar response.

(4) A fourth possible pathway is via the ponto-cerebellar pathway to the cerebellum demonstrated morphologically by Mihailoff (1993). Both the basal pontine nuclei and the nucleus reticularis tegmenti pontis were found to send fibres to the cerebellar nuclei as collaterals, most likely from the mossy fibres, that continue into the cerebellar cortex.. This is the tract which would match the timing of both the early brainstem and the late cerebellar potentials revealed in the present study, a view supported by others (Wada & Starr, 1983; Shaw, 1992).

Our results are consistent with some previous findings. There was no significant differences between latencies of responses evoked by stimulating right and left ears separately (Highstein & Coleman, 1968). The waveform evoked by simultaneous binaural stimulation retained its resemblance in shape and latency to that evoked by

monaural stimulation (Highstein & Coleman, 1968) but both subdural and epidural recordings showed binaural facilitation, the amplitude being usually greater than that to monaural stimulation, but less than the sum of the responses obtained by stimulating each ear separately. Single unit recordings have also showed such binaural facilitation, with the greatest effect if tones are of equal intensity at each ear (Aitkin & Boyd, 1975). This evidence indicates that the cerebellar neurones may effectively cross-correlate the inputs from each ear and discharge maximally when these inputs are appropriately matched in timing and intensity. The response following binaural stimuli is, however, smaller than the sum of the potentials obtained by stimulating each ear. This may be either because only a proportion of the cerebellar neurones (mainly in the vermis) receive the auditory afferents from both sides of the auditory pathway, or because facilitation occurs with cross-inhibition, similar to the more pronounced effect in the neocortical AEP, following binaural stimulation, from the contralateral side. Whatever the explanation, the practical consequence is that binaural stimulation with matched time and intensity gives the best cerebellar responses when recorded at the midline over the vermis.

Sensory inputs to the cerebellum have been proposed to play a role in sensorimotor integration (e.g. Ito; 1982; Stein 1986; Houk 1988; Miall *et al.* 1993). Our data provide further evidence that sensory inputs arrive at the cerebellum significantly earlier than at the cerebral cortex (Lorenzo *et al.* 1977; Morissette and Bower 1996). The fast sensory afferents to the cerebellum form the physiological basis for the cerebellum to play a role as a predictor in movement control. An alternative hypothesis has been proposed, that the cerebellum receives primary sensory

information from particular sets of sensory receptors involved in active exploration and then, through the motor system, adjusts those sensory receptors to an optimal position for active acquisition of sensory information on which the performance of the rest of the nervous system is based (Bower 1993; Beitel and Kaas, 1993; Knudsen *et al.* 1993; Gao *et al.* 1996).

Another contribution of the present study is that we demonstrate the potential practical implication of recording the cerebellar AEP as a novel functional index for detecting conductive dysfunction in the cerebellum. Small but significant changes of surface potential (decrease in amplitude, delay in latency and prolongation in the calculated CCT) can be induced by temporary blockade of cerebellar fibres. These responses were therefore used for monitoring experimental myelinopathies in the brainstem-cerebellar auditory pathway (see Chapter 4 and 5). However given the facts that the decrease in P4 amplitude induced by procaine injection was found to be significant but by only 11% (9.27 to 8.24 μV), and the closely similar latencies of the inferior collicular, cerebellar nuclear, and cerebellar cortical responses, it must be pointed out that the overall amplitude of wave P4 probably contains contributions from each of these sources in the rat. The surface-recorded cerebellar AEP may also be clinically applicable for detecting cerebellar disorders provided the corresponding cerebellar component can be identified and is recordable from the scalp in man.

CHAPTER 4.

THE LYSOLECITHIN-INDUCED FOCAL DEMYELINATION IN THE CEREBELLAR WHITE MATTER: MONITORED BY THE SURFACE-RECORDED CEREBELLAR AUDITORY EVOKED POTENTIAL AND DETECTION OF MYELIN BASIC PROTEIN IN THE CEREBROSPINAL FLUID.

4.1. Summary

We evaluated two novel methods for quantitative *in vivo* monitoring of the acute focal demyelination induced by injection of lysolecithin (LPC) in rat cerebellar white matter. These two methods are the measurement of surface-recorded cerebellar auditory evoked potential (AEP) and radioimmunoassay of myelin basic protein (MBP) in the cerebrospinal fluid (CSF), which might ultimately be clinically applicable. F334 rats were surgically prepared by chronic implantation of electrodes for cerebellar AEP recording and of a cannula for CSF sampling. Bilateral demyelinating lesions were induced by injection of 1% LPC (2.5 μl × 2), and then followed by repeated AEP recordings, and CSF sampling with assay for MBP. Results revealed that, as early as 6 hours after injection, a decrease in amplitude of the cerebellar AEP and release of MBP into the CSF occurred. In contrast to the transit amplitude decrease in AEP peaked at 6 hours (18.03 ± 0.83 to 15.97 ± 1.03 μV, mean ± SD, n=7), MBP in the CSF peaked at 24 hours with a value of 88.36 ± 21.50 ng/ml (n = 5), and completely disappeared by day 5. Pathologically, lesions did not completely recover until day 15. We concluded that the surface-recorded cerebellar AEP detected the peak myelin disrupting effect of LPC with decrease in amplitude of the cerebellar component but not the early components generated proximal to the cerebellum, which provided a good indication of lesion sites. The lack of a sustained decrease in responses throughout the period of demyelination, suggested however that the AEP was not a sensitive index of damage in this size. The extent and current status of demyelination was reflected by the level of MBP although this provided no information about where the lesion might be located within the central nervous system.

4.2. Introduction

It has been well demonstrated that focal acute demyelination in both the peripheral and central nervous systems in a number of species, including mouse (Hall and Gregson, 1971; Hall, 1972), rat (Blakemore, 1976), cat (Blakemore, *et al.*, 1977), rabbit (Blakemore, 1978), and primates (Dousset *et al.*, 1996), can be effectively induced by local injection of microlitre qualities of lysolecithin (lysophosphatidyl choline, LPC) which has a strongly myelinolytic action. Unlike many of the other myelinotoxic agents, LPC disrupts the myelin sheath without producing intramyelinic oedema. Such a demyelinating model was applied to study the primary demyelination (Hall, 1972; Blakemore, 1976; Ford, *et al.*, 1990; Payne, *et al.*, 1991) and the subsequent natural remyelination processes (Blakemore, *et al.*, 1977; Gilson and Blakemore, 1993; Jeffery and Blakemore, 1995). Recently, studies based on this local demyelinating model were extended to investigation of the remyelinating and migratory potential of transplanted glial cells (Duncan, *et al.*, 1981; Vignais, *et al.*, 1993; Blakemore, *et al.*, 1994). It is well understood that collapse of the myelin sheath can alter the electrophysiological properties of myelinated nerve fibre (e.g. a recent review, Shrager, 1995) and release myelin breakdown products, such as MBP, into the extracellular space and thereby into the cerebrospinal fluid circulation (Cohen, *et al.*, 1976; Whitaker and Snyder, 1982). The demyelinating and remyelinating processes associated with the injection of LPC are well described pathologically and they can be monitored morphologically *in vivo* using high-resolution magnetic resonance imaging (Ford *et al.*, 1990; Dousset *et al.*, 1996). Despite this, repeatable and quantitative clinical methods for *in vivo* functional monitoring of such lesions still required evaluation due to the importance of assessing both the current status and progression of such lesions.

This investigation was designed to evaluate both the surface-recorded cerebellar AEP (see 3.4.5.) and radioimmunoassay (Barry, *et al.*, 1990) as techniques for *in vivo* monitoring of the effects of demyelination on either neural conductivity or release of MBP into the CSF, respectively. A pathologically well defined rat model of LPC-induced focal demyelination was selected, with the modification of placing the lesions symmetrically in the cerebellar white matter, part of the cerebellar auditory pathway.

Some of these results have been presented to the British Toxicology Society (Liu *et al.*, 1995).

4.3. Materials and methods

(A general description of experimental methods was given in Chapter 2.)

Animals and LPC preparation: Twenty male Fisher/344 rats, weighting 200-250 g were used. LPC, Gamma-O-hexadecyl L-α-lysophosphatidyl choline (L5016, Sigma Chemical Co., Dorset, UK), was prepared, in a similar way to that previously reported by Payne, *et al.*, (1990), as micelles in normal saline by sonication at the concentration of 1% (10 mg/ml). The LPC was dissolved in chloroform-methanol, dried with nitrogen gas, and taken up in isotonic saline. This mixture was sonicated for 2 min × 4 with 5 min intervals between sonications to allow for cooling, then stored at 4°C, and resonicated before injection.

Implantation of cannula into the cisterna magna and placement of gross screw electrodes in the dorsal skull: Details of the cannula implantation and placement of electrodes for AEP recordings have been given in detail elsewhere (see 2.4.). The

animal was anaesthetized (Sagatal 60-70 mg/kg, i.p.) and placed in a stereotaxic frame. A 2 cm midline incision was made and the skin was retracted with the underling tissues. Burr holes were drilled in the dorsal skull for three electrodes: a recording electrode (midline, 2 mm posterior to lambda), an earth electrode (parietal region) and a reference electrode (midline, between eyes). Two more burr holes were drilled at the proposed positions for LPC injection over the cerebellum and covered by two screws before all the electrodes were embedded in dental acrylic, together with a previously attached four pin strip connector, on the dorsal surface of skull. The middle part of the occipital muscles were then dissected from the skull and retracted caudally for implanting the cannula. Finally, the cannula and electrodes were secured in place with more dental acrylic. After 3 - 4 days recovery, all the animals appeared to be in good health, and further samplings of 50 µl at each other day were achieved.

LPC injections: Injections of LPC were carried out stereotaxically under Halothane anaesthesia (< 1.5%) via a 30G needle attached to a 5µl Hamilton syringe. After removing the previously placed covering screws on the burr holes over the cerebellum, injection of 2.5 µl fresh prepared 1% LPC solution was made in one side, slowly over a period of 5 minutes with another 5 minutes before withdrawing the needle over 5 more minutes in order to reduce the possibility of LPC diffusing along the needle track. The same procedure was, then, repeated in the other side to make bilateral lesions. The reasons for inducing bilateral lesions were (1) auditory afferents to the cerebellum are bilateral, and (2) animals would cope with bilateral cerebellar lesions better than with a unilateral one. The site of the injection, as in the experiments of intracerebellar injection of procaine (see Chapter 3), was chosen to be in the cerebellar

white matter above the medial cerebellar nuclei. Control injections of sterilized normal saline of 2.5 μl were made in the same manner in 5 other animals.

Cerebellar auditory evoked potential recording and analysis. The surface cerebellar AEP was repeatedly recorded before and after LPC injection. Recordings were made via an overhead lead which was plugged into the connector while the animals were lightly anaesthetized with halothane (<1.5 %) and kept on a thermostat blanket with a rectal probe in place. Detailed recording techniques and parameters (see Chapter 2) are summarized here: Auditory stimuli were 0.5ms tone bursts of 40 kHz delivered at 5 Hz via a ultrasonic transmitter placed 34 cm directly over the rat's head for binaural stimulation. Stimulus intensity was 118 dB SPL. The responses were collected with filter bandwidth of 3 - 5,000 Hz, averaged 512 - 2048 times, displayed on a monitor. Data was stored on a PC hard disk. Recordings were repeatedly carried out before and every other day until 15 days after injection. Peak latencies of the surface-recorded cerebellar AEP were measured from the onset of stimulus, and the central conduction time (CCT) was calculated by subtracting the peak latency of wave 1a from that of the wave 4. The amplitude of each component was estimated by using a three-point analysis. The inflexions used for measuring are indicated in Fig. 2-7.

Radioimmunoassay of MBP. CSF samples of 50μl were collected before and after LPC injection at the same time as the cerebellar AEP was recorded starting 5-7 days after cannula implantation, and all samples were stored at -20°C until assayed. Prior to assay, each CSF sample was diluted 1 in 2 to 10 in buffer and heated in a boiling water

bath for 5 minutes. After centrifugation the supernatant was used for assay (for detailed assay procedure, see 2.6.).

Clearance rate of the MBP from the CSF: The clearance rate of the MBP from the CSF was determined by repeated CSF samplings of 50 μl (approximate 10% of total CSF volume) at 0.5, 1, 2, 4, and 24 hours after injection of purified MBP with known concentration of 170 μg/ml in three animals (for detailed injection procedures, see 2.5.). Samples were assayed to measure the MBP concentration, and two clearance curves were then plotted with the values of remaining MBP concentration in the CSF against time: (1) values detected in the experiments and (2) detected values plus 10% to compensate for the withdrawal of 50 μl CSF at each time point produced by CSF sampling.

Histopathology: Animals deeply anaesthetized with ether were killed for tissue examination by perfusion of fixative through the left ventricle into the aorta after survival times from 6 hours to 15 days. Histopathology was performed for light microscopy as described in Section 2.9.

4.4. Results

4.4.1. The clearance rate of the MBP from the CSF: Repeated CSF samples after injection of MBP with known concentration of 170 μg/ml were obtained and assayed to measure the concentration of the MBP in the samples against time. Figure 4-1 shows the clearance curve of MBP from the CSF circulation in three animals. The clearance curves were plotted with values, averaged from the results in three animals

and presented as mean ± SD, of remaining MBP concentration in CSF samples collected at different time points (Fig. 4-2). Clearance did not follow a simple mono-exponential relationship, being more rapid at the earlier times and slower at the later. However a mean 50% clearance time was calculated as 140 - 150 minutes with the 10% compensated values to reduce the artefact produced by repeated CSF sampling.

4.4.2. Changes in the cerebellar and neocortical AEPs: Measurements of the peak latencies, amplitudes, and calculated CCT are presented in Table 4-1. The amplitude of cerebellar component P4 was significantly decreased at 6 hours from 18.03 ± 0.83 to 15.97 ± 1.03 μV (Fig. 4-3) without significant change in its latency. There was no significant change in either amplitude and latency of the early P1a, P1b and P3 components, or the CCT over a 15 day observing period after LPC injection. There was no significant change in either amplitude (16.22 ± 1.37 μV) or latency (26.22 ± 2.11 ms) of the P2 over the same period.

4.4.3. Appearance of MBP in the CSF: Measurements of the concentration of MBP in the CSF sampled from the LPC-injected animals are presented in Table 4-2 and Fig. 4-3. MBP appeared in the CSF as early as 6 hours and peaked at 24 hours, started to fall rapidly, and completely disappeared by day 5 after LPC injection. No MBP was detectable in the control animals injected with 0.9% saline in the same manner.

Changes in the AEP amplitude and appearance of MBP in the CSF both occurred as early as 6 hours after intracerebellar injection of LPC (Fig. 4-2). In contrast to the

transient amplitude decrease in AEP, MBP in the CSF peaked at 24 hours, started to fall rapidly, and completely disappeared by day 5.

4.4.4. Histopathological findings: Cerebellar sections collected on day 3 and 15 after LPC injection, in 4 animals, revealed focal demyelinating lesions at the targeted regions around the cerebellar deep nuclei symmetrically about the midline. Under the light microscope (Fig. 4-4a), the areas of demyelination could easily be identified and were 1.0-1.2 mm in diameter. With high power viewing, the cerebellar white matter and neighbouring glial cells at the centre of lesions were found to be severely destroyed accompanying infiltration predominantly by macrophages. Such demyelinating changes reversed mostly by day 15 (Fig. 4-4b).

4.5. Discussion

The myelinolytic effects of LPC have been demonstrated in a variety of mammals in a wide range of structures in both the PNS and CNS. Microinjection of LPC into the sciatic nerve, in addition to the tibial and sural nerve (Sedal *et al.*, 1992), was a favoured PNS model (Hall and Gregson, 1972; Low *et al.*, 1983; Griffin *et al.*, 1989). In a number of studies, focal demyelinating lesions were induced by LPC in the dorsal column of the spinal cord (Hall, 1972; Blakemore 1976; Gilson and Blakemore 1993; Jeffery and Blakemore 1995). Such lesions were also satisfactorily induced in several other locations within the CNS, such as the internal capsule (Ford *et al.*, 1990), the fimbria (Payne *et al.*, 1991), the centrum semiovale (Dousset *et al.*, 1996), and the cerebellum in the present study. Some variation among different locations in time course of progression and pathological features of demyelinating lesion induced by

Table 4-1. Measurements of the cerebellar AEP in the LPC treated rats.

Components	Time Course (day)										
of AEP	0	1/4	1	2	3	4	5	6	7	9	11
Amplitudes	(μV)										
P1a	10.32 ± 1.04	10.73 ± 1.05	11.07 ± 0.49	10.15 ± 0.82	9.90 ± 0.75	9.23 ± 0.78	9.30 ± 0.32	10.78 ± 0.62	9.59 ± 0.91	9.40 ± 0.79	9.39 ± 0.67
P1b	10.31 ± 0.80	10.25 ± 0.88	10.72 ± 0.55	10.41 ± 0.89	9.89 ± 0.49	9.42 ± 0.73	9.90 ± 0.71	10.76 ± 0.71	9.66 ± 0.80	9.26 ± 0.77	9.70 ± 0.39
P3	3.77 ± 0.40	3.88 ± 0.40	4.48 ± 0.49	4.43 ± 0.41	4.19 ± 0.35	4.22 ± 0.52	3.86 ± 0.31	3.87 ± 0.69	4.31 ± 0.47	3.76 ± 0.41	3.86 ± 0.44
P4	18.03 ± 0.83	15.97 ± 1.03**	18.08 ± 0.95	18.26 ± 1.06	18.00 ± 0.80	17.40 ± 0.67	17.50 ± 0.86	18.19 ± 0.94	17.37 ± 0.89	17.23 ± 0.74	17.67 ± 1.25
Latencies	(ms)										
P1a	2.19 ± 0.01	2.21 ± 0.03	2.19 ± 0.01	2.18 ± 0.02	2.17 ± 0.02	2.19 ± 0.02	2.20 ± 0.02	2.22 ± 0.02	2.19 ± 0.02	2.21 ± 0.02	2.21 ± 0.02
P1b	2.48 ± 0.02	2.48 ± 0.01	2.46 ± 0.01	2.46 ± 0.02	2.44 ± 0.02	2.45 ± 0.02	2.47 ± 0.03	2.49 ± 0.03	2.48 ± 0.02	2.47 ± 0.02	2.47 ± 0.02
P3	3.84 ± 0.07	3.86 ± 0.10	3.85 ± 0.08	3.84 ± 0.07	3.82 ± 0.07	3.83 ± 0.06	3.88 ± 0.08	3.94 ± 0.10	3.85 ± 0.08	3.89 ± 0.08	3.87 ± 0.10
P4	4.77 ± 0.07	4.80 ± 0.07	4.84 ± 0.07	4.81 ± 0.08	4.82 ± 0.07	4.83 ± 0.07	4.88 ± 0.09	4.80 ± 0.13	4.83 ± 0.10	4.83 ± 0.09	4.87 ± 0.12
CCT	2.56 ± 0.07	2.59 ± 0.06	2.65 ± 0.07	2.63 ± 0.07	2.63 ± 0.06	2.65 ± 0.07	2.68 ± 0.07	2.62 ± 0.10	2.64 ±0.09	2.62 ± 0.07	2.66 ± 0.11

Data are presented as mean ± S.M.E.; n = 4 to 7.

**: $p<0.01$ (paired t-test)

Table 4-2. Measurements of MBP in the LPC treated rat CSF.

	Before Injection	Time Course (day) 1/4	1	2	3	4	6	10
MBP concentration (ng/ml)	< 5	84.04 ± 18.76	88.36 ± 21.50	32.58 ± 12.60	7.32 ± 1.02	3.75 ± 2.17	< 5	< 5
	n = 5	n = 5	n = 5	n = 5	n = 5	n = 4	n = 4	n = 4

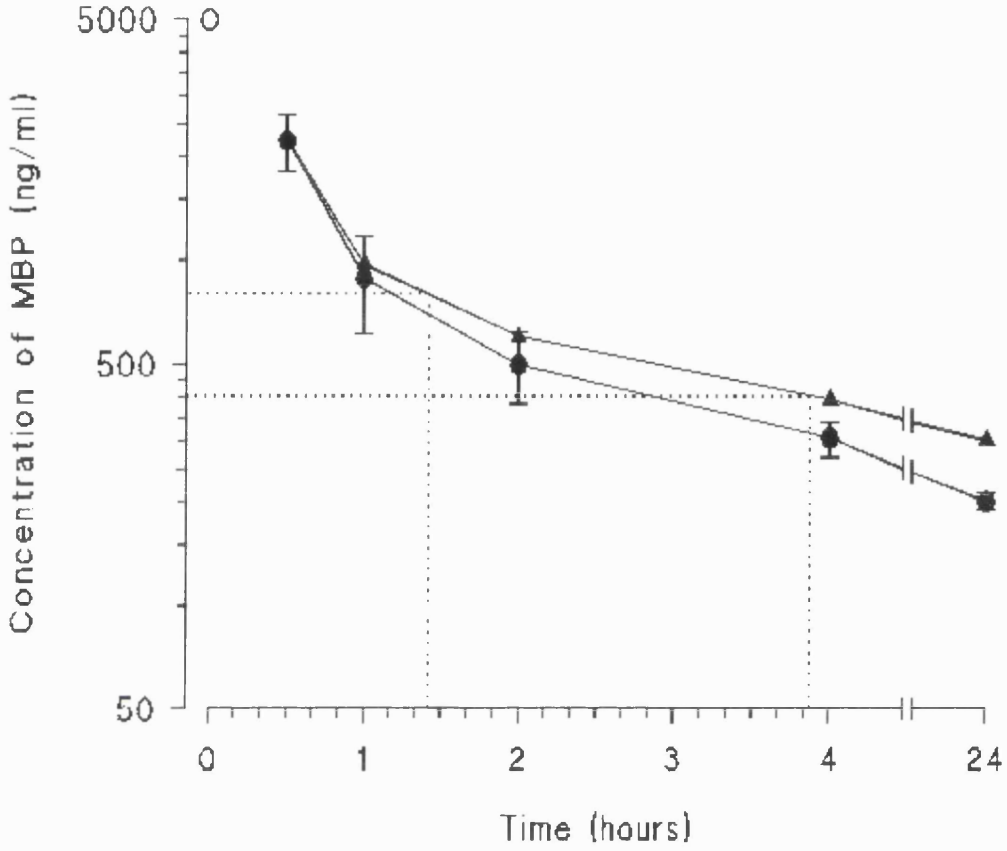

Fig. 4-1. Clearance curve of injected rat MBP in the CSF circulation detected by radioimmunoassay, which gives an approximate 140-150 minutes of fifty percent clearance rate of MBP from the CSF. (O) Theoretical value; (●) Detected values; and (▲) Detected values + 10% compensation for artificial MBP clearance by CSF samplings.

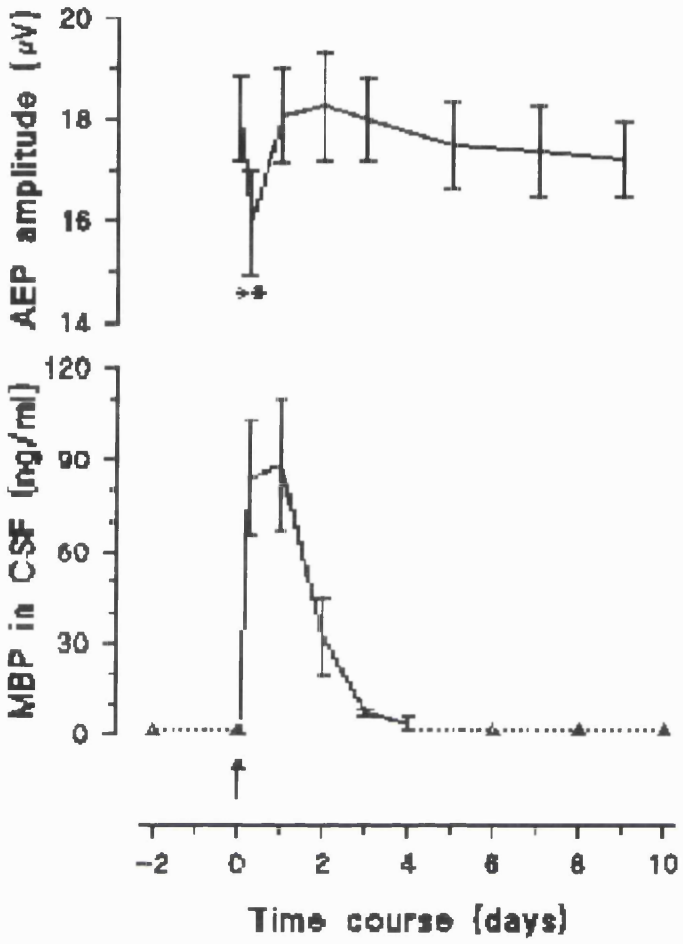

Figure 4-2. Time course of the acute focal demyelination induced by intracerebellar injection of LPC reflected by both decrease in amplitude of the cerebellar AEP (P4) and appearance of MBP-like materials in rat CSF as early as 6 hours after intoxication. Data are presented as mean ± S.E.M., n = 4 to 7. Δ: values < 5 ng/ml; ↑: Time of LPC injection; **: p < 0.01 (paired t-test).

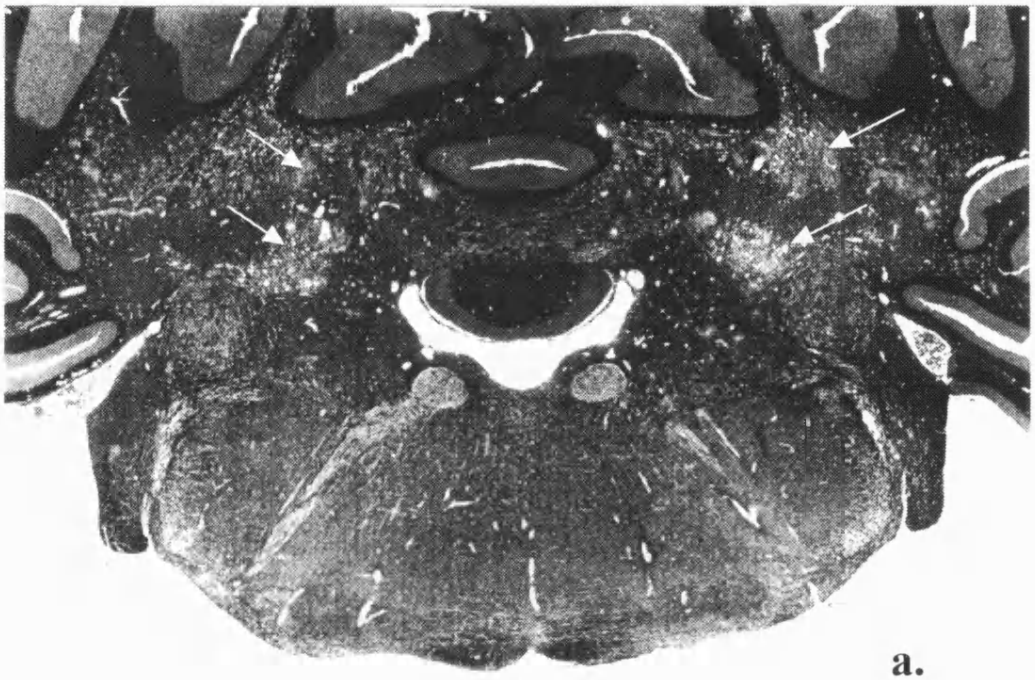

a.

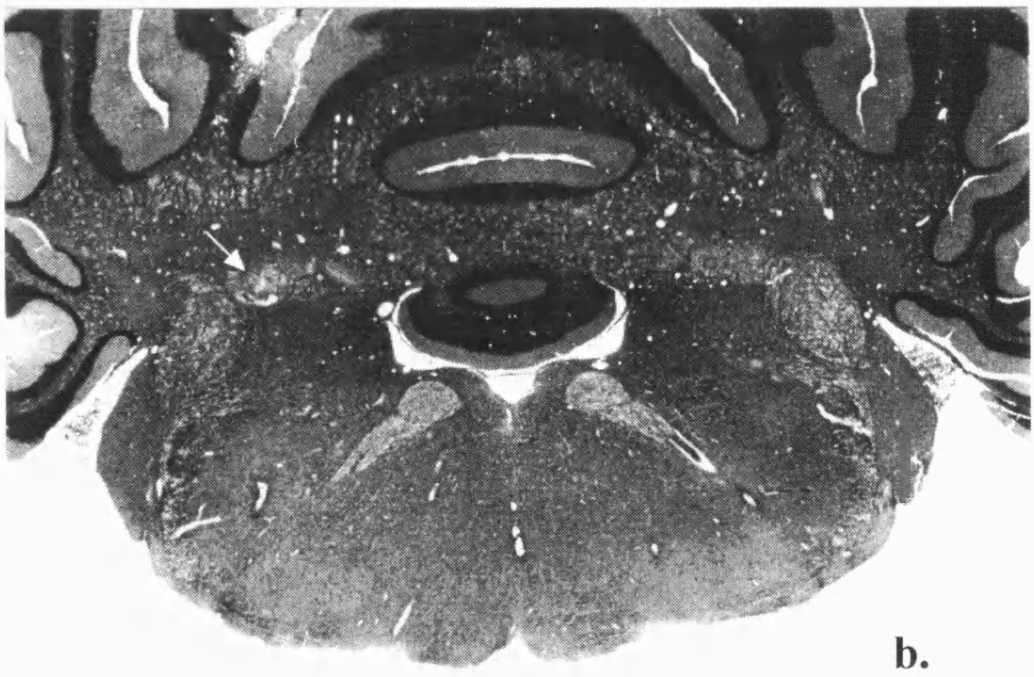

b.

Fig. 4-3. Coronal sections (7 μm) of rat brains perfused with fixative (10% formalin, 2% acetic acid) through the cerebellum and the brainstem. H & E. ×10. Electronic prints were acquired by scanning the conventional photographs.

(a) Three days after injection of LPC (2.5 μl x 2 of 10% LPC-saline solution) into cerebellar white matter, focal demyelinating lesions symmetrically appeared at the targeted regions around the cerebellar deep nuclei as seen under the light microscope. The area of demyelination (white arrows) was well defined, and the cerebellar white matter and neighbouring glial cells at the centre of lesions were severely disrupted and accompanied by predominantly macrophages infiltration.

(b) Compared with (a), the LPC-induced demyelinating lesions in the cerebellar white matter have mostly recovered fifteen days after injection.

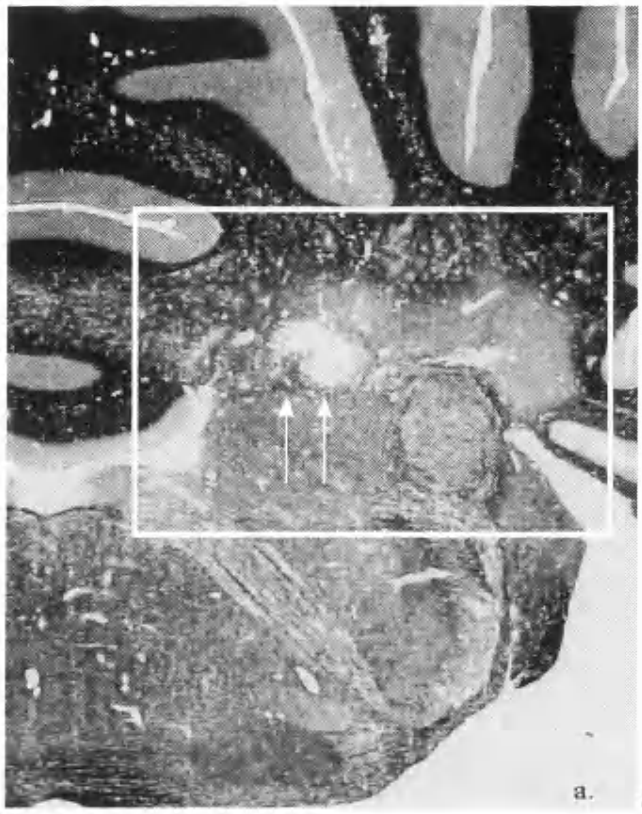

a.

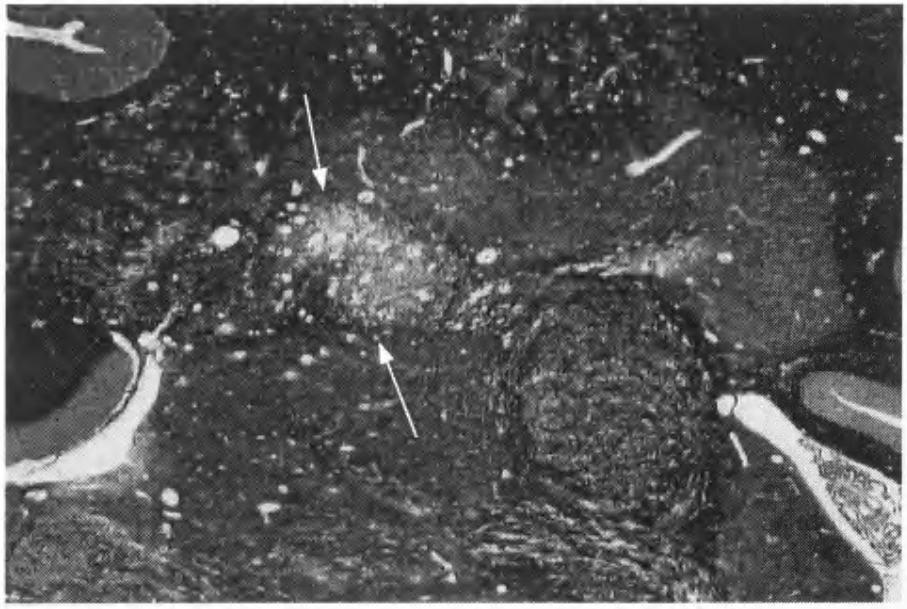

b.

Fig. 4-4. Coronal section (7 μm) from rat brain perfused with fixative (10% formalin, 2% acetic acid), stained with solochrome cyanin for myelin. Electronic prints were acquired by an electronic camera attached directly to the microscope.

(a) Three days after injection of LPC. Focal lesions, approximately 1 mm in diameter, with a sharp margin (white arrows) in the cerebellum, showing almost complete loss of myelin. x10

(b) Higher power view of the demyelinated area with intact nerve fibres and macrophage infiltration. x25

LPC injection is evident from those studies. Hall's (1972) experiment of injecting 0.2 µl, 1% LPC into the dorsal white matter of the adult mouse spinal cord showed that initial signs of myelin sheath disruption occurred within 30 min of LPC injection, with subsequent demyelination of axons. By day 5, the demyelinating process was sharply delineated. Extended observations by Jeffery and Blakemore (1995) showed that demyelination was rapidly followed by remyelination which was first evident at 7 days and involved almost all axons by 10 days. However, the time of the peak demyelinating effect observed morphologically could be different to that detected by function. Payne and co-workers (1991) found that the peak demyelinating effect detected by recording the action potential occurred as late as 6 or 7 days after injection of a small volume of 0.1µl, 1% LPC in rat fimbria. This difference may just be due to the difference in the appearance of demyelinating lesions seen by different method of observation. In confirmation of the previous studies, demyelinating lesions in the present investigation started rapidly after injection, with the peak effect of LPC at 6 or 24 hour detected by the functional indices of surface cerebellar AEP recording or radioimmunoassay of released MBP in the CSF samples, respectively. Despite the fact that the volume of LPC injected in the present study was relatively large, 2.5µl compared to 2.0µl in other studies, no clinical sign of cerebellar damage could be observed after bilateral LPC injections.

The potential application of recording surface cerebellar AEP as a gross index of conductive dysfunction in cerebellar white matter was previously evaluated by temporary inactivation of the cerebellar white matter by local anaesthetic; the cerebellar component was significantly decreased in amplitude and delayed in latency,

with prolongation of the central conduction time (see 3.4.5.). The fact that there was no significant change in the early components generated proximal to the cerebellum indicated that the cerebellar AEP could also be a cerebellum-specific indication, for which there is clear evidence in the present study. Focal demyelinating lesions in the cerebellar white matter produced a significant decrease in amplitude of only the cerebellar component rather than the early brainstem components or the neocortical AEP. Significant conductive delays occurred as reflected both by the cerebellar AEP recorded superficially following intramyelinic oedema induced by TET intoxication (see 5.4.3.) involving both the brainstem and cerebellum and by the action potential recorded locally at the immediate sites around the focal lesion in a brain slice preparation (Payne, *et al.*, 1991). In contrast to the results of procaine injection (see Chapter 3), which reduced amplitude and increased latency, there was no significant delay in the peak latencies of any components of the cerebellar AEP following LPC injection.

Possible explanations for these observations are that (1) the bilateral focal demyelinating lesions (each approximately 1.5 mm in diameter) may have only produced conduction blockade in a few percent of the fibres distributing radically from the cerebellar peduncles to the entire cerebellar cortex; (2) the latency of the cerebellar AEP was determined by the impulses conducted by the undamaged normal fibres projecting to the cortex, with a decrease in amplitude proportional to the percentage of fibres blocked; and (3) a proportion of the surface-recorded potential arising from generators located proximal to the demyelinating sites (e.g. the cerebellar deep nuclei, see 3.5.) was unaffected.

The results obtained in the present study with depth recordings of the cerebellar AEP (see 3.4.4.), focal injection of procaine (see 3.4.5.) and of LPC (in this Chapter) suggest that the interpretation of the AEP changes seen by Verschoyle *et al* (1992) may need to be re-assessed. These authors interpreted the marked decrease in AEP during systemic intoxication of diphenamid to a loss of a cerebellar cortical response, due to 'de-afferentation' via fibres passing up through the area of the cerebellar nuclei. In the light of the present results, it is more likely that much of the reduction was the result of action on generators within the nuclei themselves.

A remaining question is whether the transient decrease in amplitude of cerebellar AEP reflects the overall progression of demyelination and subsequent remyelination. The answer is clearly no. Evidence suggests that the demyelinating process lasts for several days and the earliest remyelination commences only after 7 days (not earlier) after LPC injection (Jeffery and Blakemore, 1995). In the present study, it was believed that the transient decrease in AEP amplitude only reflected the peak myelin disruption produced by focal lesions which were limited in size; in other words, the gross conductive dysfunction caused by the focal demyelinating lesions was just above the threshold of cerebellar AEP detection. The dysfunction was clearly LPC specific, not being seen after control injection, but may have reflected some other more transient and sensitive action, such as the production of local oedema. I propose that recording the cerebellar AEP for monitoring larger focal lesions would be much more effective, and that further evidence correlating changes in the cerebellar AEP recording with pathological findings could be achieved with larger lesions.

A knowledge of MBP clearance rate from the CSF circulation is crucial for the proper correlation of MBP concentration measured in the CSF following myelin breakdown with the current status of myelin collapse. The major concern is that the released MBP may accumulate in the extracellular fluid on its way to the CSF, possible bind to the ependyma, be taken up by cells, and then be released later to produce an artificially high concentration of MBP (a false-positive result) after myelin collapse has already ceased. On the other hand, a decline of MBP concentration does not necessarily mean that myelin collapse has already ceased. It could indicate, alternatively, that the release rate of MBP from the myelin sheath had fallen below the clearance rate of MBP from the CSF. This rate can be estimated by a rough calculation of the maximum quantity of MBP available to be liberated from the LPC-induced demyelinating lesions and how much of it is actually liberated to the CSF circulation over the first 24 hours. Assuming MBP is 30% of brain myelin protein, myelin protein in myelin is about 30% of dry weight, and white matter of dry weight is about 2% that of wet weight, then MBP is about 0.18% of wet white matter. Thus in $3mm^3$ LPC-induced lesions there will be a total of 5.4μg MBP. It has been shown in the present study (see MBP clearance curve with 10% compensated values in Fig. 4-1) that approximately 300ng/ml of MBP remains in CSF circulation 24 hours after an artificial injection of 5μg/ml MBP injection. Thus if a total of 5.4μg MBP were instantaneously released into the CSF, it would give a MBP concentration of 320ng/ml at 24 hours instead of the detected value of 88ng/ml. By comparing these figures it can been seen that approximately 27% (88/320) of total available MBP in the lesions would appear in the CSF over the first 24 hours. Given the approximate nature of this calculation, it is still quite difficult to estimate precisely the amount of MBP that accumulates in the

extracellular fluid on its way to the CSF, binds to the ependyma, and is taken up by cells, but it would appear that at least a substantial proportion of the MBP is released into the CSF over the first 24 hours. Part of the remaining MBP appears to continue to be released after the initial response, as indicated both in the present experiments by the appearance of MBP in the CSF lasting for up to 4-5 days after LPC injection and by the similar time course revealed pathologically by others (Hall, 1972; Jeffery and Blakemore, 1995). It is therefore that the time course of MBP appearance in the CSF correlates that of myelin collapse although this provided no information about the location of the lesion within the CNS. In comparison with the experiment of the reversible intramyelinic oedema induced by TET (see 5.4.4.), in which there is no myelin destruction and thus no MBP can be detected, MBP is a selective indicator of demyelination.

The sensitivity of the present MBP assay can be expressed in terms of its lesion threshold (the minimum quantity of demyelinating lesion to give a positive MBP detection by the assay). Such a threshold can be calculated as follows: Rat brain is about 2g or 1500 mm^3. The lesions of 1.5 mm^3 x 2 induced by LPC injections in the present experiments are therefore approximately 0.2% of total brain weight and give a peak value of 88 ng/ml MBP in CSF. If twice the detection limit of the assay, i.e. 2 x 5 ng/ml = 10 ng/ml, is used to determine the lesion threshold for MBP assay, it will be only approximately 0.022% of total brain. If the brain : CSF ratio in the rat is no higher than that in the human, then a lesion equivalent to that in the rat will be 2200 mm^3 or a focal lesion of approximately 16 mm in diameter which is slightly larger than the average size of a single plaque in multiple sclerosis, and the MBP method

would work just as well for disseminated lesions of the same total volume which may not detectable by imaging.

Abnormalities in evoked potentials (Jones, 1995) and CSF (Bentz, 1995) help support the clinical diagnosis of demyelinating disorders in the CNS such as multiple sclerosis. Multiple modality evoked potentials are usually required to detect lesions in different neural pathways. There is, however, a lack of neurophysiological indication of conductive dysfunction in the cerebellar pathway for lesions limited to the cerebellum. The surface-recorded cerebellar AEP has been shown by the present experimental results to be an index of cerebellar conduction which may be ultimately extended to clinical application if the corresponding cerebellar component can be identified and is recordable from the scalp in man. We have also demonstrated that the MBP released into the CSF following chemically-induced experimental demyelination can be detected by the assay originally designed for detection of immunologically-induced myelin breakdown, which indicates that the MBP-like materials released in both pathological conditions cross-react to the same anti-MBP antibody although the exact structure and biochemical constituents of the myelin breakdown products in both conditions are still not clearly identified.

CHAPTER 5.

TRIETHYLTIN-INDUCED ACUTE OTOTOXICITY AND MYELINOPATHY IN RATS: MONITORED BY SURFACE-RECORDED AUDITORY EVOKED POTENTIAL AND RADIOIMMUNOASSAY OF MYELIN BASIC PROTEIN IN THE CEREBROSPINAL FLUID

5.1. Summary

The acute hypothermia, ototoxicity and myelinopathy induced by a single intraperitoneal dose of 8 mg/kg triethyltin bromide (TET) in rats were investigated using two novel *in vivo* methods of surface-recording cerebellar auditory evoked potential (AEP) and radioimmunoassay of myelin basic protein (MBP) in the cerebrospinal fluid. Animals were surgically prepared with implantation of surface electrodes for AEP recording and a cannula for cerebrospinal fluid (CSF) sampling. In addition to assessments of body weight, rectal temperature and ataxia-weakness of limbs, the surface AEP was repeatedly recorded, and MBP in the CSF samples was detected. Results revealed that TET induced a transient hypothermia peaking at 24h, accompanied by significantly decreased AEP amplitudes. The first decrease occurred in the early components indicating direct cochlear damage. Motor deficits, ataxia (disturbances in co-ordination of body movement and balance) and hindlimb weakness developed gradually in parallel to the significant delay in latency of both the AEP late component (with prolongation of the CCT) and of the SEP. Furthermore, the temperature dependence of nerve conduction was significantly increased by TET. Thus TET produces two phases of toxicity: (1) a rapid transient general depression of the CNS and a rapid but persistent ototoxicity, and (2) a slower reversible myelinotoxicity. No detectable MBP was found in the CSF at any time throughout the experimental period. Pathological sections showed reversible intramyelinic vacuolation in widespread brain structures.

5.2. Introduction

Acute intoxication with triethyltin (TET) in experimental animals has been intensively studied over the past decades to investigate possible neurotoxic mechanisms. The classical rat models of TET intoxication that were used commonly included oral, intraperitoneal, intravenous, or intraventricular dosing, and acute, subacute, and chronic intoxication were then produced by varying the dosage and route. It is clear that TET produces specific pathological changes confined to the cerebral white matter that can be best described as an intramyelinic oedema with vacuoles formed by the splitting of the intraperiod line (e.g. reviewed by Watanabe, 1980; Cavanagh and Nolan, 1994). Mechanisms of TET intoxication proposed are that TET induces myelinopathy in the following ways.

(1) At low concentrations (2 μM), given the presence of an ionic gradient, rapid penetration of Cl^- takes place in exchange for OH^- by a non-energy consuming process, accompanied by an inflow of water (Aldridge, 1977).

(2) At higher concentrations of TET (up to 8 μM in the brain), there is uncoupling or inhibition of mitochondrial oxidative phosphorylation which is normally required by the ionic pumps to maintain active transport of fluid and electrolyte across cell membranes (Aldridge and Street, 1971; Aldridge, 1977; Leow *et al.*, 1979; Kauppinen *et al.*, 1988).

(3) By the direct inhibition of ATPase (Snoeij *et al.*, 1985; 1987; Stine *et al.*, 1988).

More recently, these studies of organotin toxicity have been extended to investigate peripheral neurotoxicity (Allen, *et al.*, 1980; Richman and Bierkamper, 1984), developmental neurotoxicity (Watanabe, 1977; Blaker, *et al.*, 1981; Freeman *et al.*,

1994; Barone *et al.*, 1995), behavioural neurotoxicity (Squibb *et al.*, 1980; McMillan and Wenger, 1985; Broxup *et al.*, 1989), and ototoxicity (Crofton *et al.*, 1990; Clerici *et al.*, 1991; Hoeffding and Fechter, 1991; Clerici *et al.*, 1993).

In addition to the pathological and biochemical approaches, a number of indicators have been developed and employed in monitoring TET toxicity *in vivo*. Recordings of the electroencephalogram and evoked potentials have been employed to quantify the conductive abnormality (Amochaev *et al.*, 1979; Dyer and Howell; 1982a, b), and urinary cholesterol metabolites have been measured to determine the rate of central demyelination (Nicholas and Taylor, 1994).

In the current study, we investigated the acute hypothermia, ototoxicity and myelinopathy induced by TET in rats, with emphasis on the *in vivo* monitoring of acute and reversible toxicity of TET by means of the surface-recorded auditory evoked potential (AEP) and radioimmunoassay of myelin basic protein (MBP) in the cerebrospinal fluid (CSF). These techniques may ultimately be applicable clinically.

Some of the results have been presented to the British Toxicology Society (Liu and Ray, 1995b).

5.3. Materials and methods

Animals and TET intoxication. Twenty male Fisher 344 rats, weighting 200-250 grams were used. TET (triethyltin bromide, MRC Toxicology Unit, UK), was dissolved in sterile saline to make 8 mg/ml solution. A single intraperitoneal dosage of

8mg/kg, *i.p.* was used. Controls were two rats intraperitoneally injected with the same volume of normal saline.

Clinical observations. Body weight, rectal temperature and ataxia and weakness of limbs were assessed throughout the experimental period. Ataxia and weakness of limbs were assessed by investigators according to the following 10-point scale described by Ray *et al* (1996): 0 = normal. 1 = body sways when walking. 2 = legs extended or splayed when walking. 3 = slow to pick up hind legs when walking. 4 = clear signs of hind limb weakness. 5 = occasionally drags a leg when walking. 6 = hind legs splayed out behind body. 7 = some additional forelimb weakness. 8 = cannot lift 350g with forelimbs. 9 = difficulty in righting body. 10 = full ataxia, unable to right body.

Implantation of cannula into the cisterna magna and placement of gross screw electrodes in the dorsal skull: Details for the cannula implantation have been described in detail elsewhere (see 2.4.). CSF cannula were implanted together with the electrodes for AEP and SEP recordings. The animal was anaesthetized (Sagatal 60-70 mg/kg, *i.p.*) and placed in a stereotaxic frame. A 2 cm midline incision was made and the skin was retracted with the underling tissues. Burr holes were drilled in the dorsal skull for three electrodes (1 mm diameter, stainless steel screws): a AEP recording electrode (midline, 2 mm posterior to lambda), a SEP recording electrode (parietal region) and a reference electrode (midline, between eyes). The middle part of the occipital muscles were then dissected from the skull and retracted caudally for implanting the cannula. Finally, the cannula and electrodes were secured in place with

more dental acrylic. After 3 - 4 days recovery, all the animals appeared to be in good health, and further samplings of 50 µl every other day were achieved.

Cerebellar AEP and neocortical SEP recording and analysis. The surface AEP and in some animals SEP were repeatedly recorded before and after TET injection. Recordings were made via an overhead lead which was plugged into the connector while animals were lightly anaesthetized by isoflurane (<1.5%) and kept on a thermostat blanket with a rectal probe in place. Auditory stimuli were delivered 34 cm directly over the rat's head for binaural stimulation. Stimulus intensity was 118 dB SPL. Data was stored on a PC hard disk. Recordings were repeatedly carried out before and every other day until 15 days after injection. Peak latencies were measured from the onset of the stimulus, and peak-peak measurement was used to estimate amplitudes. For cortical SEP, electrical stimuli were 0.1 ms square wave delivered at 1 Hz via a stainless steel needle over the median nerve at the wrist. Intensity (usually in the range of 4 - 10 volts) of stimuli was determined as up to 3 times above the threshold intensity producing thumb twitch. The reference electrode was subcutaneously placed 1.5 cm from the stimulating electrode.

Radioimmunoassay of MBP. CSF samples of 50µl were collected before and after LPC injection at the same time as the cerebellar AEP was recorded starting 5-7 days after cannula implantation, and all samples were stored at -20°C until assayed. Prior to assay, each CSF sample was diluted 1 in 2 to 10 in buffer and heated in a boiling water bath for 5 minutes. After centrifugation the supernatant was used for assay (for detailed assay procedure, see 2.6.).

Histopathology: Animals deeply anaesthetized with ether were killed for tissue examination by perfusion of fixative through the left ventricle into the aorta at 3 and 15 days. The brains were sliced coronally for 7 μm sections stained with Hematoxylin and Eosin. Electronic prints of the sections were acquired by scanning conventional photographs.

5.4. Results

5.4.1. Clinical assessment of acute systemic toxicity in rats. Body temperature in a controlled environmental temperature of 22±2°C was decreased soon after intoxication with TET reaching a peak effect at 24 hours, then rapidly recovered within the next two days, and slowly returned to normal over a period of 6 days afterwards (Fig. 2a). Body weight was reduced by TET intoxication reaching the lowest level on day 7 and then recovered to gain at normal growth rate compared with controls (Fig. 2b). Ataxia and weakness of the hindlimbs was developed promptly and gradually recovered over the entire 15 days of observing period (Fig. 2c).

5.4.2. Interaction of TET with anaesthetics. The decrease in body temperature induced by isoflurane anaesthesia was enhanced by intoxication with TET. Before TET intoxication, rectal temperature gradually decreased from 38°C and remained at 36°C over a period of 100 minutes under anaesthesia as the concentration of isoflurane was gradually reduced from 3% (induction concentration) to the lowest maintaining concentration of 1.2 %. In contrast, on day 1 after TET intoxication, rectal temperature was under 37°C before anaesthesia and was more rapidly decreased to 33°C under an even lower concentration of isoflurane over the same observing period. The

environmental temperature in both cases was 22 ± 2°C (Fig. 3a). It was also noticed that the lowest isoflurane concentration for maintaining the lightest anaesthesia after TET intoxication was significantly reduced from 1.5 ± 0.07% to 0.75 ± 0.07% (Fig. 3b).

5.4.3. Monitoring TET toxicity with cerebellar AEP and cortical SEP. The surface-recorded cerebellar AEP were repeatedly recorded via implanted gross screw electrodes before and every other day after TET intoxication to monitor TET toxic effects on the cerebellar auditory pathway. The amplitude and latency of each component of the auditory evoked potential over the experimental period are presented in Table 1 as mean ± S.M.E, and examples of AEP potential traces from two animals are illustrated in Fig. 4. During each recording session, body temperature was maintained by a heating blanket at 38 ± 0.5 °C. Every component was significantly affected by TET with a general feature of increase in latency and decrease in amplitude, in which the decrease in amplitudes of P1a and P1b on day 1 was the most dramatic event, and the central conduction time (P1a - 4) was significantly prolonged with the longest CCT on day 3 (Fig. 5). These changes were gradually reversed but not completely until day 15, except for the P4 latency and the CCT. Temperature dependence of impulse conduction along the normal and insulted auditory pathway was investigated by observing the effect of body temperature on the conduction time (Fig. 6). When body temperature decreased from 38°C to 36°C induced by either isoflurane or TET, the conduction time was prolonged 0.09 ± 0.04 ms (n = 8) before dosing, and 0.36 ± 0.08 ms (n = 6) on day 3 after dosing, which was a significant difference ($P<0.05$, unpaired t-test).

The cortical SEP was recorded by placing a screw electrode in the skull over the somatosensory cortex and stimulating the contralateral median nerve at the wrist with body temperature maintained at 38 ± 0.5 °C. The peak effects on day 5 - 7 (similar to AEP recording) of TET intoxication on the SEP are illustrated in Figure 6-6, and show a marked delay in latencies and decrease in amplitude indicating the extent of myelinopathies along the somatosensory pathway.

5.4.4. No MBP detectable in the CSF. Twenty-four CSF samples from 8 animals (2 controls and 6 dosed animals) at different time points pre- and post-intoxication (up to day 12) were assayed for detection of MBP like materials. There was no detectable MBP in any CSF sample.

5.4.5. Histopathological findings. Brain sections from intoxicated rats obtained at 72 hours or at day 15 and stained with H&E illustrate that TET-induced myelinopathy, presented as intramyelinic vacuoles, widely distributes in the cerebral, brainstem and cerebellar white matters (Fig. 7a), and most of such myelin oedema were spontaneously disappeared by day 15 (Fig. 7b). No obvious cellular change was found from those sections under light microscope.

5.5. Discussion

The results of the present study reveal that TET induced two phases of toxicity: (1) The early phase peaking at 24 hours after dosing; there was a rapid transient general depression of the CNS reflected by both hypothermia and increased susceptibility to

Table 5-1. Alteration of the auditory evoked potential before and after TET intoxication.

Components				Time	course	(day)			
of AEP	0	1	3	5	7	9	11	13	15
Amplitudes	(μV)								
P1a	7.24±0.53	2.70±0.43**	4.30±0.47**	4.49±0.25**	5.15±0.46*	4.41±0.54**	5.68±0.24*	5.52±0.40*	5.85±0.33*
P1b	6.64±0.41	3.28±0.49**	4.23±0.54**	4.12±0.23**	4.19±0.43**	3.48±0.51**	4.27±0.16**	4.57±0.29**	4.53±0.25**
P3	2.85±0.25	1.59±0.13**	2.19±0.11*	1.89±0.10**	1.89±0.10**	1.87±0.22*	2.05±0.16*	2.03±0.16*	2.04±0.19*
P4	12.1±0.58	8.28±0.48**	8.81±0.40**	8.89±0.50**	9.19±0.47**	8.53±0.43**	9.41±0.32**	10.1±0.52*	9.58±0.29**
Latencies	(ms)								
P1a	2.19±0.01	2.29±0.02**	2.26±0.02**	2.25±0.01**	2.24±0.01**	2.27±0.02*	2.24±0.01*	2.22±0.01	2.24±0.01*
P1b	2.49±0.01	2.73±0.05**	2.67±0.03**	2.63±0.02**	2.63±0.03**	2.63±0.04**	2.57±0.01**	2.57±0.02**	2.56±0.02**
P3	3.63±0.03	3.86±0.04**	3.77±0.05*	3.78±0.03	3.73±0.07	3.80±0.04**	3.88±0.05**	3.77±0.04*	3.78±0.03**
P4	4.86±0.04	5.03±0.06*	5.08±0.06*	5.06±0.04*	5.04±0.08	4.99±0.07	4.94±0.05	4.90±0.04	4.90±0.05
CCT	(ms)								
	2.66±0.04	2.74±0.06	2.83±0.06*	2.81±0.04*	2.80±0.07	2.72±0.06	2.71±0.05	2.68±0.04	2.66±0.05

Data are presented as mean ± S.M.E.; n=8.

**: $p<0.01$; *:$p<0.05$ (t-test).

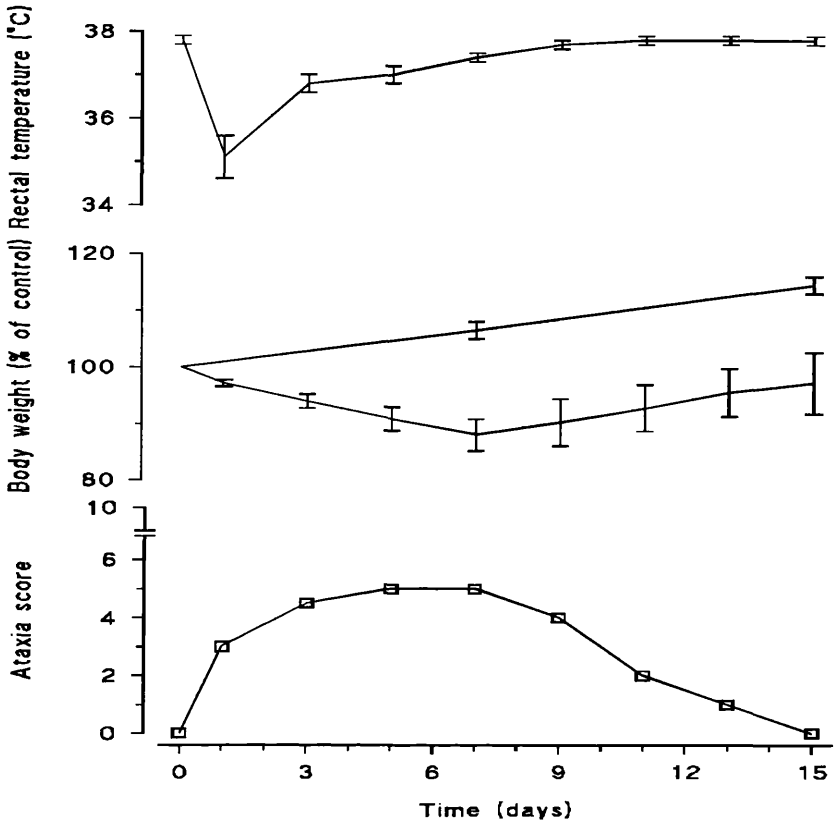

Fig. 5-1. Reversible changes of rectal temperature under controlled room temperature of 22 ± 2 °C, body weight comparing with control, and limb weakness-ataxia score over the observing period of TET (8 mg/kg, i.p.) intoxication in F344 rats. Data are presented as either mean ± SD in temperature and weight or median in ataxia; n = 8.

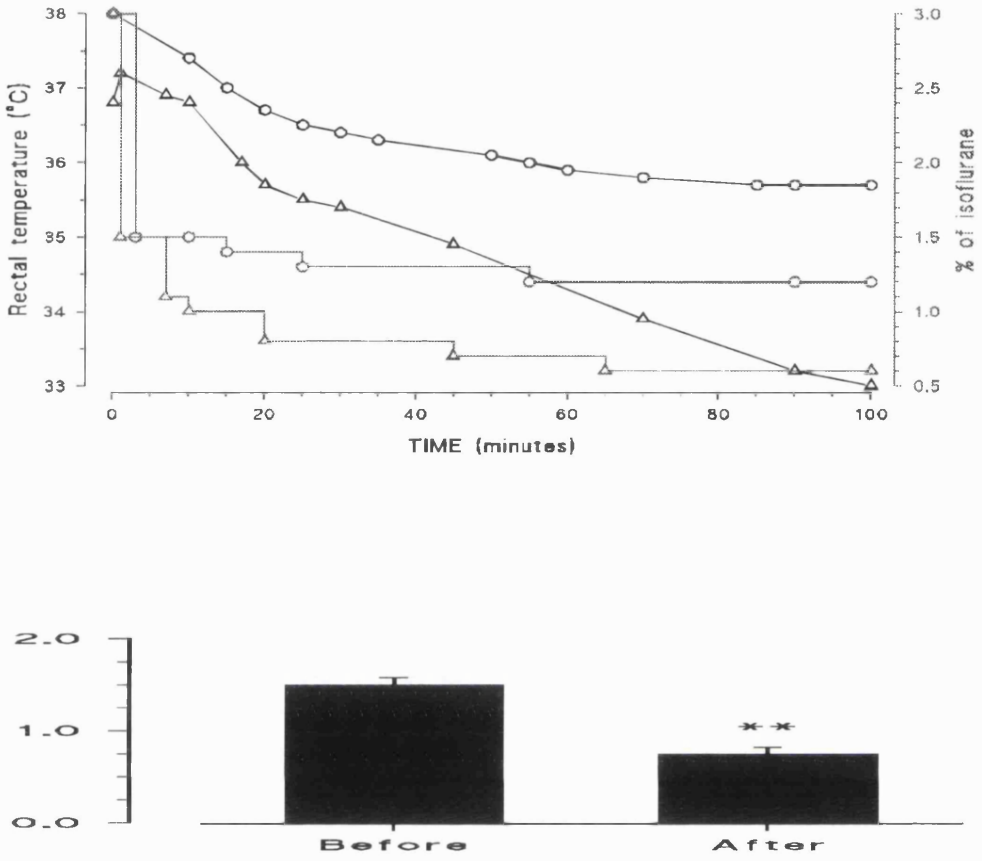

Fig. 5-2. Deeper anaesthetic hypothermia and significant reduction of isoflurane required to maintain anaesthesia caused by TET. a: An example of the lower rectal temperature decrease 72 hours after dosing (Δ) than that pre-dosing (O) under the same environment temperature of 22 ± 2°C and the same depth of anaesthesia (with reduction of the concentration of Isoflurane required to maintain that anaesthesia). b: The concentration of isoflurane required to maintain the lightest level of anaesthesia in 7 animals 72 hours after dosing was significantly reduced compared with that required in the same animals before intoxication. Data are presented as mean ± SD; n = 7; $p < 0.001$ (paired t-test).

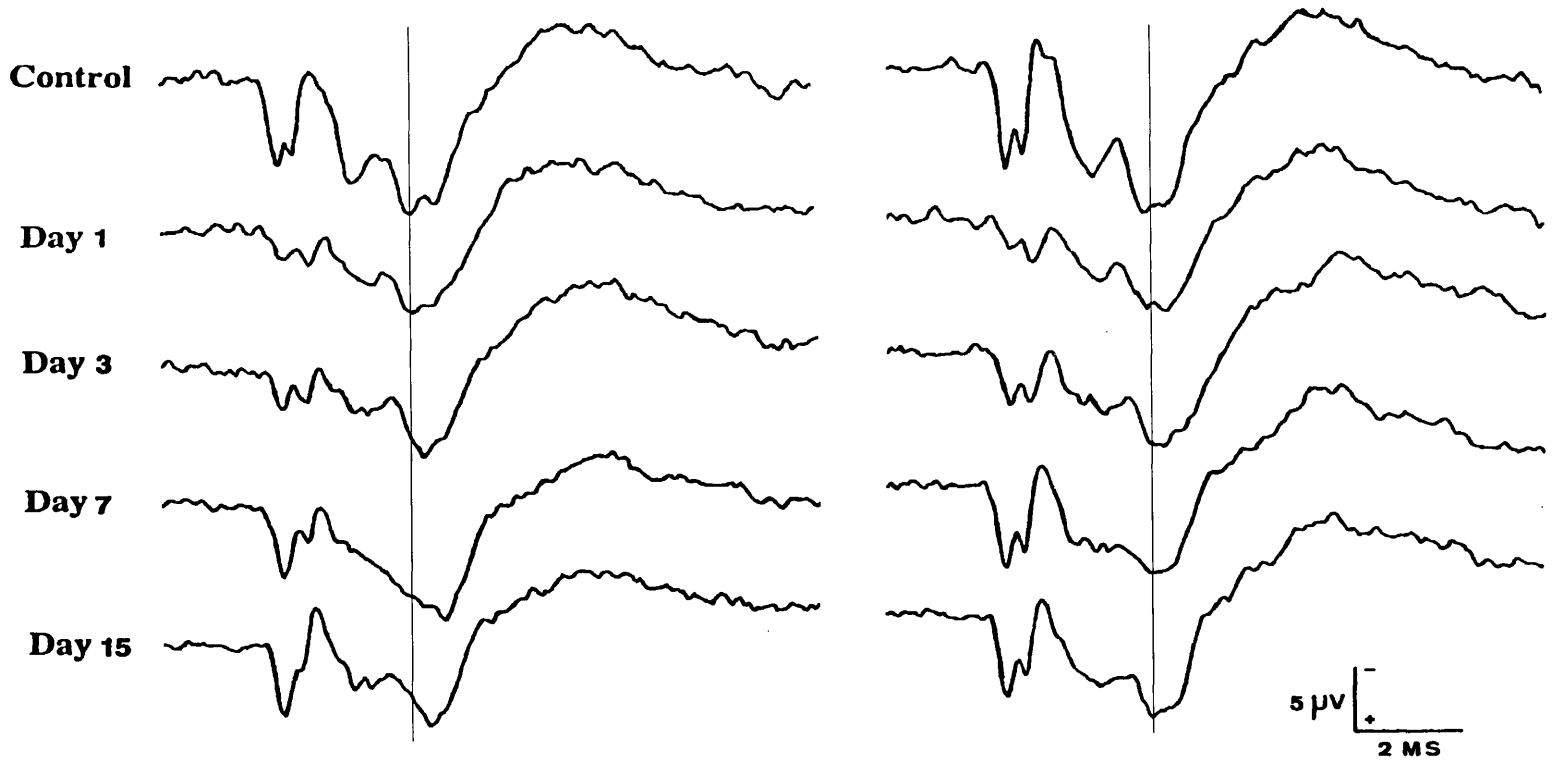

Fig. 5-3. Two examples (left half and right half) of various components of the cerebellar AEP reversibly altered over 15 days of TET intoxication reflected by the changes in amplitudes and latencies. The time point of recording is marked at the left hand side of each corresponding trace. P4 latency is marked by a line.

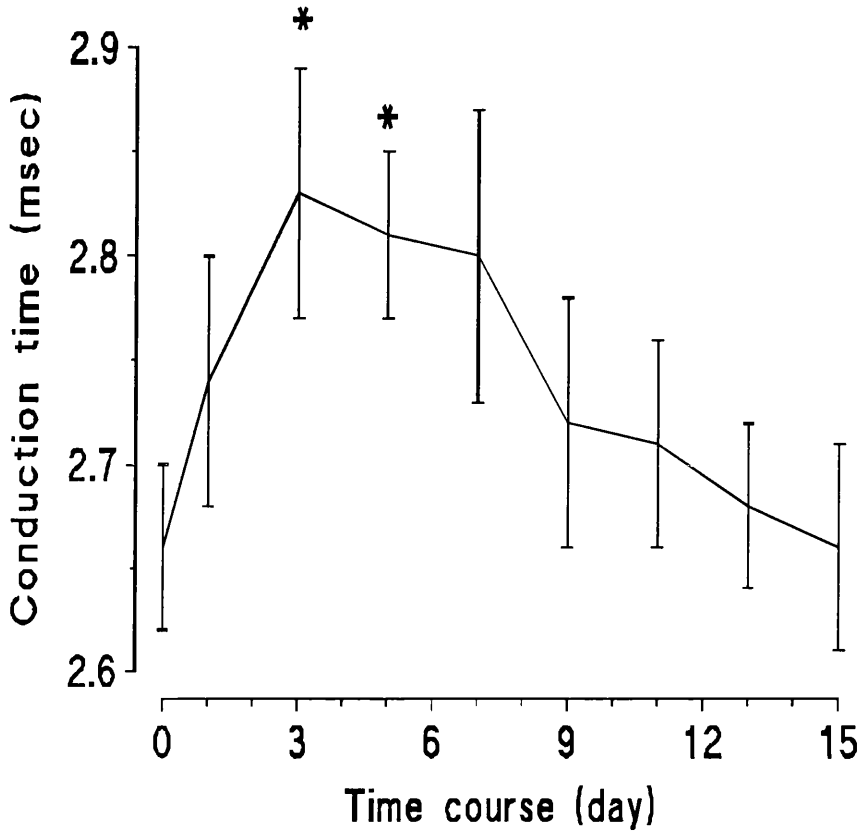

Fig. 5-4. Significant prolongation of the calculated conduction time (Interpeak interval of P1a - 4) at 72 hours after TET intoxication. Data are presented as mean ± S.M.E., n = 8; *: $p < 0.05$ (paired t-test).

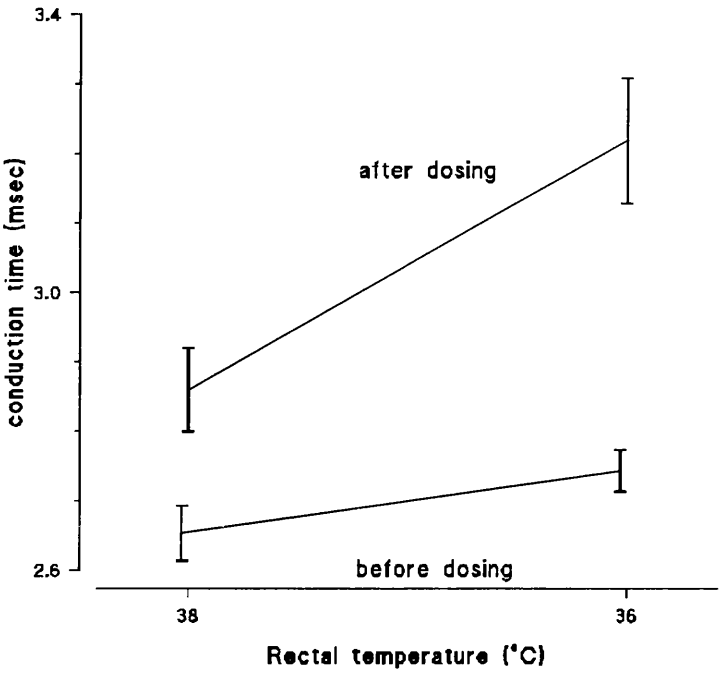

Fig. 5-5. The temperature dependence of nerve conduction significantly increased in the TET-induced myelinopathy. The prolongation of the conduction time when the rectal temperature in animals decreased under anaesthesia from 38°C to 36°C significantly increased at 72 hours after TET intoxication (top trace) compared to before dosing (bottom trace). Data are presented as mean ± S.M.E., n = 6; $p < 0.05$ (paired t-test).

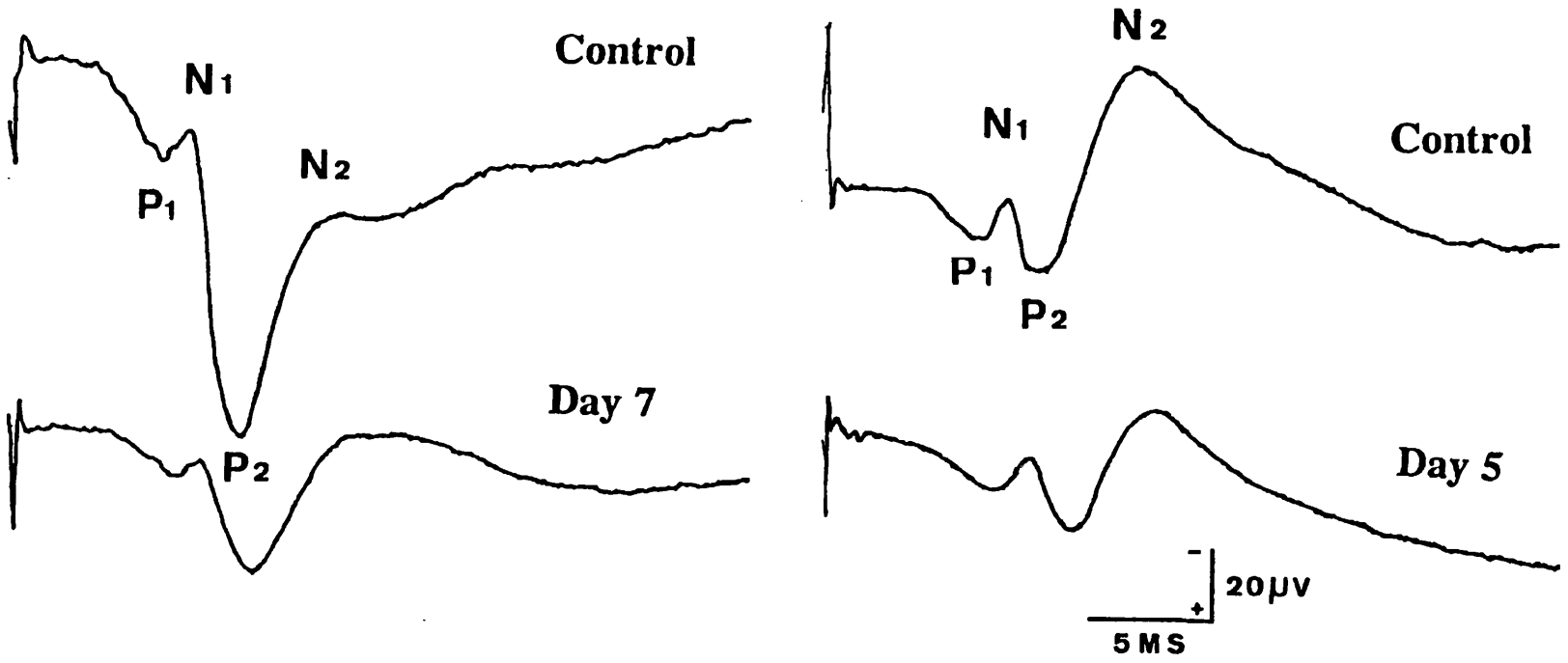

Fig. 5-6. Two examples (left half and right half) of various components of the cortical SEP altered by TET intoxication reflected by the decrease in amplitude and delay in latency peaking at day 5 and 7. The time point of recording is marked at the left hand side of each corresponding trace.

a.

b.

Fig. 5-7. Coronal sections (7 μm) through the cerebellum and the brainstem of rat brains perfused with fixative (10% formalin, 2% acetic acid). H & E. ×10. Electronic prints of the sections were acquired by scanning conventional photographs.

(a) Three days after receiving TET (8 mg/kg, i.p.), the intramyelin vacuoles (white arrows) are bilaterally distributed throughout the white matter in the cerebellum and the brainstem.

(b) Most of the intramyelin oedema has been absorbed fifteen days after TET intoxication.

anaesthesia, and a rapid but persistent ototoxicity indicated by the rapid decrease and slow recovery in amplitudes of the early AEP components; (2) The late phase peaking at day 7, with a slower reversible myelinotoxicity reflected by limb weakness-ataxia scoring and delay of nerve conduction in both the auditory and somatosensory pathways. Several mechanisms of TET toxicity have previously been proposed, including the impairment of non-energy-consuming catalytic process of chloride-hydroxyl ion exchange across cell membranes with accompanying inflow of water molecules, uncoupling of mitochondrial oxidative phosphorylation, and the inhibition of Na,K-ATPase (for a recent review, see Cavanagh and Nolan, 1994).

In addition to the absolute decrease of body temperature, we demonstrated that body temperature, under light anaesthesia, persistently fell with time after intoxication rather than falling slightly and being maintained above 35°C before intoxication, which implies loss of the mechanism of auto-regulation of body temperature after TET intoxication. The extent and duration of hypothermia are strongly dose-dependent, as shown by previous studies as well as the present work. With dosages up to 6 mg/kg, the body temperature decreased 2 - 3°C and this hypothermia lasted less than 24 hours (Leow 1980; Dyer and Howell, 1982a). At dosage of 8 mg/kg (in present study) and 9mg/kg (Dyer and Howell, 1982a), hypothermia lasted up to 72 hours. If dosage was as high as 10 mg/kg, body temperature fell between 5 and 6°C within 120 minutes and remained thus until the rats died (Leow *et al.*, 1980). The mechanism of TET induced hypothermia is far from clear, but it could be presumed that the hypothermia induced by TET reflected the general depression of the CNS function due to a reduction in the energy generation following disruption of the cellular respiratory chain (Dyer and

Howell, 1982a; Aschner and Aschner 1992). In the present study, the general depression of CNS function was also confirmed by the action of TET (in combination with anaesthetic) reducing the anaesthetic concentration needed to produce a given level of anaesthesia. Two apparent physiological consequences of the TET-induced hypothermia are: Conduction of impulses along the insulted nerve fibres is delayed even further by the hypothermia; and the temperature-dependent neurotoxicity of TET described previously by Dyer and Howell (1982b) is reduced.

In the present study, significant decreases in amplitude of the first two components of the AEP were the most dramatic alterations detected during first 24 hours after intoxication. These changes indicate the acute ototoxic effect of TET since the early components of the surface recorded AEP were generated from the cochlear nuclei (see 3.4.4.). Furthermore, such acute disruption appeared earlier than the prolongation of the conduction time, and was therefore unlikely to be caused simply by the change of conductivity due to the myelinopathy in the acoustic nerve. This conclusion is supported by the evidence of previous studies (Clerici *et al.*, 1991; Fechter, 1993; Clerici *et al.*, 1993) which showed that the inner hair cells, associated spiral ganglion and stria vascularis were the initial cochlear targets for TET. These authors found that disruption of neural function at the level of the cochlea could happen as early as 1 hour after administration, and recovery of cochlear function in the ensuring days and weeks was evident from the changes in the vasculature of the stria vascularis.

The AEP components affected by the TET-induced wide-spread myelinopathies peaking at day 7 also include P2 and P3 (generated possibly by the auditory pathway at

the brainstem level). In contrast, P4 amplitude only decreased following intracerebellar injection of either procaine (see 3.4.5.) or LPC (see 4.4.2.). This indicates the remarkable involvement of extracerebellar structures, a conclusion further supported by the decrease in amplitude and increased delay observed in the neocortical SEP, in which the spinocortical projecting pathway is involved.

It is clear that the cerebellar AEP not only responds to LPC-induced cerebellar focal demyelination (see Chapter 4); it also reacts to the procaine-induced cerebellar white matter inactivation (see Chapter 3) and non-demyelinating but wide-spread lesions induced by TET, which indicates that the cerebellar AEP, although a functional index of the cerebellar integrity, is not a demyelination-specific one.

Nerve conductivity changes with temperature in TET insulted nerve fibres as compared with normals. Results of the present study have shown that the effects of TET on nerve conductivity can be divided into two overlapping stages. A possible explanation is that in the early stage (direct toxic insult to the myelin sheath), the energy-requiring pumps maintaining electrolyte gradients across cell membranes are inhibited directly by TET via uncoupling of mitochondrial oxidative phosphorylation and inhibition of Na,K-ATPase. In the second stage (vacuolation of the lamellae), the electrophysiological properties of the myelin sheath are changed because of the splitting and accumulation of fluids at the intraperiod line. Thus, the temperature-related conduction delay in the central auditory pathway in the present study may have been due to a combination of changes in the electrophysiological properties of the myelin sheath induced directly by TET and a reduction in efficiency of ion channels

following hypothermia. This proposal is based on other studies of demyelination and temperature influences on nerve conduction (Rasminsky 1973; Bostock *et al.*, 1978; Dioszeghy and Stålberg 1992). However, demyelination and temperature reduction influence nerve conductivity via different mechanisms from that of TET-induced myelinopathy. In demyelinated nerve fibres, transverse resistance diminishes, outward leakage currents increase and impulse transmission becomes impaired due to the alterations of myelin thickness, internodal distance and nodal properties (McDonald 1963; McDonald and Sears 1970; Waxman 1977; Kaji and Kimura, 1991). Temperature reduction primarily affects the kinetics of sodium channels. The outward current tending to depolarise the nodal membrane to threshold is prolonged and this may result in slower impulse conduction.

The present study also throws light on the question of whether there is myelin breakdown in acute TET intoxication. In contrast to the appearance of MBP in the CSF detected by radioimmunoassay following the focal demyelination produced by lysolecithin (see Chapter 5), the fact that there was no detectable MBP in the CSF samples in the present study suggests that any demyelination would have been very limited in extent. This negative result was seen despite the much more extensive damage seen after TET than in the LPC model, which was strictly focal. In addition, the rapid disappearance of vacuoles in the myelin sheath, and the prompt recovery of both delayed conduction time in the auditory pathway and clinical sensory and motor deficits as found in the present study and elsewhere (Dyer and Howell 1982a), indicates that, with a single intraperitoneal dose of up to 9mg/ml, the recovery would be very much a process of absorption of the oedema rather than remyelination

following the breakdown of myelin sheath, which would take longer. These findings argue against suggestions that TET induced myelinopathy was not only an accumulation of extracellular fluid at the intraperiod line, but also a collapse of the myelin sheath based on increased activity of synthesising myelin proteins (Smith, 1972) and increased expression of MBP-mRNA (Veronesi, *et al.*, 1991) in the brain response to the TET intoxication.

The pathological observation in the present study of acute TET intoxication in the adult rat produces widely-spread severe intramyelin oedema in the CNS parallels those reported previously (Bakay 1965; Watanabe 1980; Aschner and Aschner 1992; Cavanagh and Nolan 1994). With myelin as the primary target site, TET causes the sheath to split and allows fluid from extracellular compartments to accumulate and produce myelinopathy with vacuolation of the myelin sheath at the intraperiod line of the lamellae. In addition to the toxic effect of TET on white matter in the CNS, there is evidence that TET can induce vacuoles within the intraperiod line of the myelin sheath in the peripheral nerve and produce occasional Wallerian degeneration of the nerve fibre (Graham and Gonatas 1973; Richman and Bierkamper 1984).

CHAPTER 6.

CONCLUSIONS

6.1. CONCLUSIONS FROM THE PRESENT INVESTIGATION: The main conclusions of the present investigation can be summarized as follows.

Repeated sampling of CSF of up to 100 µl from conscious animals as small as the rat offers an experimental method for repeatedly monitoring changes in specific elements of the brain released into the CSF circulation in normal cerebral metabolism or pathological conditions. The modified method of implanting the cannula in the rat cisterna magna via an occipital approach for repeated CSF sampling has proved to be more efficient, allowing a better view of the cistern during implantation and improved long term patency of 50% over 2 - 4 weeks. The intracranial space occupied by the cannula is also reduced, a crucial factor in maintaining the intracranial pressure while brain volume increases because of intracerebral lesions.

Components of the surface-recorded cerebellar AEP could be used as indices of conductivity of the cerebellar fibres, which are susceptible targets of several demyelinating agents, so that the surface-recorded cerebellar AEP could be employed for monitoring myelinopathies involving cerebellar white matter. The surface-recorded cerebellar AEP has been explored in this study via a number of electrophysiological approaches with three main results. Firstly, the surface-recorded cerebellar AEP is a complex of multiple components with both high and low frequency waves superimposed. The slow component of the AEP behaves in a manner characteristic of near field activity which is generated by the structures within the cerebellum, whereas the fast early components are evidently generated from relatively distant structures within the brainstem. The cerebellar AEP can be best recorded over the vermis,

following binaural stimulation. Secondly, the cerebellar AEP appears not to be generated exclusively in the cerebellar cortex: other generators within (possibly the cerebellar nuclei) or even outside (e.g. the inferior colliculi) the cerebellum may also contribute to the surface-recorded potential. Finally, the fact that such a response is altered by temporary inactivation of the cerebellar central white matter, seen as a decrease in amplitude, delay in latency and prolongation in the calculated CCT, confirms that the cerebellar AEP can be employed as an electrophysiological index for monitoring focal abnormalities of impulse conduction within the cerebellum.

The present study has showed that 50 % clearance of artificially injected MBP from the CSF circulation is achieved in about 140-150 minutes. Such a clearance rate is slower than the natural CSF turnover time of approximately 100 minutes and faster than the interval of appearance of MBP induced by LPC lasting over several days. MBP liberated from demyelinating lesions into the CSF following myelin collapse is neither cleared so rapidly from the CSF as to give a false negative detection while myelin breakdown is still active nor accumulated in the CSF to yield a false positive detection after demyelination has already ceased. Thus the level of the MBP in the CSF does provide a measure of the current status of myelin breakdown.

Two animal models of acute myelinopathies have been re-established in the present studies. In the first model, focal demyelination in the central white matter of the cerebellum was induced by bilateral micro-injection of 2.5μl of 1% LPC. The injection of LPC produced no clinical motor deficits, but a transient decrease in amplitude of the cerebellar AEP occurred at 6 hours after injection, with the rapid

appearance of MBP in the CSF peaking at 24 hours and clearing after 4 days. Each LPC lesion was approximately 1.5 mm in diameter at 72 hours in pathological sections, and was characterised by extensive demyelination which had largely recovered at 15 days. In the second model, wide-spread but non-demyelinating myelinopathies were induced by a single *i.p.* injection of TET at dose of 8 mg/kg. TET produces two phases of toxicity: an rapid transient general depression of the CNS with a rapid but persisting otoxicity, and a slower reversible myelinotoxicity. Clinical observation showed an transient hypothermia peaking at 24 hours and accompanied by an increased sensitivity to isoflurane anaesthesia, even in rats maintained at normal body temperature by external heating. Reversible ataxia and limb weakness peaked at 7 days. There was also a parallel body weight loss of 20%. Both phases of TET intoxication could be monitored satisfactorily by changes in the cerebellar AEP. The amplitude of the cerebellar AEP showed a peak decrease at 24 hours and a slow recovery, most marked in the early components, suggesting direct cochlear damage. There was also a later change in the cerebellar AEP with significant delay in latency, prolongation of CCT and increase in the temperature dependence of conduction velocity, complemented by the parallel changes in the cortical SEP, all indicating myelin damage. Nevertheless, there was no MBP detectable in the CSF throughout the observation period, presumably because there was no significant liberation of MBP from the intraperiod line of the myelin sheaths. Pathological examination showed a widespread but reversible intramyelinic vacuolation in the upper spinal cord, brainstem, cerebral and cerebellar white matter.

Thus AEP measurement has been confirmed as an effective method for monitoring progression of conduction deficits along myelinated fibres subsequent to temporal inactivation of cerebellar fibres induced by procaine, myelin oedema induced by TET and complete collapse of myelin sheaths induced by LPC. Useful indices are decrease in amplitude, delay in latency and prolongation in the CCT, with evidence of the location of the lesion according to which component is involved. The direct ototoxicity of TET could also be clearly shown from the early waves. But the AEP is not a demyelination-specific index, and other interpretations of the later wave changes, and hence of central conduction deficits may exist because the precise afferent pathway of the auditory input to the cerebellum and location of possible generators contributing to the surface-recorded cerebellar AEP are still unclear.

Although the nature of the MBP-like materials released from the myelin sheath following the chemical insult is not conclusively identified, and despite the volume limitation of the CSF samples in the small animal experiments, the MBP released from the LPC-induced demyelination in rats cross-reacts to the anti-human MBP antibody, and the previously designed radioimmunoassay of MBP in the CSF for detecting immune mediated demyelination is also applicable for detecting chemically-induced demyelination. The method is effective even for relatively small lesions. Such a RIA is sensitive and selective, allowing monitoring of the progress of focal demyelination induced by LPC but not responding to the widespread myelin oedema induced by TET without myelin breakdown.

Both AEP recording and MBP detection could be clinically applicable provided the corresponding cerebellar component is identified and recordable from the scalp in man, and sufficient CSF samples are obtainable from patients. However, the AEP lacks both specificity (not distinguishing myelin oedema from demyelination) and sensitivity, although changes in its components could be used to localise the lesion.

Some of the results contained in this thesis have been presented either as demonstrations, oral communications or poster presentations at Physiological Society or British Toxicology Society Meetings (see appendices or Liu and Ray, 1993; Liu and Ray, 1994; 1995a, Liu and Ray, 1995b; Liu, *et al.*, 1995).

6.2. POINTERS FOR FURTHER INVESTIGATIONS: Further studies based on the present investigation can be pursued in both the short and long terms along neurophysiological, immunochemical and toxicological lines. The following suggestions may be made:

In the short term, the surface-recorded cerebellar AEP could be studied experimentally to obtain further evidence of how the deep cerebellar nuclei contribute to the surface-recorded field potential. Two ways to approach this are to record single unit activity from the nuclei occurring in response to an auditory stimulus, and to observe the effects of inactivating the entire nuclei following focal injection of local anaesthetic. This would not be a simple task, however, since the cerebellar nuclei are large structures. In addition, the corresponding auditory potential in the human should be identified. Long term studies to investigate the auditory afferent pathway(s) to the

cerebellum, their physiological role in cerebellar functions and the clinical application of cerebellar AEP recording are of interest and should be pursued because of their potential to provide a useful monitor of cerebellar function.

Since MBP-like materials released under different pathological conditions can have differences in size, appearance and immunoreactivity, the nature of these MBP products of chemical intoxication could usefully be separated and analysed to investigate mechanisms of chemically-induced myelin damage. Techniques for detection of MBP in human CSF samples need to be developed to enable routine monitoring of acute and, more frequently, chronic intoxication of demyelinating chemicals in order to improve the diagnoses of such clinical cases.

Finally, the experimental techniques, protocols and functional indices developed in the present studies can be applied to other experimental studies of the toxic effect of other demyelinating chemicals which primarily affect the CNS (see 1.4.1.), particularly the brainstem and the cerebellum. Focal injection of LPC provides an effective tool to damage selectively and reversibly a grey or white matter target of interest. Such a technique is frequently required in a wide range of *in vivo* experimental investigations of the nervous system.

REFERENCES

Adams R. D., Victor M. and Mancall E. L. Central pontine myelinolysis: a hitherto undescribed disease occurring in alcoholic and malnourished patients. *Archives in Neurology and Psychiatry* 1959; **81**: 154-172.

Aitkin L. M. and Boyd J. Responses of single units in cerebellar vermis of the cat to monaural and binaural stimuli. *Journal of Neurophysiology* 1975; **38**:418-429.

Alajouanine T., Dérobert L. and Thieffry S. Étude clinique d'ensemble de 210 cas d'intoxication par les sels organiques d'étain. *Revue Neurologique* 1958; **98**:85-96.

Aldridge W. N. and Street B. W. Oxidative phosphorylation: The relation between the specific binding of trimythyltin and triethyltin to mitochondria and their effects on various mitochondrial functions. *Journal of Biochemistry* 1976; **124**:221-234.

Aldridge W. N. The influence of organotin compounds on mitochondrial functions. *Advances in Chemistry Series* 1976; **157**:186-196.

Aldridge W. N., Street B. W. and Skilleter D. N. Oxidative phosphorylation. Halide-dependent and halide-independent effects of triorganotin and triorganolead compounds on mitochondrial functions. *Journal of Biochemistry* 1977; **168**:353-364.

Aleu F. P., Katzman R. and Terry R. D. Fine structure and electrolyte analyses of cerebral edema induced by alkyl tin intoxication. *Journal of Neuropathology and Experimental Neurology* 1963; **22**:403-413.

Allen J. E., Gage P. W., Leaver D. D. and Leow A. C. T. Triethyltin depresses evoked transmitter release at the mouse neuromuscular junction. *Chemical and Biological Interactions* 1980; **31**:227-231.

Allt G., Ghabriel M. N. and Sikri K. Lysophosphatidyl choline-induced demyelination. A freeze-fracture study. *Acta Neuropathology* (Berl.) 1988; **75**:456-464.

Altman J. A., Becheerev N. N., Radionova E. A. *et al.* Electrical responses of the auditory area of the cerebellar cortex to acoustic stimulation. *Experimental Brain Research* 1976; **26**:285.

Amochaev A., Johnson R. C., Salamy A. and Shah S. N.. Brain stem auditory evoked potentials and myelin changes in triethyltin-induced edema in young adult rats. *Experimental Neurology* 1979; **66**:629-635.

Aschner M., Aschner J. L. Cellular and Molecular Effects of Trimethyltin and Triethyltin: Relevance to Organotin Neurotoxicity. *Neuroscience and Biobehavioral Reviews* 1992; **16**:427-435.

Bakay L. Morphological and chemical studies in cerebral edema: Triethyl tin-induced edema. *Journal of the Neurological Sciences* 1965; **2**:52-67.

Banik N. L. Pathogenesis of myelin breakdown in demyelinating diseases: Role of proteolytic enzymes. *Critical Reviews in Neurobiology* 1992; **6**:257-271.

Banik N. L., Mauldin L. B. and Hogan E. L. Activity of 2',3'-cyclic nucleotide 3' - phsophohydrolase in human cerebrospinal fluid. *Annals of Neurology* 1979; **5**:534-541.

Barker A. T., Jalinous R. and Freeston I. L. Noninvasive stimulation of the human motor cortex. *Lancet* 1985; **1**:1106-1107.

Barone S. Jr., Stanton M. E. and Mundy W. R. Neurotoxic effects of neonatal triethyltin (TET) exposure are exacerbated with aging. *Neurobiology of Aging* 1995; **16**:723-735.

Barry R., Lawrence M., Thompson A., McDonald I. and Groome N. An improved radioimmunoassay for myelin basic protein-link immunoreactive material in cerebrospinal fluid. *Neurochemistry International* 1990; **16**:549-558.

Bartsch U. Myelination and axonal regeneration in the central nervous system of mice deficient in the myelin-associated glycoprotein. *Journal of Neurocytology* 1996; **25**: 303-313.

Becker F. O., Michael J.A. and Ritchie J. M. Acute effects of oral phosphate on visual function in multiple sclerosis. *Neurology* 1974; **24**:601-607.

Beitel R. E. and Kaas J. H. Effects of bilateral and unilateral ablation of auditory cortex in cats on the unconditioned head orienting responses to acoustic stimuli. Journal of Neurophysiology 1993; **70**: 351-369.

Bentz J. S. Laboratory investigation of multiple sclerosis. *Laboratory Medicine* 1995; **26**: 393-399.

Blakemore W. F. Demyelination of the superior cerebellar peduncle in the mouse induced by cuprizone. *Journal of Neurological Science* 1973a; **20**:63-72.

Blakemore W. F. Invasion of Schwann cells into the spinal cord of the rat following local injections of lysolecithin. *Neuropathology and Applied Neurobiology* 1976; **2**:21-39.

Blakemore W. F. Myelination, demyelination and remyelination in the CNS. In *Recent advances in Neuropathology*, Chapter 3, edited by W. Thomas Smith and J. B. Cavanagh. Churchill Livingstone, Edinburgh, London, Melbourne, and New York. 1982, pp 53-81.

Blakemore W. F. Observations on oligodendrocyte degeneration, the resolution of status spongiosus and remyelination in cuprizone intoxication in mice. *Journal of Neurocytology* 1972; **1**: 413-426.

Blakemore W. F. Observations on remyelination in the rabbit spinal cord following demyelination induced by lysolecithin. *Neuropathology and Applied Neurobiology* 1978; **4**: 381-392.

Blakemore W. F. Remyelination of the superior cerebellar peduncle in the mouse following demyelination induced by feeding cuprizone. *Journal of Neurological Science* 1973b; **20**:73.

Blakemore W. F., Franklin R. J. M. and Crang A. J. Repair of demyelinated lesions by glial cell transplantation. *Journal of Neurology* (Supplement) 1994; **242**: S61-63.

Blakemore W.F., Eames R. A., Smith K. J. and McDonald W. I. Remyelination in the spinal cord of the cat following intraspinal injections of lysolecithin. *Journal of the Neurological Sciences* **22**: 31-43; 1977.

Blaker W. D., Krigman M. R., Thomas D. J., Mushak P. and Morell P. Effect of triethyl tin on myelination in the developing rat. *Journal of Neurochemistry* 1981; **36**: 44-52.

Blight A. R. Effect of 4-AP on axonal conduction block in chronic spinal cord injury. *Brain Research Bulletin* 1989; **22**: 47-52.

Boniface S. J., Schubert M. and Mills K. R. Suppression and long latency excitation of single spinal motor neurone by transcranial magnetic stimulation in health, multiple sclerosis, and stroke. *Muscle and Nerve* 1994; **17**: 642-646.

Bostock H., Sears T. A. and Sherratt R. M. The effects of 4-aminopyridine and tetraethylammonium ions no normal and demyelinated mammalian nerve fibres. *Journal of Physiology (Lond.)* 1981; **313**: 301-315.

Bostock H., Sherratt R. M. and Sears T. A. Overcoming conduction failure in demyelinated nerve fibres by prolonging action potentials. *Nature* 1978; **274**: 385.

Bower J. M. Is the cerebellum a motor control device? Commentary on "Functional heterogeneity with structural homogeneity: how dose the cerebellum operate?" by Bloedel J. R. *Behaviour Brain Science* 1993; **15**: 714-715.

Brown A. W., Aldridge W. N., Street B. W. and Verschoyle R. D. The behavioural and neuropathologic sequelae of intoxication by trimethyltin compounds. *American Journal of Pathology* 1979; **97**: 59-82.

Brown A. W., Cavanagh J. B., Verschoyle R. D., Gysbers M. F., Jones H. B. and Aldridge W. N. Evolution of the intracellular changes in neurones caused by trimethyltin. *Neuropathology and Applied Neurobiology* 1984; **10**: 267-283.

Broxup B., Robinson K., Losos G. and Beyrouty P. Correlation between behavioural and pathological changes in the evaluation of neurotoxicity. *Toxicology and Applied Pharmacology* 1989; **101**: 510-520.

Cammer W. Toxic demyelination: Biochemical studies and hypothetical mechanisms. Chapter 17. In *Experimental and Clinical Neurotoxicology*, edited by P. S. Spencer and H. H. Schaumburg, Williams and Wilkins, Baltimore/ London, 1980, pp239-256.

Carlton W. W. Response of mice to the chelating agents sodium diethyldithocarbamate, α-bensoinoxime, and biscyclohexanone oxaldihydrazone. *Toxicology and Applied Pharmacology* 1966; **8**:512-521.

Carlton W. W. Spongiform encephalopathy induced in rats and guinea pigs by cuprizone. *Experimental and Molecular Pathology* 1969; **10**:274- 287.

Carnegie and Moore. Myelin basic protein. In: *Proteins of the nervous system*, 2nd edition (Ed.) Bradshaw, R.A. & Schneider, D.M. New York: Raven Press., 1980. pp 119-143.

Cavanagh J. B. and Nolan C. C. The neurotoxicity of organolead and organotin compounds. In: *Handbook of Clinical Neurology* Vol 64. Intoxications of the Nervous System (Part 1). (Ed.) Vinken PJ and de Bruyn GW; (volume ed) de Wolff FA. Elsevier Science BV, Amsterdam, 1994.

Cavanagh J. B., Chen F. C. K., Kyu M. H. and Ridley A. The experimental neuropathy in rats caused by p-bromophenylacetylurea. *Journal of Neurology, Neurosurgery and Psychiatry* 1968; **31**: 471-478.

Cavatorta P., Giovanelli S., Bobba A., Riccio P. and Quagliariello E. Interaction of cations with lipid-free myelin basic protein. A spectroscopy study. *Acta Neurol Napoli* 1991; **13**: 162-169.

Chiappa K. H. *Evoked potentials in clinical medicine*. 2nd ed., Reven Press, New York, 1990.

Chiu S. Y. and Ritchie J. M. Evidence for the presence of potassium channels in the paranodal region of acutely demyelinated mammalian nerve fibres. *Journal of Physiology (Lond.)* 1981; **313**: 415-437.

Chiu S. Y. and Ritchie J. M. Potassium channels in nodal and internodal axonal membrane in mammalian myelinated fibres. *Nature* 1980; **284**: 170-171.

Clerici W. J., Chertoff M. E., Brownell W. E. and Fechter L. D. In vitro organotin administration alters guinea pig cochlear out hair cell shape and viability. *Toxicology and Applied Pharmacology* 1993; **120**: 193-202.

Clerici W. J., Ross B. Jr. and Fechter L. D. Acute ototoxicity of trialkyltin in the guinea pig. *Toxicology and Applied Pharmacology* 1991; **109**: 547-556.

Cohen S. R. Myelin Basic Protein in cerebrospinal fluid: Index of active demyelination. In *Neurobiology of cerebrospinal fluid*, Chapter 34. edited by James H, Wood. Plenum Press, New York, pp 487-494, 1980.

Cohen S. R., Herndon R. M. and McKhann G. M. Radioimmunoassay of myelin basic protein in spinal fluid: An index of active demyelination. *New England Journal of Medicine* 1976; **296**: 1455-1457.

Compston, D. A. S., Scolding N., Wren D. and Noble M. The pathogenesis of demyelinating disease-insights from cell biology. *Trends in Neurosciences* 1991; **14**: 175-182.

Cooper R. and Binnie C. D. Techniques. Part 1. Origins and techniques. In: *Clinical Neurophysiology: EMG, Nerve Conduction and Evoked Potentials*. ed. Binnie C. D., Cooper R., Fowler C. J., Mauguière F. and Prior P. F., editor-in-chief Osselton J. W., Butterworth-Heinemann Ltd/Oxford, 1995.

Cooper R. Murray N. M. F. and Mauguière F. Methods and instrumentation. Part 3. Evoked Potentials. In: *Clinical Neurophysiology: EMG, Nerve Conduction and Evoked Potentials*. ed. Binnie C. D., Cooper R., Fowler C. J., Mauguière F. and Prior P. F., editor-in-chief Osselton J. W., Butterworth-Heinemann Ltd/Oxford, 1995.

Cremer J. E. Selective inhibition of glucose oxidation by triethyltin in rat brain in vivo. *Journal of Biochemistry* 1970; **67**: 95-102.

Crofton K. M., Dean K. F., Menache M. G. and Janssen R. Triethyltin effects on auditory function and cochlear morphology. *Toxicology and Applied Pharmacology* 1990; **105**: 123-132.

Davis F. A., Stefoski D. and Rush J. Orally administered 4-aminopyridine improves clinical signs in multiple sclerosis. *Annals of Neurology* 1990; **27**: 186-192.

Demura N., Kuroda J., Tanaka K. I., Seno N. and Kanazawa I. Effects of continual intravenous posttreatment with D-CPP-ene, a potent competitive M-metyl-D-aspartate receptor antagonist, on rat brain edema induced by injection of triethyltin onto the cerebral hemisphere. Neuroscience Letters 1995; **192**: 109-112.

Dioszeghy P. and Stålberg E. Changes in motor and sensory nerve conduction parameters with temperature in normal and diseased nerve. *Electroencephologram and clinical Neurophysiology* 1992; **85**:229-235.

Dousset V., Braochet B., Vital A., Gross C. and Benazzouz A. Preliminary in vivo study with MR and magnetization transfer. *American Journal of Neuroradiology* 1995; **16**: 225-231.

Duncon I. D., Aguayo A. J., Bunge R. P. and Wood P. M. Transplantation of rat Schwann cells grown in tissue culture into the mouse spinal cord. *Journal of the Neurological Sciences* 1981; **49**: 241-252.

Dyer R. S. and Howell W. E. Acute triethyltin exposure: Effects on visual evoked potential and hippocampal afterdischarge. *Neurobehavioral Toxicology and Teratology* 1982a; **2**: 259-266.

Dyer R. S. and Howell W. E. Triethyltin: Ambient temperature alters visual system toxicity. *Neurobehavioral Toxicology and Teratology* 1982b; **4**:267-271.

Earl C., Chantry A., Mohammad N. And Glynn P. Zinc ions stabilise association of basic protein with brain myelin membranes. *Journal of Neurochemistry* 1988; **51**: 718-723.

Eberstein A., Goodgold J. and Pechter B. R. Effect of curare on EMG and contractile responses in the myotonic mouse. *Experimental Neurology* 1975; **49**:612.

Eto Y., Suzuki K. and Suzuki K. Lipid composition of rat brain myelin in triethyltin-induced edema. *Journal of Lipid Research* 1971; **12**: 570.

Fabiani M., Sohmer H., Tait C., Gafni M. and Kinarti R. A functional measure of brain activity: brain stem transmission time. *Electroencephologram and clinical Neurophysiology* 1979; **47**: 483-491.

Fechter L. D., Young J. S. and Nuttall A. L. Triethyltin ototoxicity: Evidence for a cochlear site of injury. *Hearing Research* 1986; **23**: 275-282.

Filippi M., Campi A., Dousset V., Baratti C, Martinelli V., Canal N. *et al.* A magnetization transfer imaging study of normal-appearing white matter in multiple sclerosis. *Neurology* 1995a; **45**: 478-482.

Filippi M., Horsfield M. A., Tofts P. S., Barkhof F., Thompson A. J. and Miller D. H. Quantitative assessment of MRI lesion load in monitoring the evolution of multiple sclerosis. *Brain* 1995b; **118**: 1601-1612.

Finean J. B. Further observation on the structure of myelin. *Experimental cell Research* 1953; **5**: 202-215.

Flecknell P. *Laboratory animal anaesthesia.* 2nd edition, Academic Press, London, 1996.

Ford C. C., Ceckler T. L., Karp J. and Herndon R. M. Magnetic resonance imaging of experimental demyelinating lesions. *Magnetic Resonance in Medicine* 1990; **14**: 461-481.

Foster R. E., Kocsis J. D., Malenka R. C. and Waxman S. G. Lysophosphatidyl choline-induced focal demyelination in the rabbit corpus callosum. *Journal of Neurological Sciences* 1980; **48**: 221-231.

Fox D. A., Lowndes H. E. and Bierkamper G. G.. Electrophysiological techniques in neurotoxicology. In *Nervous system toxicology*, edited by C. L. Mitchell. Raven Press, New York, 1980, pp299-335.

Freeman J. H. Jr., Barone S. Jr. and Stanton M. E. Cognitive and neuroanatomical effects of triethyltin in developing rats: Role of age of exposure. *Brain Research* 1994; **634**: 85-95.

Fressinaud C. and Vallat J. M. Basic fibroblast growth factor improves recovery after chemically induced breakdown of myelin-like membranes in pure oligodendrocyte cultures. *Journal of Neuroscience Research* 1994; **38**: 202-213.

Fujita N., Ishiguro H., Sato S., Kurihara T., Kuwano R., Sakimura K., Takahashi Y. and Miyatake T. Induction of myelin-associated glycoprotein mRNA in experimental remyelination. *Brain Research* 1990; **513**: 152-155.

Funai H. and Funasaka S. Experimental study on the effect of inferior colliculus lesions upon auditory brain stem response. *Audiology* 1983; **22**:9-19.

Gao J-H., Parsons L. M., Bower J. M., Xiong J., Li J. and Fox P. T. The role of the cerebellum in sensory discrimination: a functional magnetic resonance imaging study. *Science* 1996; **272**: 545-547.

Gilman S., Bloedel J. R. and Lechtenberg R. *Disorders of the cerebellum.* F. A. Davis Company, Philadelphia, 1981, pp15-51; 95-118.

Gilson J. and Blakemore W. F. Failure of remyelination in area of demyelination produced in the spinal cord of old rats. *Neuropathology and Applied Neurobiology* 1993;**19**: 173-181.

Glynn P. and Linington C. Cellular and molecular mechanism of autoimmune demyelination in the central nervous system. *CRC Critical Reviews in Neurobiology* 1989; **4**: 367-385.

Goldstein S. and Rall W. Changes of action potential shape and velocity for changing core conductor geometry. *Biophysics Journal* 1974; **14**: 731-757.

Graham D. I. and Gonatas N. K. Triethyltin sulphate-induced splitting of peripheral myelin in rats. *Laboratory investigation* 1973; **29**: 628-632.

Griffin J. W., Stocks E. A., Fahnestock K., Van Praagh A. and Trapp B. D.. Schwann cell proliferation following lysolecithin-induced demyelination. *Journal of Neurocytology* 1990; **19**: 367-384.

Griffiths I. R., Schneider A. Anderson J. and Nave K. A. Transgenic and natural mouse models of proteolipid protein (PLP)-related dysmyelination and demyelination. *Brain Pathology* 1995; **5**: 275-281.

Griot C., Vandevelde M., Richard A., Peterhans E. and Stocker R. Selective degeneration of oligodendrocytes mediated by reactive oxygen species. *Free Radical Research* 1990; **11**: 181-193.

Gutmann L. Metabolic-toxic neuropathies. *Current Opinion in Neurology and Neurosurgery* 1991; **4**: 707-711.

Hall S. M. and Gregson N. A. The in vivo and ultrastructural effects of injection of lysophosphatidyl choline into myelinated peripheral nerve fibres of the adult mouse. *Journal of Cell Science* 1971; **9**:769-789.

Hall S. M. The effect of injections of lysophosphatidyl choline into white matter of the adult mouse spinal cord. *Journal of Cell Science* 1972; **10**:535-546.

Harris C. P., Townsend J. J. and Baringer J. R. Symptomatic hyponatremia: Can myelinolysis be prevented by treatment? *Journal of Neurology, Neurosurgery and Psychiatry* 1993; **56**: 626-632.

Hashimoto I., Ishiyama Y., Yoshimoto T. and Nemoto S. Brain-stem auditory-evoked potentials recorded directly from human brainstem and thalamus. *Brain* 1981; **104**: 841-859.

Hayakawa T., Ushio Y., Mori T., Arita N., Yoshimine T., Maeda Y., Shinizu K. and Myoga M. Levels in stroke patients of CSF astroprotein and astrocyte-specific cerebroprotein. *Stroke* 1979; **10**: 685-689.

Hemm R. D. and Carlton W. W. Ultrastructural changes of Cuprizone Encephalopathy in mice. *Toxicology and Applied Pharmacology* 1971; **18**:869-882.

Hershviz R., Mor F., Gilat D., Cohen I. R. and Lider O. T cells in the spinal cord in experimental autoimmune encephalomyelitis are matrix adherent and secrete tumor necrosis factor alpha. *Journal of Neuroimmunology* 1993; **41**: 161-166.

Highstein S. and Coleman P. D. Responses of the cerebellar vermis to binaural auditory stimulation. *Brain Research* 1968; **10**: 470-473.

Hillborn M. and Weinberg A. Prognosis of alcoholic peripheral neuropathy. *Journal of Neurology, Neurosurgery and Psychiatry* 1984; **47**: 699-703.

Hirano A., Becker H. M. and Zimmerman H. M.. The distribution of peroxidase in the triethyltin-intoxicated rat brain. *Journal of Neuropathology and Experimental Neurology* 1969; **28**: 507-511.

Hoeffding V. and Fechter L. D. Trimethyltin disrupts function and cochlear morphology in pigmented rats. *Neurotoxicology and Teratology* 1991; **13**: 135-145.

Honmou O., Felts P. A., Waxman S. G. and Kocsis J. D. Restoration of normal conduction properties in demyelinated spinal cord axons in the adults rat by transplantation of exogenous Schwann cells. *Journal of Neuroscience* 1996; **16**: 3199-3208.

Houk J. C. Schema of motor control utilizing a network model of the cerebellum. In: Anderson DZ (ed) *Neural information processing systems.* Am Inst Phys, New York, 1988. pp367-376.

Howe J. F., Calvin W. H. and Loeser J. D. Impulses reflected from dorsal root ganglia and from focal nerve injuries. *Brain Research* 1976; **116**: 139.

Holz A., Schaeren-Wiemers N., Schaefer C., Pott U., Colello R. J. and Schwab M. E. Molecular and developmental characterization of novel cDNAs of the myelin-associated/oligodendrocytic basic protein. *The Journal of Neuroscience* 1996; **16**: 467-477.

Hudson L. D. Molecular biology of myelin proteins in the central and peripheral nervous systems. *Seminars in Neuroscience* 1990; **2**: 483-496.

Hughes R. A. C. Inflammatory neuropathies. *Bailiere's Clinical Neurology* 1994; **3**: 45-72.

Huxley A. F. and Stampfli R: Evidence for saltatory conduction in peripheral myelinated nerve fibres. *Journal of Physiology* 1949; **108**: 315.

Ito M. Cerebellar control of the vestibulo-ocular reflex. Around the floccular hypothesis. *Annals Review of Neuroscience* 1982; **12**: 275-296.

Jacobs J. M., Cremer J. E. and Cavanagh J. B. Acute effects of triethyltin on the rat myelin sheath. *Neuropathology and Applied Neurobiology* 1977; **3**: 169-181.

Jacobs K. S., Lemasters J. J. and Reiter L. W. Inhibition of ATPase activities of brain and live homogenates by triethyltin (TET). In: *Developments in the science and practice of toxicology.* Hayes A, Schnell RC, Miya TS, eds., Amsterdam, Elsevier Science Publishers, 1983.

Jeffery N. D. and Blakemore W. F. Remyelination of mouse spinal cord axons demyelinated by local injection of lysolecithin. *Journal of Neurocytology* 1995; **24**: 775-781.

Jewett D. L. and Romano M. N. Neonatal development of auditory system potentials averaged from the scalp of rat and cat. *Brain Research* 1972; **36**: 101-115.

Jewett, D. L. Volume-conducted potentials in response to auditory stimuli as detected by averaging in the cat. *Electroencephologram and clinical Neurophysiology.* 1970; **28**: 609-618.

Johnson B. L. Electrophysiological methods in neurotoxicity testing. Chapter 49. In *Experimental and Clinical Neurotoxicology*, edited by P. S. Spencer and H. H. Schaumburg. Williams and Wilkins, Baltimore/ London, 1980, pp726-742.

Johnson E. S. and Ludwin S. K. The demonstration of recurrent remyelination and demyelination of axons in the central nervous system. *Acta Neuropathology* 1981; **53**:93.

Jones S. J. Clinical assessment of central nervous system axons: Evoked potentials. Section 31. In *The axon: Structure, function and pathophysiology*, edited by Waxman SG, Kocsis JD and Stys PK, Oxford University Press, Oxford/New York, 1995, pp629-647.

Kaji R. and Kimura J. Nerve conduction block. *Current Opinion in Neurology and Neurosurgery* 1991; **4**: 744-748.

Kaji R. and Sumner A. J. Quabain reverses conduction disturbances in single demyelinated nerve fibre. *Neurology* 1989; **39**: 1364-1368.

Kaji R., Happel L. and Sumner A. J. Effect of digitalis on clinical symptoms and conduction variables in patients with multiple sclerosis. *Annals of Neurology* 1990; **28**: 582-584.

Kauppinen R. A., Komulainen H. and Taipale H. T. Chloride-dependent uncoupling of oxidative phosphorylation by triethyllead and triethyltin increase cytosolic free calcium in guinea pig cerebral cortical synaptosomes. *Journal of Neurochemistry* 1988; **49**: 1617-1625.

Kesterson J. W. and Carlton W. W. Histopathologic and enzyme histochemical observations of the cuprizone-induced brain edema. *Experimental and Molecular Pathology* 1971; **15:**82-96.

Knudsen E. I., Knudsen P. F. and Masino T. Parallel pathway mediating both sound localization and gaze control in forebrain and midbrain of the barn owl. *Journal of Neuroscience* 1993; **13**: 2837-2852.

Komoly S., Jeyasingham M. D., Pratt O. E. and Lantos P. L. Decrease in oligodendrocyte carbonic anhydrase activity preceding myelin degeneration in cuprizone induced demyelination. *Journal of the Neurological Sciences* 1987; **79**: 141-148.

Komoly S., Hudson L. D., DeF W. H. and Bondy C.A. Insulin-like growth factor I gene expression is induced in astrocytes during experimental demyelination. *Proceedings of the National Academy of Sciences of the United States of America* 1992; **5**: 1894-1898.

Lampert P. and Garrett R. Mechanism demyelination in tellurium neuropathy. Electron microscopic observations. *Laboratory investigation* 1971; **25**: 380.

Le Quesne P. M. Clinically used electrophysiological end-points. Chapter 4. In *Electrophysiology in Neurotoxicology*, Volume I, edited by Herbert E. Lowndes. CRC Press, Inc., Boca Raton, Florida, 1987, pp103-116.

Le Quesne P. M. Electrophysiological investigation of toxic neuropathies. *Acta Neurol Scand* 1982; **66**: 75-87.

Le Quesne P. M. Neuropathy due to drugs. In: Dyck P. J., Thomas P. K., Griffin J. W., *et al.*, eds. Peripheral Neuropathy. W. B. Saunders, Philadelphia, 1993.

Lee J. C. and Bakay L. Ultrastructural changes in the oedematous central nervous system: I. Triethyltin edema. *Archives Neurology* 1965; **13**: 48.

Lee K. H., Hashimoto S. A., Hooge J. P., Kastrukoff L. F., Oger J. J. F., Li D. K. B. and Paty D. W.. Magnetic resonance imaging of the head in the diagnosis of multiple sclerosis: A prospective 2-year follow-up with comparison of clinical evaluation, evoked potentials, oligocolonal banding, and CT. *Neurology* 1991; **41**: 657-660.

Leow A. C. T., Anderson R. McD., Little R. A. and Leaver D. D. A sequential study of changes in the brain and cerebrospinal fluid of the rat following triethyltin poisoning. *Acta Neuropathology* (Berl.) 1979; **47**: 117-121.

Leow A. T. C., Towns K. M. and Leaver D. D. Effect of organotin compounds and hexachlorophene on brain adenosine cyclic 3',5'-monophosphate metabolism. *Chem Biol Interactions* 1979; **27**: 125-132.

Leow A. T. C., Towns K. M. and Leaver D. D.. The effects of triethyltin in the rat following systemic and intracerebroventricular injection. *Chemical and Biological Interactions* 1980; **31**: 233-238.

Liu H., Oteiza P. I., Gershwin M. E., Golub M. S. and Keen C. L. Effects of maternal marginal zinc deficiency on myelin protein prfiles in the sucking rat and infant rhesus monkey. *Biol Trace Elem Res* 1992; **34**: 55-66.

Liu X. and Ray D. E. An improved method for repeated cerebrospinal fluid sampling in the rats. *Journal of Physiology* 1993; **467**: 214p.

Liu X. and Ray D. E. Cerebellar surface auditory evoked potential: The effect of intracerebellar injection of procaine in anaesthetised rats. *Journal of Physiology* 1995a; **483**: 29p.

Liu X. and Ray D. E. Neurotoxic effects of triethyltin: A model of physiological monitoring neurotoxicity. *Human and Experimental Toxicology*. 1995b; **14**: 375.

Liu X., Glynn P. and Ray D. E. Chemically-induced myelinopathy in the central nervous system: Electrophysiological and biochemical monitoring. *Human and Experimental Toxicology* 1995; **14**: 375.

Liu X., Ray D. E. Comparison of surface responses evoked by the high frequency monaural and binaural stimulation. *Journal of Physiology* 1994; **480**: 104-105p.

Liuzzi G. M., Ventola A., Rizzo T., Riccio P. and Quagliariello E. Zinc as an inhibitor of myelin basic protein proteolytic breakdown in the central nervous system. *Acta Neurol Napoli* 1991; **13**: 153-161.

Lock A. E. and Aldridge W. N. The binding of triethyltin to rat brain myelin. *Journal of Neurochemistry* 1975; **25**:871-876.

Lock A. E. The action of triethyltin in the respiration of rat brain cortex slices. *Journal of Neurochemistry*. 1976; **26**:887-892.

Lorenzo D., Velluti J. C., Crispino L. and Velluti R.. Cerebellar sensory functions: Rat auditory evoked potentials. *Experimental Neurology* 1977; **55**: 629-636.

Love S. Cuprizone neurotoxicity in the rat: Morphologic observations. *Journal of Neurological Science* 1988; **84**:223-237.

Low P. A. and Mcleod J. G. Refractory period, conduction of trains of impulses, and effect of temperature on conduction in chronic hypertrophic neuropathy. *Journal of Neurology, Neurosurgery and Psychiatry* 1977; **40**: 434.

Low P. A., Schmelzer J. D., Yao J. K., Dyck P. J., Parthasarathy S. and Baumann W. J. Structural specificity in demyelination induced by lysophospholipids. *Biochimica et Biophysica Acta* 1983; **754**: 298-304.

Lowenthal A. Biochemical cerebrospinal fluid analysis. *Current opinion in Neurology and Neurosurgery* 1991; **4**: 914-918.

Ludolph A. C. and Spencer P. S. Toxic neuropathies and their treatment. *Bailliere's Clinical Neurology* 1995; **4**: 505-527.

Ludwin S. K. Central nervous system remyelination: Studies in chronically damaged tissue. *Annuls of Neurology* 1994; **36**: S143-S145.

Ludwin S. K. An autoradiographic study of cellular proliferation in remyelination of the central nervous system. *American Journal of Pathology* 1979; **95**:683.

Ludwin S. K. and Johnson, E. S. Evidence for a "dying-back" gliopathy in demyelinating disease. *Annals Neurology* 1981; **9**:301-305.

Ludwin S. K. Central nervous system demyelination and remyelination in the mouse: An ultrastructural study of cuprizone toxicity. *Laboratory Investigation* 1978; **39**:597-612.

Ludwin S. K. Chronic demyelination inhibits remyelination in the central nervous system: an analysis of contributing factors. *Laboratory Investigation* 1980; **43**:382-387.

Magee P. N., Stoner H. B. and Barnes J. M.. The experimental production of oedema in the central nervous system of the rat by triethyltin compounds. *Journal of Pathology and Bacteria* 1957; **73**: 107-124.

Magos L. Tin. In: Friberg L, Nordberg G. F., Vouk V. B. eds. *Handbook on the toxicology of metals.* Amsterdam: Elsevier Science Publishers; 1986; pp 569-593.

Maimone D., Gregory S., Arnason B. G. And Reder A. T. Cytokine levels in the cerebrospinal fluid and serum of patients with multiple sclerosis. *Journal of Neuroimmunology* 1991; **32**: 67-74.

Martenson R. E. ed., *Myelin: biology and chemistry.* CRC Press, Boca Raton, 1992.

Mattieu J. M. and Amiguet P. Myelin/oligodendrocyte glycoprotein expression during development in normal and myelin-deficit mice. *Developmental Neuroscience* 1990; **12**: 293-302.

Maugh T. H. The EAE model: a tentative connection to multiple sclerosis. *Science* 1977; **195**: 969-971.

Mauguière F. Definitions and introductory remarks. Part 3. Evoked potentials. In: *Clinical Neurophsyiology: EMG, Nerve Conduction and Evoked Potentials.* ed. Binnie C. D., Cooper R., Fowler C. J., Mauguière F. and Prior P. F., editor-in-chief Osselton J. W., Butterworth-Heinemann Ltd/Oxford, 1995.

Maxwell W. L., McCreath B. J. Graham D. I. and Gennarelli T. A. Cytochemical evidence for redistribution of membrane pump calcium-ATPase and ecto-Ca-ATPase activity, and calcium influx in myelinated nerve fibres of the optic nerve after stretch injury. *Journal of Neurocytology* 1995; **24**: 925-942.

Mayer R. F. Conduction velocity in the central nervous system of the cat during experimental demyelination and remyelination. International *Journal of Neuroscience* 1971; **1**: 287-308.

McDonald W. I. and Sears T. A. The effects of experimental demyelination on conduction in the central nervous system. *Brain* 1970; **93**: 583-598.

McDonald W. I. The effects of experimental demyelination on conduction in peripheral nerve: A histological and electrophysiological study: II Electrophysiological observations. *Brain* 1963; **86**:501-524.

McMahon R. E. and Sullivan H. R. The metabolism of the herbicide diphenamid in rats. *Biochemical Pharmacology* 1965; **14**: 1085-1092.

McMillan D. E. and Wenger G. R. Neurobehavioral toxicology of Trialkyltins. *Pharmacology Reviews* 1985; **37**: 365-379.

Meyer B. U., Roricht S., Grafin-von-Einsiedel H., Kruggel F. and Weindl A. Inhibitory and excitatory interhemispheric transfers between motor cortical areas in normal human and patients with abnormalities of the corpus callosum. *Brain* 1995; **118**: 429-440.

Miall R. C., Weir D. J., Wolpert D. M., Stein J. F. Is the cerebellum a Smith predictor?. *Journal of Motor Behaviour* 1993; **25**: 203-216.

Michetti F., Massaro A. and Murazio M. The nervous system-specific S-100 antigen in cerebrospinal fluid of multiple sclerosis patients. *Neuroscience Letters* 1979; **11**: 171-175.

Mihailoff G. A. Cerebellar nuclear projections from the basilar pontine nuclei and nucleus reticularis tegmenti pontis as demonstrated with PHA-L tracing in the rat. *Journal of Comparative Neurology* 1993; **330**: 130-146.

Miller D. B. Pre- and postsreening indices of neurotoxicity in rats: Effects of triethyltin (TET). *Toxicology and Applied Pharmacology* 1984; **72**:557-565.

Miller S. D., McRea B. L., Vanderlugt C. L., Nikcevich K. M., Pope J. G., Pope L. and Karpus W. J. Evolution of the T-cell repertoire during the course of experimental immune-mediated demyelinating diseases. *Immunological Reviews* 1995; **144**: 225-244.

Miyatani N. Saito N. Argia T. Yoshino H. And Yu R. K. Glycosphingolipid in the cerebrospinal fluid of patients with multiple sclerosis. *Molecular and Chemical Neuropathology* 1990; **13**: 205-216.

Monuki E. S. and Lemke G. Molecular biology of myelination. Section 7. In *The axon: Structure, function and pathophysiology*, edited by Waxman SG, Kocsis JD and Stys PK, Oxford University Press, Oxford/New York, 1995, pp144-163.

Morell P. ed. *Myelin.* Plenum Press, New York, 1984.

Morin F., Catalano J. V. and Lamarche G. Wave form of cerebellar evoked potentials. *American Journal of Physiology* 1957; **188**: 263-273.

Morissette J., Bower J. M. Contribution of somatosensory cortex to responses in rat cerebellar granule cell layer following peripheral tactile stimulation. *Experimental Brain Research* 1996; **109**: 240-250.

Nagamatsu M., Mokuno K., Sugimura K., Kiyosawa K., Aoki S., Takahashi A. and Kato K. Cerebrospinal fluid levels of S-100b protein and neuron-specific enolase in chronic inflammatory demyelinating polyneuropathy. *Acta Neurol Scand* 1995; **91**: 483-487.

Nicholas H. J. and Taylor J. Central nervous system demyelinating diseases and increased release of cholesterol into the urinary system of rats. *Lipids* 1994; **29**: 611-617.

Offenbacher H., Fazekas F., Schmidt R., *et al.*, Assessment of MRI criteria for a diagnosis of MS. Neurology 1993; **43**: 905-909.

Olsson T. Cytokines in neuroinflammatory disease-role of myelin autoreactive T-cell production of interferon-gamma. *Journal of Neuroimmunology* 1992; **40**: 211-218.

Otto D. K., Boyes H. W., Janssen R. and Dyer R. Electrophysiological measures of visual and auditory function as indices of neurotoxicity. *Toxicology* 1988; **49**: 205-218.

Owen T and Sriram S. The immunology of multiple sclerosis and its animal model, experimental allergic encephalomyelitis. Neurologic Clinics 1995; **13**: 51-73.

Paxinos G. and Watson C. The rat brain in stereotaxic coordinates. 2nd edition, Academic Press, Sydney. 1986.

Payne T., Newmark J. and Reid K. H. The focally demyelinated rat fimbria: A new in vitro model for the study of acute demyelination in the central nervous system. *Experimental Neurology* 1991; **114**: 66-72.

Peter B. J., Baig W. M., Huang S., Kingery W. S. and Date E. Temperature correction factors derived from normal subjects may be invalid in demyelinating neuropathies. *Am J Phys Med Rehabil* 1993; **72**: 369-371.

Pluta R. and Ostrowska B. Acute poisoning with triethyltin in the rat. Changes in cerebral blood flow, cerebral oxygen consumption, arterial and cerebral venous blood gases. *Experimental Neurology* 1987; **98**: 67-77.

Povlishock J. T. Traumatically induced axonal injury: pathogenesis and pathobiological implication. *Brain Pathology* 1992; **2**:1-12.

Purves D. C., Garrod I. J. and Dayan A. D. A comparison of spongiosis induced in the brain by hexachlorophene, cuprizone and triethyl tin in the Sprague-Dawley rat. *Human & Experimental Toxicology* 1991; **10**: 439-444.

Rasminsky M. and Sears T. A. Internodal conduction in undissected demyelinated nerve fibres. *Journal of Physiology* 1972; **227**: 323.

Rasminsky M. Ectopic generation of impulses and cross-talk in spinal nerve roots of "dystrophic" mice. *Annals of Neurology* 1978; **3**: 351.

Rasminsky M. Physiological consequences of demyelination. Chapter 18. In *Experimental and Clinical Neurotoxicology*, edited by Spencer P. S. and Schaumburg H. H., Williams and Wilkins, Baltimore/ London, 1980, pp257 - 271.

Rasminsky M. The effects of temperature on conduction in demyelinated single nerve fibres. *Archives Neurology* 1973; **28**: 287.

Ray D. E. Electroencephalographic and evoked response correlates of trimethyltin induced neuronal damage in the rat hippocampus. *Journal of Applied Toxicology* 1981; **1**: 145-148.

Ray D. E., Cavanagh J. B., Nolan C. C. and Williams S. C. R. Neurotoxic effects of gadopentatate dimeglumine: behavioural disturbance and morphology after intracerebroventricular injection in rats. *American Journal Neuroradiology* 1996; **17**: 365-373.

Riccio P., Giovannelli S., Bobba A., Romito E., Fasano A., Bleve-Zacheo T., Favilla R., Quagliariello E. And Cavatorta P. Specificity of zinc bind to myelin basic protein. *Neurochemical Research* 1995; **20**: 1107-1113.

Richman E. A. and Bierkamper G. G. Histopathology of spinal cord, peripheral nerve, and muscle of rats treated with triethyltin bromide. *Toxicology and Applied Pharmacology* 1984; **90**: 122-133.

Ritchie J. M. and Rogart R. B. The density of sodium channels in mammalian myelinated nerve fibres and the nature of the axonal membrane under the myelin sheath. *Proc Natl Acad Sci USA* 1977; **74**: 211-215.

Robertson J. D. The unit membrane of cells and mechanisms of myelin formation. Ultrastructure and metabolism of the nervous system. *Res Publ Ass Res Nerv Ment Dis* 1962; **40**: 94-158.

Robinson and Rudge P. Auditory evoked responses in multiple sclerosis. *Lancet* 1975; **1**: 1164-1166.

Rose M. S. and Aldridge W. N. The interaction of triethyltin with components of animal tissue. *Journal of Biochemistry* 1968; **106**: 821.

Rothwell J. C., Thompson P. D., Day B. L. *et al.* Stimulation of the human motor cortex through the scalp. *Experimental Physiology* 1991; **76**: 159-200.

Ruppert P. H., Dean K. F. and Reiter F. W. Comparative developmental toxicity of triethyltin using split-litter and whole-litter dosing. *Journal of Toxicology and Environmental Health* 1983; **12**: 73-87.

Schmitt F. O. Nerve ultrastructures as revealed by X-ray diffraction and polarised light studies. *Cold Spring Harbor Symp Quant Biol* 1936; **4:** 7-12.

Schwab M. E. Oligodendrocyte inhibition of nerve fiber growth and regeneration in the mammalian central nervous system. Section 57. In *Neuroglia.* edited by Kettenmann H. and Ransom B. R., Oxford University Press, New York/Oxford, 1995, pp859-868.

Scolding N. J., Morgan B. P., Campbell A. K. and Compston D. A. S. The role of calcium in rat oligodendrocyte injury and repair. *Neuroscience Letters* 1992; **135**: 95-98.

Sedal L., Jennings K. H., Allt G., Ghabriel M. N. and Harrison M. J. G. Influence of fatty acid content of lysophosphatidyl choline on its myelinotoxic properties. *European Neurology* 1992; **32**: 4-10.

Selmaj K., Raine C. S. and Cross A. H. Anti-tumor necrosis factor therapy abrogates autoimmune demyelination. *Annals of Neurology* 1991; **30**: 649-700.

Seppäläinen A. M. H. Neurophysiological approaches to the detection of early neurotoxicity in humans. *CRC Critical Reviews in Toxicology* 1988; **18**: 245-298.

Shah S. N., Bhargava V. K., Johnson R. C and McKean C. M. Latency changes in brain stem auditory evoked potentials associated with impaired brain myelination. *Experimental Neurology* 1978; **58**: 111-118.

Shaw N. A. A possible collicular component of the auditory evoked potential and its relationship to brainstem and cerebellar auditory potentials. *Electromyography and Clinical Neurophysiology* 1992; **32**: 570-590.

Shaw N. A. Effects of low pass filtering on the brainstem auditory evoked potential in the rat. *Experimental Brain Research* 1987; **65**: 686-690.

Shaw N. A. The auditory evoked potential in the rat - a review. *Progress in Neurobiology* 1988; **33**: 19-45.

Shaw N. A. The temporal relationship between the brainstem and primary cortical auditory evoked potentials. *Progress in Neurobiology* 1995; **47**: 95-103.

Shofer R. J. Firing patterns induced by sound in single units of the cerebellar cortex. *Experimental Brain Research* 1969; **8**: 327-345.

Shrager P. Action potential conduction recorded optically in normal, demyelinated, and remyelinated axons. Section 18. In *The axon: Structure, function and pathophysiology*, edited by Waxman SG, Kocsis JD and Stys PK, Oxford University Press, Oxford/New York, 1995, pp341-354.

Smith J. F., Mclaurin R. L., Nichols J. B. and Asbury A.. Studies in cerebral edema and cerebral swelling: I. The changes in lead encephalopathy in children compared with those in alkyltin poisoning in animals. *Brain* 1960; **83**: 411.

Smith K. J. and Hall S. M. Peripheral demyelination and remyelination initiated by the calcium-selective ionophore ionomycin: In vivo observations. *Journal of Neurological Sciences* 1988; **83**: 37-53.

Smith K. J. and McDonald W. I. Spontaneous and mechanically evoked activity due to central demyelinating lesions *Nature* 1980; **286**: 154-155.

Smith M. E. Studies on the mechanism of demyelination: Triethyltin-induced demyelination. *Journal of Neurochemistry* 1973; **21**: 357-372.

Smith M. E. Turnover of myelin proteins. *Neurobiology* 1972; **2**: 35-40.

Snider R. S. and Stowell A. Receiving areas of the tactile, auditory, and visual systems in the cerebellum. *Journal of Neurophysiology* 1944; **7**: 331-357.

Snoeij N. J., Ven Iersel A. A. J., Penninks A. H. and Seinen W. Toxicity of triorganotin compounds: Comparative *in vivo* studies with a series of trialkyltin compound and triphenyltin chloride in male rats. *Toxicology and applied Pharmacology*. 1985; **81**: 274-286.

Snoeij N. J., A. H. Penninks and W. Seinen. Biological activity of organotin compound - an overview. *Environmental Research* 1987; **44**: 335-353.

Sokal R. R. and Rohlf F. J. Introduction to biostatistics. 2nd ed., Freeman, New York, 1987.

Spencer P. S. and Schaumburg H. H. *Experimental and Clinical Neurotoxicology.* Williams and Wilkins, Baltimore/London, 1980, pp119-138.

Sprinkle T. J. and McKhann G. M. Activity of 2',3'-phosphodiesterase in cerebrospinal fluid of patients with demyelinating disorders. *Neuroscience Letters* 1978; **7**: 203-206.

Squibb R. E., Carmichael N. G. and Tilson H. A. Behavioural and neuromorphological effects of triethyltin bromide in adult rats. *Toxicology and Applied Pharmacology* 1980; **55**: 188-197.

Stein J. F. Role of the cerebellum in the visual guidance of movement. *Nature* 1986; **323**: 217-221

Stine K. E., Retter L. W. and Lemasters J. J. Alkyltin inhibition of ATPase activities in tissue homogenates and subcellular fractions from adult and neonatal rats. *Toxicology and Applied Pharmacology* 1988; **94**: 394- 406.

Stockard J. J. and Rossiter V. S. Clinical and pathologic correlates of brain stem auditory response abnormalities. *Neurology* 1977; **27**: 316- 325.

Streicher E. The thiocyanate space of rat brain in experimental cerebral edema. *Journal of Neuropathology and Experimental Neurology* 1962; **21**: 437.

Studer R. K., Siegel B. A., Morgan J. and Potchen J. Dexamethasone therapy of triethyltin induced cerebral edema. *Experimental Neurology* 1973; **38**: 429-437.

Stys P. K., Waxman S. G. and Ransom B. R. Ionic mechanism of anoxic injury in mammalian CNS white matter: role of Na+ channels and Na+-Ca+ exchanger. *Journal of Neuroscience* 1992; **12**: 430-439.

Suzuki K. and Kikkiwa Y. Status spongiosus of CNS and hepatic changes induced by cuprizone (biscyclohexanone oxalidihydrazone). *American Journal of Pathology* 1969; **54**:307.

Targ E. F. and Kocsis J. D. Action potential characteristics of demyelinated rat sciatic nerve following application of 4-aminopyridine. *Brain Research* 1986; **363**: 1-9.

Thomas D. G. T., Palfreyman J. W. and Radcliffe D. I. G. Serum myelin basic protein assay in diagnosis and prognosis of patients with head injury. *Lancet* 1978; **1**: 113-115.

Thompson E. J. Cerebrospinal fluid. *Journal of Neurology, Neurosurgery and Psychiatry* 1995; **59**: 349-357.

Torack R. M., Gordon J. and Prokop J. Pathobiology of acute triethyltin intoxication. In: *International Review of Neurobiology* Volume XII, p45, edited by C. C. Pfeiffer and J. R. Smythes. Academic Press, New York, 1970.

Trotter J. L., Wegescheid C. and Lieberman L. Myelin proteolipid protein (PLP) in sera and CSF after CNS damage. *Transactions of the American Neurological Association* 1980; **105**: 302-303.

Tuohy V. K. Peptide determinants of myelin proteolipid protein (PLP) in autoimmune demyelinating disease: A review. *Neurochemical Research* 1994; **19**: 935-944.

Venturini G. Enzymic activities and sodium, potassium and copper concentrations in mouse brain and liver after cuprizone treatment in vivo. *Journal of Neurochemistry* 1973; **21**:1147-1151.

Veronesi B. and Bondy S. Triethyltin-induced neuronal damage in neonatally exposed rats. *Neurotoxicology* 1986; **7**: 69-80.

Veronesi B., Jones K., Gupta S., Pringle J. and Mezei C. Myelin basic protein-messenger RNA (MBP-mRNA) expression during triethyltin-induced myelin edema. *Neurotoxicology* 1991; **12**: 265-276.

Verschoyle R. D., Brown A. W., Nolan C. C., Ray D. E. and Lister T. A comparison of the acute toxicity, neuropathology, and electrophysiology of N,N-Diethyl-m-toluamide and N,N-Dimethyl-2,2-diphenylacetamide in rats. *Fundamental and Applied Toxicology* 1992; **18**: 79-88.

Vignais L., Naitouesmar B., Mellouk F., Gout O., Labourdette G., Baron-Van Evercooren A. and Gumpel M. Transplantation of oligodendrocyte precursors in the adult demyelinated spinal cord: migration and remyelination. *Developmental Neuroscience* 1993; **11**: 603-612.

Voodg J. Section16. Cerebellum. In: Paxinos G (ed) *The rat nervous system.* 2nd edition. Academic Press, Inc., Sydney. 1995; pp332-342

Wada S. I. and Starr A. Generation of auditory brain stem responses (ABRs). III. Effects of lesions of superior olive, lateral lemniscus and inferior colliculus on the ABR in guinea pig. *Electroencephalography and Clinical Neurophysiology* 1983; **56**: 352-366.

Watanabe I. Effect of triethyltin on the developing brain of the mouse. In: *Neurotoxicology.* Roizin L, Shiraki H, Greevie H., eds.,. New York, Raven Press, 1977, pp317-326.

Watanabe I. Organotins (Triethyltin). Chapter 37. In *Experimental and Clinical Neurotoxicology*, edited by Spencer P. S. and Schaumburg H. H., Williams and Wilkins, Baltimore/ London, 1980, pp545-557.

Waxman S. G. Conduction in myelinated, unmyelinated, and demyelinated fibres. *Archives Neurology* 1977; **34**: 585-589.

Waxman S. G. and Geschwind N. Major morbidity related to hypothermia in multiple sclerosis. *Annual Neurology* 1983; **13**: 348.

Waxman S. G., Kocsis J. D. and Black J. A. Pathophysiology of demyelinated axons. Section 23. In *The axon: Structure, function and pathophysiology*, edited by Waxman SG, Kocsis JD and Stys PK, Oxford University Press, Oxford/New York, 1995, pp438-461.

Waxman S. G., Utzschneider D. A. and Kocsis J. D. Enhancement of action potential conduction following demyelination: Experimental approaches to restoration of function in multiple sclerosis and spinal cord injury. *Progress in Brain Research* 1994; **100**: 233-243.

Whitaker J. N. and Snyder S. D. Myelin components in the cerebrospinal fluid in diseases affecting central nervous system myelin. *Clinics in Immunology and Allergy* 1982; **2**: 469-482.

Whitaker J. N., Layton B. A., Herman P. K., Kachelhofer R. D., Burgard S. and Bartolucci A. A. Correlation of myelin basic protein-like material in cerebrospinal fluid of multiple sclerosis patients with their response to glucocorticoid treatment *Annals of Neurology* 1993; **33**: 10-17.

Whitaker J. N., Lisak R. P., Bashir R. M., Fitch O. H., Seyer J. M, Krance R, Lawrance J. A., Ch'ien L. T., and O'Sullivan P. Immunoreactive myelin basic protein in the cerebrospinal fluid in neurological disorders. *Annals of Neurology* 1980; **7**: 58-64.

Whitaker J. N., Williams P. H., Layton B. A., McFarland H. F., Stone L. A., Smith M. E., *et al.* Correlation of clinical features and findings on cranial magnetic resonance imaging with urinary myelin basic protein-like material in patients with multiple sclerosis. *Annals of Neurology* 1994; **35**: 577-585.

Williams K. A. and Deber C. B. The structure and function of central nervous system myelin. *Critical Reviews in Clinical Laboratory Sciences* 1993; **30**: 29-64.

Wolfe J. W. Responses of the cerebellar auditory area to pure tone stimuli. *Experimental Neurology* 1972; **36**: 295-309.

Wolman M. Patterns of spread of different demyelinating processes in the myelin sheath. *Progress in Neurobiology* 1992; **38**: 511-521.

Xiao B. G., Linington C. and Link H. Antibodies to myelin-oligodendrocytes glycoprotein in cerebrospinal fluid from patients with multiple sclerosis and controls. *Journal of Neuroimmunology* 1991; **31**: 91-96.

Young I. R., Hall A. S., Pallis C. A., Legg N. J., Bydder G. M. and Steiner R. E. Nuclear magnetic resonance imaging of the brain in multiple sclerosis. *Lancet* 1981; **2**: 1063-1066.

Young W., Rosenbluth J., Wojak J. C., Sakatani K. and Kim H. Extracellular potassium activity and axonal conduction in spinal cord of the myelin-deficient mutant rat. *Experimental Neurology* 1989; **106**: 41-51.

Zamvil S. S. and Steinman L. The T lymphocyte in experimental allergic encephalomyelitis. *Annals Review of Immunology* 1990; **8**: 579-621.

Appendix 1. Failure of inducing central demyelination by chronic intoxication of Cuprizone in Fisher/334 rats

Introduction

Cuprizone (C14H22N4O2, FW 278.4) has limited industrial use as a chelating agent in the detection of copper in food products. There are no reports of accidental human or animal intoxication; however, experimental studies have shown it to be toxic and results in both CNS and hepatic pathology. Unlike other demyelinating compounds, chronic intoxication of cuprizone in mice induces demyelination by damaging oligodendrocytes and astrocytes. The experiment was carried out to induce such lesions in the larger animal of Fisher/344 rats in order to evaluate methods of repeated AEP recording and detection of MBP in the CSF for *in vivo* monitoring chronic demyelination.

Experimental Protocol

Experimental animals: A group of ten F344 rats (120-140g) was used, among them eight were experimental and two were controls. Standard rat diets (2,000g each) in powder form were separately mixed with 10 and 20g Cuprizone (biscyclohexanone oxaldihydrazone, C-9012, SIGMA) to make 0.5 % and 1.0 % toxic diets. This procedure were carried out in a fume cupboard and with gloves, coat and mask on. Dosing procedures: All animals were accommodated in isolators, and the experimental animals were put on the 0.5 % toxic diet in individual cage for four weeks, and four of them then were transferred to 1.0 % toxic diet. The control animals were provided with standard diet. By the end of eighth week, all animals were killed

by perfusion with fixative under terminal anaesthesia. Pathological sections with H&E stein were obtained.

Results

Body weight, diet consumption and rectal temperature of both experimental and control animals were assessed weekly over the entire eight week dosing period, as illustrated in Figure 1. There was a significant and reversible decrease in rectal temperature in the intoxicated rats compared with the controls at week one. Significant decrease in body weight growth was only found in the group of four animals which was put on 1.0 % toxic diet for further two weeks after four weeks on 0.5 % toxic diet. No significant difference in diet consumption between intoxicated and control animals. Comparing the body weight gain between experimental and control animals during first four-week and second-four week intoxication (Fig. 2), body weight gain in all animals slowed down in the second four-week compared with the first one. There was a significant decrease in the animals on 1.0 % toxic diet during the second four-week compared with the controls and no significant difference between control and animals on 0.5 % toxic diet in both dosing periods was found.

There were no signs of demyelination in pathological sections of the whole brain with standard H&E stain at the light microscope level.

Discussion

Intoxication with Cuprizone in mice. The extensive demyelination which cuprizone produces in certain areas of the brain has been the subject of considerable interest and

experimental studies have provided much information both on CNS demyelination and the ability of the CNS to be remyelinated. Most of the studies of cuprizone intoxication were carried on mice (Cammer, 1980), the same investigation on rats has not be extensively achieved except the report from Carlton in 1969. Carlton (1966) administered three groups of mice with α-benzoinoxime, sodium diethyldithiocarbamate, and cuprizone which were incorporated into chicken mash diets, each at levels of 0.1 % and 0.5 %. The results shown that the α-benzoinoxime, sodium diethyldithiocarbamate were non toxic even at a level of 0.5 % of the diet and did not induce lesions in the brain. Cuprizone was found to be extremely toxic when fed as 0.5 % of the diet. Oedema with demyelination, especially prominent in the cerebellar white matter, was observed at both the 0.1 % and 0.5 % levels, but hydrocephalus was restricted to the group fed 0.5 % of this compound.

Pathological and biochemical findings of cuprizone-induced demyelination. Pathological and biochemical changes produced by cuprizone on mice have been studied by many investigators (Suzuki and Kikkiwa, 1969; Kesterson and Carlton, 1971; Hemm and Carlton, 1971; Blakemore, 1972; 1973a; 1973b; Ludwin, 1978; 1979; 1980; Ludwin and Johnson, 1981; Johnson and Ludwin, 1981) and summarised by Cammer (1980). Gross changes in the mice brains include hydrocephalus and status spongiosus of cerebellar white matter and the brain stem. Blakemore (1972) identified the demyelinating/remyelinating nature of the lesion seen in cuprizone toxicity. The first microscopical change to be noted in the brain is astrocytic hypertrophy and hyperplasia. Shortly thereafter, the first evidence of degeneration of oligodendrocytes begins (Blakemore, 1972; 1973a) with degeneration of mitochondria, loss of

ribosomes, increased microtubules, cytoplasmic swelling, and inner tongue abnormalities. At about the same time, vacuolation of myelin begins with myelin splitting at the intraperiod line. Demyelination is seen between 3 and 4 weeks. Vacuolated myelin is removed and phagocyteosed by microglial cells or by a variety of other means. By 5 weeks, almost all axons in the superior cerebellar peduncles are demyelinated. During the course of intoxication, remyelination is rare, but if cuprizone is terminated, remyelination occurs rapidly and by 4 weeks after termination of dosing, almost all axons are re- unsheathed (Blakemore, 1973b). Ludwin (1979) carried out an electron microscopic autoradiographic study in cuprizone-intoxicated mice. He discovered that immature glial cells divided 5 to 6 weeks after demyelination and oligodendrocyte-labelled nuclei were associated with remyelinating oligodendrocytes. In chronic cuprizone intoxication, however, the initial phase of remyelination after termination of dosing would have disappeared and with continued poisoning of oligodendrocytes, few of these cells or their precursors would be available to commence remyelination when intoxication was stopped (Ludwin, 1980). Once remyelination has occurred, demyelination can occur again if a cuprizone is add to the diet although the second bout of demyelination is protracted unlike the first (Ludwin and Johnson, 1981; Johnson and Ludwin, 1981). In this situation, degeneration of oligodendrocytes appears to start within the inner cytoplasmic tongue and it has been suggested that this may indicate a "dying-back" gliopathy, i.e., the most distal part of the oligodendrocyte is most susceptible.

Intoxication with cuprizone in rats. In parallel to previous experiments of chronic intoxication of cuprizone, cuprizone failed to induce pathological changes in

Fisher/344 rats similar to those in mice despite the fact that several strains of Fisher/344 (the present study), albino (Carlton, 1969), Sprague-Dawley (Purves *et al.*, 1991) rats were tested. The reported experiments are summarized here: Carlton (1969) administrated cuprizone incorporated into chicken mash at concentrations of 0.1, 0.5, 1.0, and 1.5 % for up to 8 weeks. Cuprizone at the dietary concentration of 0.1% was not clinically toxic and the average weight of test rats were equal to controls after 8 weeks of feeding. Cuprizone at the concentration of 0.5 % reduced weight gains by about half and 4 of 10 animals died during the experimental period of 8 weeks. At concentrations of 1.0 and 1.5%, cuprizone was extremely toxic; the animals did not grow and half of the rats of each group had died by 3 and 4 weeks of dosing. Other signs of toxicity in addition to failure to gain weight included an unkempt coat, but signs of neurological disturbance were not observed. Pathological alterations were very mild in the 0.1 % fed animals consisting of scattered vacuole formation around the nuclei of the cerebellar white matter. Lesions were most severe in the animals fed 0.5 % cuprizone. Sites of preference for the lesion extended from the level of the telecephalon to the medulla oblongata and the cerebellum. The site with the most consistent and severe alterations was the white matter around the nuclei of the cerebellar white matter. In the medulla oblongata of a few rats, tissue changes involved the vestibular regions and the descending root of the trigeminal nerve. Lesions were not observed in the cerebral cortex or corpus striatum. In severe involved brains, the tissue changes were consistent with a severe oedema creating a status spongiosus characterised by vacuolar changes in both white and grey matter. In the Kuluver-Barrera preparation for observing myelin, the spongy tissue boarding the cerebellar nuclei and the white matter above dentate nucleus of cerebellum of rat

showed reduced staining suggestive of demyelination in those areas. No hydrocephalus was found in experimental animals. In agreement with the above results, recent observations (Love, 1988; Purves *et al.*, 1991) also shown that cuprizone induced myelin damages in rats were very limited. Thus, rats are relatively insensitive to cuprizone intoxication which may be brought on by greater maturity of the brain (Carlton, 1969). Only high dose of cuprizone (>0.5% in diet) may induce myelin damage with a costly price of loosing majority or all of the intoxicated animals during initial a few weeks because of non-neurological damages. The practical implication is that neither mouse nor rat models of cuprizone-induced chronic demyelination are appropriate for the present study of *in vivo* monitoring because of the small size of mice and the insensitivity to cuprizone of rats.

References

Blakemore W. F. Demyelination of the superior cerebellar peduncle in the mouse induced by cuprizone. *Journal of Neurological Science* 1973a; **20**:63-72.

Blakemore W. F. Remyelination of the superior cerebellar peduncle in the mouse following demyelination induced by feeding cuprizone. *Journal of Neurological Science* 1973b; **20**:73.

Blakemore W. F.. Observations on oligodendrocyte degeneration, the resolution of status spongiosus and remyelination in cuprizone intoxication in mice. *Journal of Neurocytology* 1972; **1**:413-426.

Cammer W. Toxic demyelination: Biochemical studies and hypothetical mechanisms. Chapter 17. In *Experimental and Clinical Neurotoxicology*, edited by P. S. Spencer and H. H. Schaumburg, Williams and Wilkins, Baltimore/ London, 1980, pp239-256.

Carlton W. W. Response of mice to the chelating agents sodium diethyldithocarbamate, α-bensoinoxime, and biscyclohexanone oxaldi-hydrazone. *Toxicology and Applied Pharmacology* 1966; **8**:512-521.

Carlton W. W. Spongiform encephalopathy induced in rats and guinea pigs by cuprizone. *Experimental and Molecular Pathology* 1969; **10**:274- 287.

Hemm R. D. and Carlton W. W. Ultrastructural changes of Cuprizone Encephalopathy in mice. *Toxicology and Applied Pharmacology* 1971; **18**:869-882.

Johnson E. S. and Ludwin S. K. The demonstration of recurrent remyelination and demyelination of axons in the central nervous system. *Acta Neuropathology* 1981; **53**:93.

Kesterson J. W. and Carlton W. W. Histopathologic and enzyme histochemical observations of the cuprizone-induced brain edema. *Experimental and Molecular Pathology* 1971; **15:**82-96.

Love S. Cuprizone neurotoxicity in the rat: Morphologic observations. *Journal of Neurological Science* 1988; **84**:223-237.

Ludwin S. K. and Johnson, E. S. Evidence for a "dying-back" gliopathy in demyelinating disease. *Annals Neurology* 1981; **9**:301-305.

Ludwin S. K. An autoradiographic study of cellular proliferation in remyelination of the central nervous system. *American Journal of Pathology* 1979; **95**:683.

Ludwin S. K. Central nervous system demyelination and remyelination in the mouse: An ultrastructural study of cuprizone toxicity. *Laboratory Investigation* 1978; **39**:597-612.

Ludwin S. K. Chronic demyelination inhibits remyelination in the central nervous system: an analysis of contributing factors. *Laboratory Investigation* 1980; **43**:382-387.

Ludwin S. K. Central nervous system remyelination: Studies in chronically damaged tissue. *Annuls of Neurology* 1994; **36**: S143-S145.

Purves D. C., Garrod I. J. and Dayan A. D. A comparison of spongiosis induced in the brain by hexachlorophene, cuprizone and triethyl tin in the Sprague-Dawley rat. *Human & Experimental Toxicology* 1991; **10**: 439-444.

Suzuki K. and Kikkiwa Y. Status spongiosus of CNS and hepatic changes induced by cuprizone (biscyclohexanone oxalidihydrazone). *American Journal of Pathology* 1969; **54**:307.

Venturini G. Enzymic activities and sodium, potassium and copper concentrations in mouse brain and liver after cuprizone treatment in vivo. *Journal of Neurochemistry* 1973; **21**:1147-1151.

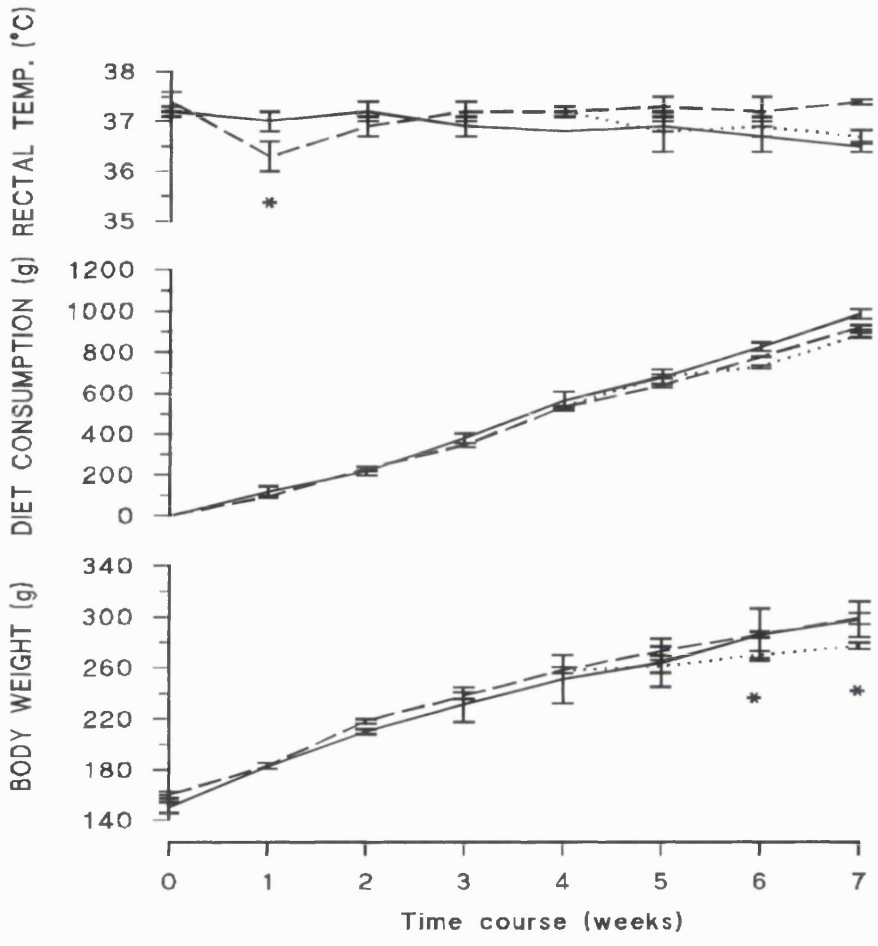

Fig. 1. Chronic intoxication of cuprizone in F334 rats: Changes in body weight, diet consumption and rectal temperature in two animals as control (solid line), four animals on 0.5% toxic diet (interrupted line) and four animals on 1.0% toxic diet after four weeks of 0.5 % diet (dotted line). Data are presented as mean ± S.M.E.; *: $P < 0.05$, paired t-test.

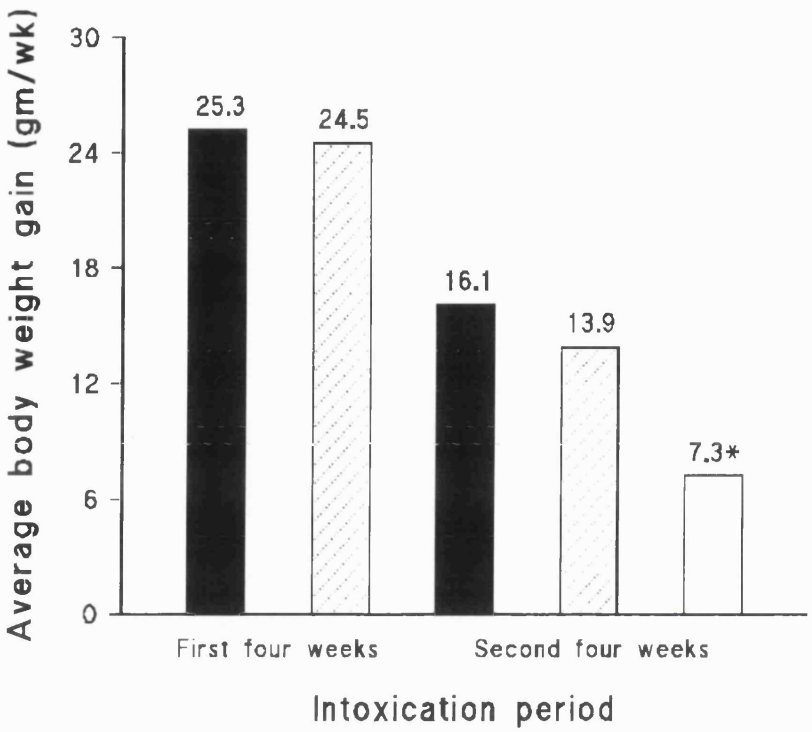

Fig. 2. Chronic intoxication of cuprizone in F334 rats: Average body weight gain in two animals as control (solid bar), four animals on 0.5% toxic diet (filled bar) and four animals on 1.0% toxic diet after four weeks of 0.5% diet (open bar). Mean values are labelled on top of each bar; *: $P < 0.05$, paired t-test.

Appendix 2. Oral intoxication of diphenamid in Fisher/334 rats

Introduction

The herbicide diphenamid (*N,N*-Dimethyl-2,2,-diphenylacetamide, DPM) is one of a number of dialkylamides which have neuropathological potential. It produces an myelinopathy similar to that produced by the insect repellent, *N,N*-diethyl-*m*-toluamide (DEET) but with only moderate CNS hyperexcitability (Verschoyle, *et al.*, 1992). On oral dosing diphenamid induces focal myelinopathy in the fibres travelling through the cerebellar nuclei, which could be detected by recording cerebellar AEP. Practically, such an animal model can be useful for an alternative pathological pattern of systemically-induced focal myelinopathy.

Experimental protocol

Ten female F344 rats were dosed according to Verschoyle's methods (1992) by oesophageal intubation with diphenamid at 800, 1,000, 1,200 and 1,400 mg/kg (as a 100 or 150 mg/ml solution in glycerinformal) after overnight starvation. The most common neurological signs of poor coordination, ataxia, prostration and death were observed and listed in Table 1.

Results and discussion

The results of the present study shows results similar to those obtained in previous study on female Lac:P Wister rats. At 800 mg/kg diphenamid produced no sedation but a marked increase in exploratory behaviour which began approximately 1 hour after dosing and persisted for 24 hours. High dose diphenamid produced a progressive

Table 1. Clinical observation of oral dosing diphenamid in F344 rats.

DOSAGES (mg/kg)	POOR COORDINATION	ATAXIA	PROSTRATION	DEATH (TIME)
700	0/2	0/2	0/2	0/2
800	0/2	0/2	0/2	0/2
1,000	2/2	1/2	1/2	0/2
1,200	2/2	2/2	2/2	2/2 (2,8 days)
1,400	2/2	2/2	2/2	2/2 (30 hours)

severe ataxia leading to prostration. Deaths were seen at a dose of 1,200 mg/kg at 2 and 8 days, and 1,400 mg/kg at as early as 30 hours. Previous studies have shown that one or two days after dosing with diphenamid, oedema fluid accumulates in the inner myelin loop and bilaterally symmetrical vacuolation of myelinated fibres in the cerebellar roof nuclei occurs with splitting at the intraperiod line, as seen under the light microscope. Similar vacuolation involved the vestibular nuclei and also the reticular formation in some rats, but less severely. Less severe vacuolation was also found in the cerebellar roof nuclei after six days of dosing suggesting that the lesions were reversible. No reactive glial or secondary neuronal changes were found in the myelin damaged area at day 1, 2, or 6. A few necrotic neurones with shrunken eosinophilic cytoplasm were seen in the region. This would have been an useful alternative to TET, in providing a more localised myelin oedema. However given the lack of effect of TET on MBP detection, this model was not, in fact, used.

Reference

Verschoyle R. D., Brown A. W., Nolan C. C., Ray D. E. and Lister T. A comparison of the acute toxicity, neuropathology, and electrophysiology of *N,N*-Diethyl-*m*-toluamide (DEET) and *N,N*-Dimethyl-2,2-diphenylacetamide (Diphenamid) in rats. *Fundamental and Applied Toxicology* 1992; **18**: 79-88.

Appendix 3. Publications related to this study so far:

3.1. An improved method for repeated cerebrospinal fluid sampling in the rat. *Journal of Physiology (Lond.)* 1993; 467: 241p.

X. Liu & D. E. Ray, MRC Toxicology Unit, University of Leicester, Leicester LE1 9HN.

A capacity for repeated cerebrospinal fluid (CSF) sampling is required in experimental models intended to simulate clinical applications, and Sarna, *et al.* (1983) developed such a method applicable to freely moving rats. However in our hands it proved very difficult both to position the cannula and to puncture the cisternum magnum with a wire pushed down the cannula whilst avoiding intracranial haemorrhage. We modified the technique by using a shorter approach and by opening the dura directly with a needle. Penetration could then be monitored by viewing the efflux of CSF.

Rats were anaesthetized by Sagatal (60 mg/kg, i.p.) and placed in a stereotaxic frame. A midline incision was made and a screw placed at the back of the skull. The middle part of the occipital muscles were dissected from the skull down to the upper edge of the foramen magnum. A burr hole (1 x 2 mm) was made in the midline 2 mm dorsal to the foramen magnum. Under a dissecting microscope the dura was bluntly dissected away from the burr hole down to the subarachnoid cistern, which was then opened by using a curved 23G needle, when the effux of CSF could be observed. A "J" shaped polyethylene (PE10) cannula was inserted into the cisterna magna using a manipulator. The cannula and supporting screw were then fixed to the skull with dental acrylic. Finally, the free end of cannula was covered by a piece of heat-sealed PE50 tubing (Fig. 1). After 3-4 days recovery, further sampling could be achieved by connecting a Hamilton syringe directly to the cannula.

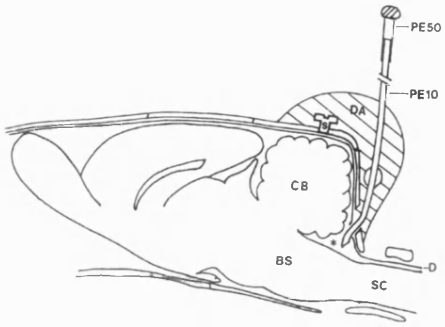

Fig. 1. Cannula implantation into the cisterna magna for repeated CSF sampling in rats. *: Cisterna magna; BS: Brain-stem; CB: Cerebellum; D: Dura; DA: Dental acrylic; PE10: Implanted polyethylene size 10 tube; PE50: Heat-sealed polyethylene size 50 tube; S: Supporting screw; SC: Spinal cord.

This technique allows a shorter intracranial approach with better visibility and wider opening of the subarachnoid cistern. It reduces the intracranial space occupied by the cannula and frees the dorsal skull for further implantation (in our case, electrodes for evoked potentials). Of 30 cannula placed using the new approach, all were patent 24 hours post implantation, and 15 remained patent for 2 - 4 weeks. The most common reason for later failures was probably placement in the subdural rather than the subarachnoid space.

Supported by EC grant PL900705 (BIOMED).

REFERENCE

Sarna, *et al.,* (1983). *J. Neurochem.* **40**, 383-388.

3.2. A comparison of surface auditory potentials evoked by high frequency monaural and binaural stimulation in the anaesthetised rat. *Journal of Physiology (Lond.)* 1994; 480:104p.

X. Liu & D. E. Ray, MRC Toxicology Unit, University of Leicester, PO Box 138, Lancaster Road, Leicester LE1 9HN.

Various investigators have studied auditory evoked potentials (AEPs) in rats (e.g. Shaw, N.A., 1988). To compare the surface responses evoked by monaural and binaural stimulation, we recorded AEPs from seven rats under anaesthesia (urethane, 140mg/kg, i.p.). Auditory stimuli were 1 ms tone bursts of 40KHz delivered at 10Hz via a RS transmitter that was either connected to a hollow stereotaxic earbar (monaural) or placed 34cm over the rat's head (binaural). Nine stainless steel screw electrodes were placed in the rat's dorsal skull and two over the auditory cortices. A reference screw was placed between the eyes. The auditory responses were recorded with a bandwidth of 3 - 5,000Hz and averaged 1024 times. Amplitudes were estimated by peak-peak measurement and presented as mean ± SE (n=5). Simultaneous recordings showed that the spatial distribution of far-field potentials over the dorsal skull was contralateral and caudal following the monaural stimulation, whereas they were larger at the midline and caudal following the binaural stimulation (Fig. 1). With

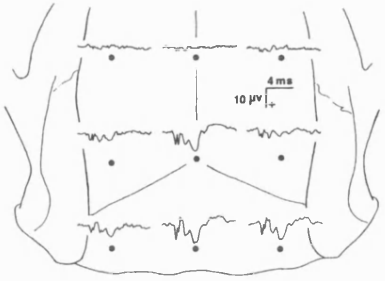

Fig. 1. Typical distribution of AEPs on the dorsal skull following binaural stimulation. Recording sites are indicated by '•' marks.

matched stimulus intensities of 100dB, the amplitude of the early component (1.2msec) to binaural stimuli was 185 ± 11% of that to monaural stimuli, but the comparable value for the late component (4.1msec) was 129 ± 5%. In contrast, the near-field cortical responses (P2) to binaural stimuli were 59 ± 4% of that to contralateral monaural stimuli.

We conclude that the distribution of far-field potentials is altered under different stimulation conditions. Following binaural stimulation, the brainstem components summate, whereas the decreased near-field cortical responses indicate that contralateral inhibition predominates in the cortex.

X. L. was supported by EC grant PL900705 (BIOMED).

REFERENCE

Shaw, N.A. (1988). *Progress in Neurobiology* **31**, 19-45.

3.3. Cerebellar surface auditory evoked potential: the effect of intracerebellar injection of procaine in anaesthetized rats. *Journal of Physiology (Lond.)* 1995; 483:29P.

Xuguang Liu and David E. Ray, MRC Toxicology Unit, University of Leicester, Lancaster Road, Leicester LE1 9HN.

The cerebellar surface response to auditory stimuli was initially described in 1944 by Snider and Stowell. Although it has been suggested that the surface positive component at a latency of 4 ms in rats represents a response of the cerebellar cortex (Shaw, 1992), questions still remain about the afferent pathway and generators contributing to the surface-recorded activity. In order to test whether such a response can be used as an index of cerebellar function, we recorded the surface potential from five rats under anaesthesia (urethane, 1.4 g kg^{-1}, i.p.) before and after injection of procaine into the central white matter of the cerebellum. Auditory stimuli were 1 ms tone bursts of 40 kHz delivered at 5 Hz with intensity of 100 dB SPL via a transmitter placed 34 cm over the rat's head. A stainless steel screw electrode was placed in the skull over the vermis in the midline. A reference was placed in the skull between the eyes. The cerebellar response was recorded with a bandwidth of 0.3-5,000 Hz and averaged 1024 times. Latency was measured from the onset of stimuli, amplitude was estimated by three-point measurement, and central conduction time was assessed relative to the cochlear nuclear peak. Body temperature was maintained at 38 ± 0.3 °C. The cerebellar white matter at AP: interaural -2.0 mm; LR: 2.0 mm; DV: interaural 3.5 - 4.5 mm was targeted, and 5 µl of 4 % procaine in saline was injected on each side using a Hamilton syringe with a 30 G needle. Data are presented as means ± S. D.

The peak latency of the response was delayed from 4.98 ± 0.05 to 5.22 ± 0.16 ms ($P < 0.05$, paired t test), wholly due to an increase in conduction time (2.79 ± 0.06 to 3.04 ± 0.15 ms, $P < 0.05$). Amplitude decreased from 9.27 ± 0.77 to 8.22 ± 0.94 μV ($P < 0.05$), while the early far field components were unchanged in both amplitude and latency. This significant but smaller than expected change suggests that either blockade of the fibres conducting the afferent impulse was insufficient, or that other generators outside the cerebellar cortex contribute to the response. Additional depth recordings showed that a large response with a similar waveform and latency could be recorded at the level of the cerebellar nuclei. We conclude that the decreased conductivity in the cerebellar white matter induced by procaine injection alters the surface-recorded response. This potential, however, appears not to be generated exclusively in the cerebellar cortex.

X.L. was supported by an EC BIOMED grant (EV5V-CT91-0005).

REFERENCES

Shaw, N. A. (1992). *Electromyogr. Clin. Neurophysiol.* **32**: 570-590.

Snider, R.S. & Stowell, A. (1944). *J. Neurophysiol.* **7**:331-357.

3.4. Chemically-induced myelinopathy in the central nervous system: Electrophysiological and immunochemical monitoring. *Human and Experimental Toxicology* 1995; 14:375.

Xuguang Liu, Paul Glynn & David E. Ray, MRC Toxicology Unit, Hodgkin Building, University of Leicester, PO Box 138, Lancaster Road, Leicester LE1 9HN.

We have studied chemically-induced myelinopathy in the central nervous system with the objective of identifying sensitive quantitative electrophysiological and immunochemical indicators which might ultimately be clinically applicable for the monitoring of such lesions.

Preliminary acute experiments were carried out to identify the cerebellar auditory evoked potentials (AEPs) which can be recorded superficially and to apply a radioimmunoassay[1] for measurement of myelin basic protein-like materials (MBP) in the cerebrospinal fluid (CSF) and determination of clearance rate of MBP from the normal CSF circulation (50% clearance time of MBP from CSF is approx. 2.5 hours). Experimental animals for toxicological studies were surgically prepared by chronic implantation of electrodes for recordings of AEPs and a cannula in the cisterna magna for CSF sampling[2]. Two animal models of gross and focal myelinopathies were established and employed: systemic triethyltin intoxication (8 mg/kg, i.p.) and bilateral intracerebellar microinjection of lysolecithin (LPC, 5 - 20 μg/rat), which were monitored by repeated recording of AEPs and immunoassay of CSF samples. The AEP was altered by triethyltin intoxication with a significant prolongation of the central conduction time (2.6 ± 0.04 to 2.8 ± 0.06, on 3d) accompanied a significant decrease in amplitude of the cochlear nuclear response (7.2 ± 0.5 to 2.7 ± 0.4, at 24hs). The MBP in the CSF was normally <1 ng/ml but increased following LPC injection up to 26 ng/ml at 24hs.

We conclude that the prolongation of the central conduction time indicates disturbance of myelinated fibres in triethyltin induced myelinopathy. The appearance of MBP in CSF in the LPC induced myelinopathy reflects the release of MBP into CSF following the collapse of the myelin sheaths.

X. L. was supported by EC grant PL900705 (BIOMED).

REFERENCES

1. Barry, R., Lawrence, M., Thompson, A., McDonald, I., & Groome, N. (1990) *Neurochem. Int.* 16, 549-558.

2. Liu, X. & Ray, D.E. (1993) *J. Physiol.* 467, P241.

3.5. Neurotoxic effects of triethyltin: A model of physiological monitoring neurotoxicity. *Human and Experimental Toxicology* 1995; 14:375.

Xuguang Liu & David E. Ray, MRC Toxicology Unit, Hodgkin Building, University of Leicester, PO Box 138, Lancaster Road, Leicester LE1 9HN.

The neurotoxicity of triethyltin (TET) has been intensively studied[1]. In the current study, we investigated the acute hypothermia, ototoxicity and myelinopathy induced by a single dose of 8 mg/kg TET, i.p. in rats by clinical observation and evoked potential recordings throughout intoxication and recovery.

Animals were surgically prepared by chronic implantation of surface electrodes for auditory and somatosensory evoked potentials (EPs) recordings. Body temperature, ataxia-weakness score and EPs were repeatedly assessed. Data are presented as mean ± s.e.m. and tested with the t-test. TET induced a transient hypothermia peaking at 24h (37.8 ± 0.1 to 35.1 ± 0.5 °C), accompanied by a 50% reduction of the isoflurane (1.5 ± 0.08% to 0.75 ± 0.07%) required to maintain anaesthesia in both hypothermic and normothermic rats. Motor deficits: ataxia and hindlimb weakness (score 5/10) developed gradually, accompanied by body weight loss (20% of control), peaking at 7d and recovering by 15d. Amplitudes of auditory EPs were significantly decreased in normothermic rats with a peak effect at 24h and slow recovery. The decrease occurred in the early components indicating direct cochlear damage. There were significant delay of EPs latency and prolongation of conduction time, which is parallel to the time course of motor deficits development. The temperature dependence of nerve conduction was significantly increased by TET (0.09 ± 0.04 ms/2°C to 0.36 ± 0.08 ms/2°C), consistent with myelin damage. Pathological sections showed widespread

reversible intramyelinic vacuolation in the brainstem, cerebral and cerebellar white matter.

Thus TET produces two phases of toxicity: (1) a rapid transient general depression of the CNS and a rapid but persistent ototoxicity, and (2) a slower reversible myelinotoxicity.

X. L. was supported by EC grant PL900705 (BIOMED).

REFERENCE

[1] Cavanagh J. B. and Nolan C.C. The neurotoxicity of organolead and organotin compounds. In: Handbook of Clinical Neurology Vol 64. Intoxications of the Nervous System (Part 1). (Ed.) Vinken PJ and de Bruyn GW; (volume ed) de Wolff FA. Elsevier Science BV, Amsterdam, 1994.